

**DEVELOPMENT OF FINE PARTICULATE EMISSION FACTORS AND  
SPECIATION PROFILES FOR OIL- AND GAS-FIRED COMBUSTION  
SYSTEMS**

**OTHER REPORT: PILOT-SCALE DILUTION SAMPLER DESIGN AND  
VALIDATION TESTS (LABORATORY STUDY)**



When citing this document, please use the following citation:  
Chang, M.C. and England, G.C., “Development of Fine Particulate Emission Factors and Speciation Profiles for Oil and Gas-fired Combustion Systems, Other Report: Pilot-Scale Dilution Sampler Design And Validation Tests (Laboratory Study),” 2004.

**DEVELOPMENT OF FINE PARTICULATE EMISSION FACTORS AND  
SPECIATION PROFILES FOR OIL- AND GAS-FIRED COMBUSTION  
SYSTEMS**

**OTHER REPORT: PILOT-SCALE DILUTION SAMPLER DESIGN AND  
VALIDATION TESTS (LABORATORY STUDY)**

Prepared by:

Ming-Chih Chang and Glenn C. England  
GE Energy and Environmental Research Corporation  
18 Mason  
Irvine, CA 92618

Prepared for:

National Petroleum Technology Office  
National Energy Technology Laboratory  
United States Department of Energy  
(DOE Contract No. DE-FC26-00BC15327)

Gas Research Institute  
California Energy Commission – Public Interest Energy Research (PIER)  
New York State Energy Research and Development Authority  
(GRI contract No. 8362)

American Petroleum Institute  
(API Contract No. 00-0000-4303)

Revision 0 (Draft): April 22, 2002  
Revision 1 (Version 3): June 18, 2004  
Revision 2 (Version 1): July 28, 2004

## LEGAL NOTICES

### **United States Department of Energy:**

This report was prepared as an account of work sponsored by an agency of the United States Government. Neither the United States Government nor any agency thereof, nor any of their employees, makes any warranty, express or implied, or assumes any legal liability or responsibility for the accuracy, completeness, or usefulness of any information, apparatus, product, or process disclosed, or represents that its use would not infringe privately owned rights. Reference herein to any specific commercial product, process, or service by trade name, trademark, manufacturer, or otherwise does not necessarily constitute or imply its endorsement, recommendation, or favoring by the United States Government or any agency thereof. The views and opinions of authors expressed herein do not necessarily state or reflect those of the United States Government or any agency thereof.

### **Gas Research Institute:**

This report was prepared by GE EER as an account of contracted work sponsored by the Gas Research Institute (GRI). Neither GE EER, GRI, members of these companies, nor any person acting on their behalf:

- a. Makes any warranty or representation, expressed or implied, with respect to the accuracy, completeness, or usefulness of the information contained in this report, or that the use of any apparatus, methods, or process disclosed in this report may not infringe upon privately owned rights; or
- b. Assumes any liability with respect to the use of, or for damages resulting from the use of, any information, apparatus, method, or process disclosed in this report.

### **California Energy Commission:**

This report was prepared as a result of work sponsored by the California Energy Commission (Commission). It does not necessarily represent the views of the Commission, its employees, or the State of California. The Commission, the State of California, its employees, contractors, and subcontractors make no warranty, express or implied, and assume no legal liability for the information in this report; nor does any party represent that the use of this information will not infringe upon privately owned rights. This report has not been approved or disapproved by the Commission nor has the Commission passed upon the accuracy or adequacy of the information in this report.

### **New York State Energy Research and Development Authority:**

This report was prepared by GE Energy and Environmental Research Corporation in the course of performing work contracted for and sponsored by the New York State Energy Research and Development Authority (NYSERDA). The opinions expressed in this report do not necessarily reflect those of the NYSERDA or the State of New York, and reference to any specific product, service, process, or method does not constitute an implied or expressed recommendation or endorsement of it. Further, NYSERDA and the State of New York make no warranties or representations, expressed or implied, as to the fitness for particular purpose or merchantability of any product, apparatus, or service, or the usefulness, completeness, or accuracy of any processes, methods, or other information contained, described, disclosed, or referred to in this report. NYSERDA, the State of New York, and the contractor make no representation that the

use of any product, apparatus, process, method, or other information will not infringe privately owned rights and will assume no liability for any loss, injury, or damage resulting from, or occurring in connection with, the use of information contained, described, disclosed, or referred to in this report.

**American Petroleum Institute:**

API publications necessarily address problems of a general nature. With respect to particular circumstances, local state and federal laws and regulations should be reviewed.

API is not undertaking to meet the duties of employers, manufacturers, or suppliers to warn and properly train and equip their employees, and others exposed, concerning health and safety risks and precautions, nor undertaking their obligations under local, state, or federal laws. Nothing contained in any API publication is to be construed as granting any right, by implication or otherwise, for the manufacture, sale, or use of any method, apparatus, or product covered by letters patent. Neither should anything contained in the publication be construed as insuring anyone against liability for infringement of letters patent.

**GE Energy:**

This report was prepared by GE Energy & Environmental Research Corporation (as part of GE Energy and General Electric Company, collectively hereinafter “GE Energy”) as an account of sponsored work. GE Energy, nor any of their employees, makes any warranty, express or implied or otherwise, or assumes any legal liability or responsibility of the accuracy, completeness, or usefulness of any information, apparatus, processes, systems, products, methodology or the like disclosed herein, or represents that its use would not infringe privately owned rights. Reference herein to any specific commercial product process or service by trade name, trademark, manufacturer, or otherwise do not necessarily constitute or imply an endorsement, recommendation, or favoring by GE Energy. The views and opinions of the authors expressed herein do not necessarily state or reflect those of GE Energy. This report has not been approved or disapproved, endorsed or otherwise certified by GE Energy nor has GE Energy passed upon the accuracy or adequacy of the information in this report.

## ACKNOWLEDGEMENTS

The following people are recognized for their contributions of time and expertise during this study and in the preparation of this report:

### GE ENERGY AND ENVIRONMENTAL RESEARCH CORPORATION

#### PROJECT TEAM MEMBERS

Glenn England, Project Manager  
Stephanie Wien, Project Engineer  
Dr. Oliver M.C. Chang, Project Engineer  
Brian Jacobs, Test Specialist  
Andrew Furlong, Test Specialist  
Prof. Barbara Zielinska, Desert Research Institute  
Prof. John Watson, Desert Research Institute  
Prof. Judith Chow, Desert Research Institute  
Prof. Philip Hopke, Clarkson University  
Prof. Glen Cass, Georgia Institute of Technology

#### AD HOC COMMITTEE MEMBERS

Dr. Karl Loos, Shell Global Solutions  
Prof. Jaime Schauer, University of Wisconsin  
Dr. Praveen Amar, NESCAUM  
Thomas Logan, U.S. EPA  
Ron Myers, U.S. EPA  
Karen Magliano, California Air Resources Board

#### PROJECT SPONSORS

Kathy Stirling, U.S. Department of Energy National Petroleum Technology Office  
Marla Mueller, California Energy Commission  
Dr. Paul Drayton, Gas Research Institute  
Karin Ritter, American Petroleum Institute  
Barry Liebowitz, New York State Energy Research and Development Authority  
Janet Joseph, New York State Energy Research and Development Authority

## FOREWORD

In 1997, the United States Environmental Protection Agency (EPA) promulgated new National Ambient Air Quality Standards (NAAQS) for particulate matter, including for the first time particles with aerodynamic diameter smaller than 2.5 micrometers (PM<sub>2.5</sub>). PM<sub>2.5</sub> in the atmosphere also contributes to reduced atmospheric visibility, which is the subject of existing rules for siting emission sources near Class 1 areas and new Regional Haze rules. There are few existing data regarding emissions and characteristics of fine aerosols from oil, gas and power generation industry combustion sources, and the information that is available is generally outdated and/or incomplete. Traditional stationary source air emission sampling methods tend to underestimate or overestimate the contribution of the source to ambient aerosols because they do not properly account for primary aerosol formation, which occurs after the gases leave the stack. These deficiencies in the current methods can have significant impacts on regulatory decision-making. The current program was jointly funded by the U.S. Department of Energy National Energy Technology Laboratory (DOE/NETL), California Energy Commission CEC), Gas Research Institute (GRI), New York State Energy Research and Development Authority (NYSERDA) and the American Petroleum Institute (API) to provide improved measurement methods and reliable source emissions data for use in assessing the contribution of oil, gas and power generation industry combustion sources to ambient PM<sub>2.5</sub> concentrations. More accurate and complete emissions data generated using the methods developed in this program will enable more accurate source apportionment and source receptor analysis for PM<sub>2.5</sub> NAAQS implementation and streamline the environmental assessment of oil, gas and power production facilities.

The goals of this program were to:

- Develop improved dilution sampling technology and test methods for PM<sub>2.5</sub> mass emissions and speciation measurements, and compare results obtained with dilution and traditional stationary source sampling methods.
- Develop emission factors and speciation profiles for emissions of fine particulate matter, especially organic aerosols, for use in source-receptor and source apportionment analysis;
- Identify and characterize PM<sub>2.5</sub> precursor compound emissions that can be used in source-receptor and source apportionment analysis.

This report is part of a series of progress, topical and final reports presenting the findings of the program.

## TABLE OF CONTENTS

LEGAL NOTICES.....	IV
ACKNOWLEDGEMENTS.....	VI
FOREWORD.....	VII
LIST OF FIGURES.....	X
LIST OF TABLES.....	XII
EXECUTIVE SUMMARY.....	1
PILOT-SCALE TEST PROGRAM.....	2
FINDINGS.....	3
1. INTRODUCTION.....	4
PROJECT OVERVIEW.....	4
BACKGROUND.....	5
Formation of Fine Particles.....	5
Traditional PM/PM10/PM2.5 Test Methods.....	7
Formation of Aerosols and Sampling Conditions.....	10
Dilution Sampling Methods.....	13
2. DILUTION SAMPLER CHARACTERIZATION APPROACH AND METHODS.....	16
TEST OBJECTIVES.....	16
PILOT-SCALE COMBUSTOR.....	17
FUELS.....	19
TEST MATRIX.....	19
Phases 1 and 2 Tests – Design Development.....	21
Phase 3 Tests – Design Validation.....	22
MEASUREMENTS.....	22
DRI Dilution Sampler.....	22
GE Energy and Environmental Research Corporation (GE EER) Dilution Sampler.....	25
Sample Collection Methods.....	26
3. DESIGN DEVELOPMENT TEST RESULTS.....	29
DILUTION SAMPLER Flow Field Characterization.....	29
PARTICLE CONCENTRATION TRENDS.....	33
ULTRAFINE PARTICLE SIZE DISTRIBUTION AND CONCENTRATION.....	34
Effects of Dilution Ratio.....	35
Effects of Residence Time.....	38
H <sub>2</sub> SO <sub>4</sub> and Zinc Oxide (ZnO) Doping Results.....	38
Effect of Exhaust Temperature.....	42
Particle Losses.....	45
Ambient Air.....	45
GRAVIMETRIC AND CHEMICAL ANALYSIS RESULTS.....	48
4. DESIGN VALIDATION TEST RESULTS.....	54
DILUTION SAMPLER CHARACTERIZATION.....	54
CO Tracer Profiles.....	54
Particulate Concentration Profiles.....	55
COMBUSTION TESTS.....	57
Natural Gas Tests.....	57



No. 6 Oil Tests .....	58
Natural Gas H <sub>2</sub> SO <sub>4</sub> Doping.....	61
5. DISCUSSION AND FINDINGS.....	63
FINDINGS.....	63
REFERENCES .....	65
APPENDIX A LIST OF ABBREVIATIONS.....	67
APPENDIX B SI CONVERSION FACTORS.....	69

## LIST OF FIGURES

Figure 1-1. U.S. EPA Method PRE-004/202 Sampling Train.....	8
Figure 1-2. Typical Particle Size Distribution in Combustion Exhaust.....	11
Figure 1-3. Theoretical effect of cooling with and without dilution on saturation ratio for 35 ppm H <sub>2</sub> SO <sub>4</sub> in air.....	12
Figure 2-1. Pilot-Scale Combustion Facility. ....	17
Figure 2-2. FEF exhaust cooling and sampling section. ....	18
Figure 2-3. DRI Dilution Sampler Setup and the Sampling Locations Corresponding to Different Residence Times in the Sampler.....	24
Figure 2-4. Compact (GE EER) Dilution Sampler. ....	25
Figure 3-1. Concentration profiles at different cross-sectional planes in the DRI dilution sampler.....	30
Figure 3-2. Dilution sampler geometry and reference locations for computational simulation. .	31
Figure 3-3. Calculated temperature profile predicted by CFD simulation showing mixing between sample and dilution air in dilution tunnel for dilution ratio of 10:1 (left) and 50:1 (right). ....	31
Figure 3-4. Velocity profiles in dilution tunnel sampler by CFD: left 10:1 and right 50:1.....	32
Figure 3-5. PM concentration trend from coal combustion measured from dilution sampler with 50:1 dilution ratio and flue gas temperature of 645 K.....	34
Figure 3-6. Effect Of Dilution Ratio On Ultrafine Particle Size Distribution And Number Concentration (Coal, Sample Temperature 450 K, Residence Time 80 Seconds). ....	36
Figure 3-7. Effect Of Dilution Ratio On Ultrafine Particle Size Distribution And Number Concentration (No. 6 Fuel Oil, Sample Temperature 450 K, Residence Time 80 Seconds).36	36
Figure 3-8. Effect Of Dilution Ratio On Ultrafine Particle Size Distribution And Number Concentration (Natural Gas, Exhaust Temperature 450 K, Residence Time 80 Seconds)...	37
Figure 3-9. Effect Of Residence Time On Ultrafine Particle Size Distribution And Number Concentration (Coal, Exhaust Temperature 450 K, Dilution Ratio 50:1). ....	39
Figure 3-10. Effect Of Residence Time On Ultrafine Particle Size Distribution And Number Concentration (No. 6 Fuel Oil, Exhaust Temperature 450 K, Dilution Ratio 50:1).....	39
Figure 3-11. Effect Of Residence Time On Ultrafine Particle Size Distribution And Number Concentration (Natural Gas, Exhaust Temperature 450 K, Dilution Ratio 50:1).....	40
Figure 3-12. Effect Of Residence Time On Ultrafine Particle Size Distribution And Number Concentration (Natural Gas + 30 ppm H <sub>2</sub> SO <sub>4</sub> , Exhaust Temperature 450 K, Dilution Ratio 50:1). ....	41
Figure 3-13. Effect Of Solid and Liquid Aerosol Doping On Ultrafine Particle Size Distribution And Number Concentration (Natural Gas, Exhaust Temperature 450 K, Dilution Ratio 10:1, Residence Time 80 Seconds). ....	41
Figure 3-14. Effect Of Residence Time On Ultrafine Particle Size Distributions (Coal, Exhaust Temperature 645 K, Dilution Ratio 50:1).....	43
Figure 3-15. Effect Of Residence Time On Ultrafine Particle Size Distributions (No. 6 Fuel Oil, Exhaust Temperature 645 K, Dilution Ratio 50:1).....	43
Figure 3-16. Effect Of Dilution Ratio And Exhaust Temperature On Ultrafine Particle Size Distributions (Coal, Residence Time 80 Seconds). ....	44
Figure 3-17. Effect Of Dilution Ratio And Exhaust Temperature On Ultrafine Particle Size Distributions (No. 6 Oil, Residence Time 80 Seconds).....	44

Figure 3-18. Size distributions of number concentration ( $\#/cm^3/mm$ ) measured from the center aligned sampling port and the sampling port on the wall using a SMPS for the coal combustion with a ten times dilution ratio.....	46
Figure 3-19. Size distributions of number concentration ( $\#/cm^3/\mu m$ ) measured from the center aligned sampling port and the sampling port on the wall using a SMPS for the coal combustion with 50:1 dilution ratio.....	46
Figure 3-20. Ultrafine particle size and number concentration measured at the centerline and near the wall of the aging chamber exit (natural gas, 645 K, dilution ratio 10:1). ....	47
Figure 3-21. Ambient Air Aerosol Concentrations During Pilot-Scale Tests. ....	47
Figure 3-22. Species Concentrations at Different Residence Times in the Dilution Sampler (Natural Gas, 50:1 Dilution Ratio, Exhaust Gas Temperature 445 K, February 4, 2002)....	49
Figure 3-23. Species Concentrations at Different Residence Times in the Dilution Sampler (Natural Gas, 50:1 Dilution Ratio, Exhaust Gas Temperature 445 K, February 5, 2002)....	50
Figure 3-24. Concentrations of aerosol species at 2 and 80 seconds residence time, expressed as in-stack concentration (natural gas, 50:1 dilution ratio, exhaust gas temperature 445 K)....	50
Figure 3-25. Concentrations of aerosol species at 10 and 80 seconds residence time, expressed as in-stack concentration (natural gas, 50:1 dilution ratio, exhaust gas temperature 445 K). .....	51
Figure 3-26. Concentrations of aerosol species at 2 seconds and 80 seconds residence time, expressed as in-stack concentration (coal, 50:1 dilution ratio, exhaust gas temperature 445 K). ....	52
Figure 3-27. Concentrations of aerosol species at 10 seconds and 80 seconds residence time, expressed as in-stack concentration (coal, 50:1 dilution ratio, exhaust gas temperature 445 K). ....	52
Figure 4-1. Sample gas concentration profile in the cross-sectional plane 12 inches downstream of the mixing plate (end of the mixing zone).....	55
Figure 4-2. Sample gas concentration profile in the cross-sectional plane 18 inches downstream of the mixing plate. ....	56
Figure 4-3. Radial particle number concentration profiles at the cross-sectional plane 12 inches downstream of the mixing plate (end of mixing zone, natural gas, exhaust temperature 450 K, 20:1 dilution ratio). ....	56
Figure 4-4. Axial particle concentration profile at centerline of dilution sampler (natural gas, exhaust temperature 450 K, 20:1 dilution ratio). ....	57
Figure 4-5. Partitioning of particulate to different sample fractions for dilution methods and EPA Methods 201A/202 (No. 6 Fuel Oil, exhaust temperature 450 K). ....	60

## LIST OF TABLES

Table 2-1. Fuel Characteristics for Pilot-Scale Tests.....	20
Table 2-2. Phase 1 and 2 Test Matrix.....	21
Table 2-3. Phase 3 Test Matrix.....	23
Table 2-4. Design Specification Comparison for DRI and GE EER Dilution Samplers.....	26
Table 2-5. Sample Collection Media, Analysis, and Location.....	27
Table 3-1. Calculated Mean Residence Times and Standard Deviations for 1 $\mu\text{m}$ Particles in the Residence Time Chamber at 10:1 and 50:1 Dilution.....	33
Table 3-2. Fraction of PM <sub>2.5</sub> Mass and Elements Smaller Than 0.32 $\mu\text{m}$ .....	48
Table 4-1. Comparison of PM <sub>2.5</sub> Mass Concentrations Measured by New Dilution Sampler and EPA Methods 201A/202 (Natural Gas, Exhaust Temperature 450 K).....	58
Table 4-2. Comparison of PM <sub>2.5</sub> Mass Concentrations Measured by DRI Dilution Sampler, EER Dilution Sampler, and EPA Methods PRE-004/202 (No. 6 Oil, Exhaust Temperature 450 K).....	60
Table 4-3. Sulfate Results for Dilution Sampler and Controlled Condensation Train.....	62

## EXECUTIVE SUMMARY

In 1997, the United States Environmental Protection Agency (EPA) promulgated new National Ambient Air Quality Standards (NAAQS) for particulate matter, including for the first time particles with aerodynamic diameter smaller than 2.5 micrometers ( $\mu\text{m}$ ) referred to as PM<sub>2.5</sub>. PM<sub>2.5</sub> in the atmosphere also contributes to reduced atmospheric visibility, which is the subject of existing rules for siting emission sources near Class 1 areas and new Regional Haze rules. There are few existing data regarding emissions and characteristics of fine aerosols from oil, gas and power generation industry combustion sources, and the information that is available is generally outdated and incomplete. Traditional stationary source air emission sampling methods tend to underestimate or overestimate the contribution of the source to ambient aerosols because they do not properly account for primary aerosol formation, which occurs after the gases leave the stack. Primary aerosol includes both filterable particles that are solid or liquid aerosols at stack temperature plus those that form as the stack gases cool through mixing and dilution processes in the plume downwind of the source. These deficiencies in the current methods can have significant impacts on regulatory decision-making. PM<sub>2.5</sub> measurement issues were extensively reviewed by the American Petroleum Institute (API) (England et al., 1998), and it was concluded that dilution sampling techniques are more appropriate for obtaining a representative particulate matter sample from combustion systems for determining PM<sub>2.5</sub> emission rate and chemical speciation. Dilution sampling is intended to collect aerosols including those that condense as the exhaust plume mixes and cools to near-ambient temperature in the atmosphere. These techniques have been widely used in recent research studies. For example, Hildemann et al. (1994) and McDonald et al. (1998) used filtered ambient air to dilute the stack gas sample followed by 80-90 seconds residence time to allow aerosol formation and growth to stabilize prior to sample collection and analysis. More accurate and complete emissions data generated using the methods developed in this program will enable more accurate source-receptor and source apportionment analysis for PM<sub>2.5</sub> NAAQS implementation and streamline the environmental assessment of oil, gas and power production facilities.

The goals of this research program were to:

- Develop improved dilution sampling technology and test methods for PM<sub>2.5</sub> mass emissions and speciation measurements, and compare results obtained with dilution and traditional stationary source sampling methods.
- Develop emission factors and speciation profiles for emissions of fine particulate matter, especially organic aerosols, for use in source-receptor and source apportionment analyses.
- Identify and characterize PM<sub>2.5</sub> precursor compound emissions that can be used in source-receptor and source apportionment analyses.

This report is part of a series of progress, topical and final reports presenting the findings of the research program. The research program includes field tests at several different types of gas- and oil-fired combustion sources, pilot-scale tests to help develop an improved measurement technology and methods, and technology transfer activities designed to disseminate results and incorporate scientific peer review into project plans and results. The reports present results and identify issues, procedures, methods and results that can be useful for future studies.

#### PILOT-SCALE TEST PROGRAM

The benchmark dilution sampler design developed and extensively characterized by Hildemann et al. (1989) has been used in several recent research studies. It has been successfully applied to several stationary sources; however, improvements need to address the following limitations before the technology can be widely applied:

- Large physical size and weight, which precludes application on many stationary sources due to a lack of sufficiently large or robust sampling platforms on the exhaust stack;
- Costly and time-consuming to setup and operate at stationary source sites;
- Losses of particles within the sampler that are difficult and time consuming to recover.
- Complex operation requiring highly skilled and experienced personnel.

Therefore, the overall goal of the pilot-scale evaluation was to experimentally understand and quantify design criteria for a more compact and easier-to-use dilution sampler that preserves comparability of results to the existing design. A pilot-scale research furnace was used to

produce combustion exhaust from real fuels (natural gas, No. 6 fuel oil, and coal) and from natural gas doped with sulfuric acid and solid (zinc oxide) particles, simulating a wide range of exhaust matrices. Measurements were made with the existing dilution sampler to evaluate the effects of dilution ratio, residence time and exhaust temperature on PM<sub>2.5</sub> mass and ultrafine particle size distributions. Based on these results a new compact dilution sampler was designed, built and tested. Side-by-side tests were conducted with the existing and compact dilution samplers for a preliminary evaluation of comparability. Supplementary tests and engineering analysis were undertaken to understand the characteristics of the current dilution tunnel performance to aid in interpreting pilot-scale test results.

## FINDINGS

The key findings from these tests are:

- Scanning mobility particle sizer and chemical speciation results at different residence time in dilution sampler suggest that an aging time after dilution of 10 seconds or more is necessary for vapor condensation growth and particle agglomeration. Shorter residence times may be adequate for sampling sources with high aerosol and/or condensable vapor concentrations.
- Preliminary tests of a new, more compact dilution sampler design demonstrated reduced particle losses in the undiluted sample components and more rapid mixing of the dilution air and sample. Aerosol concentration measurements within the sampler indicate negligible losses of particles within the sampler after dilution.
- A minimum dilution ratio of 20:1 is necessary to obtain representative particle size distributions. The total mass of PM<sub>2.5</sub> was not affected by dilution ratio.
- Particles smaller than 0.1  $\mu\text{m}$  in aerodynamic diameter rapidly accumulate into larger particles (typically in less than 10 seconds).
- Deposits of particles in the undiluted portions of the sampling system (i.e., sample nozzle, sample probe, venturi, etc.) can be significant and should be recovered for each sample run. Further development of recovery procedures for these components is needed to reduce imprecision and improve accuracy.
- Further tests are needed to validate the new dilution sampler against the current benchmark Hildemann design for a range of aerosol and condensable vapor concentrations.

## 1. INTRODUCTION

### PROJECT OVERVIEW

In 1997, the United States Environmental Protection Agency (EPA) promulgated new National Ambient Air Quality Standards (NAAQS) for particulate matter, including for the first time particles with aerodynamic diameter smaller than 2.5 micrometers ( $\mu\text{m}$ ) referred to as PM<sub>2.5</sub>. PM<sub>2.5</sub> in the atmosphere also contributes to reduced atmospheric visibility, which is the subject of existing rules for siting emission sources near Class 1 areas and new Regional Haze rules. There are few existing data regarding emissions and characteristics of fine aerosols from oil, gas and power generation industry combustion sources, and the information that is available is generally outdated and incomplete. Traditional stationary source air emission sampling methods tend to underestimate or overestimate the contribution of the source to ambient aerosols because they do not properly account for primary aerosol formation, which occurs after the gases leave the stack. Primary aerosol includes both filterable particles that are solid or liquid aerosols at stack temperature plus those that form as the stack gases cool through mixing and dilution processes in the plume downwind of the source. These deficiencies in the current methods can have significant impacts on regulatory decision-making. PM<sub>2.5</sub> measurement issues were extensively reviewed by the American Petroleum Institute (API) (England et al., 1998), and it was concluded that dilution sampling techniques are more appropriate for obtaining a representative particulate matter sample from combustion systems for determining PM<sub>2.5</sub> emission rate and chemical speciation. Dilution sampling is intended to collect aerosols including those that condense as the exhaust plume mixes and cools to near-ambient temperature in the atmosphere. These techniques have been widely used in recent research studies. For example, Hildemann et al. (1994) and McDonald et al. (1998) used filtered ambient air to dilute the stack gas sample followed by 80-90 seconds residence time to allow aerosol formation and growth to stabilize prior to sample collection and analysis. More accurate and complete emissions data generated using the methods developed in this program will enable more accurate source-receptor and source apportionment analysis for PM<sub>2.5</sub> NAAQS implementation and streamline the environmental assessment of oil, gas and power production facilities.



This study reports experimental results to determine (1) the minimum aging time and dilution air ratio required to achieve stable particle number distributions and mass emission rates, and (2) the dependence of particle size distributions on fuel types (coal, oil and natural gas) and exhaust temperature. The study was undertaken to develop improved design criteria for a new generation of relatively compact, lightweight dilution samplers. The U.S. Department of Energy National Energy Technology Laboratory (DOE/NETL), California Energy Commission (CEC), Gas Research Institute (GRI), New York State Energy Research and Development Authority (NYSERDA) and the API jointly funded the study.

The goals of this research program were to:

- Develop improved dilution sampling technology and test methods for PM<sub>2.5</sub> mass emissions and speciation measurements, and compare results obtained with dilution and traditional stationary source sampling methods.
- Develop emission factors and speciation profiles for emissions of fine particulate matter, especially organic aerosols, for use in source-receptor and source apportionment analyses.
- Identify and characterize PM<sub>2.5</sub> precursor compound emissions that can be used in source-receptor and source apportionment analyses.

## BACKGROUND

### Formation of Fine Particles

The EPA defines particulate matter in source emissions as follows (U.S. EPA, 2003):

- PRIMARY PARTICULATE MATTER (PM): Particles that enter the atmosphere as a direct emission from a stack or an open source. It is comprised of two components: Filterable PM (FPM) and Condensable PM (CPM).
- FILTERABLE PM: Particles that are directly emitted by a source as a solid or liquid at stack or release conditions and captured on the filter of a stack test train.

- CONDENSIBLE PM: Material that is vapor phase at stack conditions, but which condenses and/or reacts upon cooling and dilution in the ambient air to form solid or liquid PM immediately after discharge from the stack.
- SECONDARY PM: Particles that form through chemical reactions in the ambient air well after dilution and condensation have occurred. Secondary PM is usually formed at some distance downwind from the source.

This study is limited to measurement of primary particles. Particles in combustion exhaust derive from: mineral matter and elements in fuels, lubricants and feedstocks; carbonaceous particles formed during combustion; incomplete combustion of fuel particles and droplets; particles in the combustion air; and chemical reactions in the exhaust. After leaving the stack, the hot exhaust plume is rapidly cooled as it mixes with ambient air. Vapor species convert to particles through homogeneous and heterogeneous nucleation or condensation on the surface of existing particles, the rates for which will depend on many factors including how quickly the gases are cooled and the number of existing particles present. Rapid chemical reactions between species in the exhaust such as sulfuric acid ( $\text{H}_2\text{SO}_4$ ), hydrochloric acid (HCl) and ammonia ( $\text{NH}_3$ ) contribute to solid particles such as ammonia salts. The particle size distribution is dynamic, shifting with time as aerosol particles collide, coagulating and agglomerating to form larger particles. Condensational growth of particles in the diluted plume also occurs. These processes depend on the chemical species present and their concentrations, mixing and quench rates, time, temperature, partitioning of species between the gas and solid phase, and other factors.

Therefore, particles in the exhaust of combustion sources can have sizes covering a very wide range from sub-micron “ultrafine” particles resulting from homogeneous nucleation or gas-phase soot formation to coarse particles exceeding 100  $\mu\text{m}$  in diameter resulting from native fuel particles or growth of smaller particles. Because the amount of ambient PM<sub>2.5</sub> that is formed from stack emissions is strongly dependent on both stack emissions and atmospheric transformations and reactions (much more so than particulate with aerodynamic diameter less than 10  $\mu\text{m}$  (PM<sub>10</sub>) or total particulate), it is essential that emissions measurements accurately represent conditions controlling these reactions and transformations.

## Traditional PM/PM10/PM2.5 Test Methods

Regulatory source testing methods used for measuring particulate emissions from stationary source emissions typically employ hot filters (e.g., U.S. EPA Methods 5, 201A, PRE-004, 17) followed by bubblers (impingers) containing water placed in an ice bath (e.g., U.S. EPA Method 202). In-stack cyclones or cascade impactors may be placed ahead of the filter to enable size segregation of aerosols present at stack conditions, for measurement of PM10 and/or PM2.5 emissions (e.g., Figure 1-1). These methods tend to underestimate PM2.5 (e.g., because the hot front filter does not collect condensable species) or overestimate it (e.g., because the cold aqueous impingers may collect gaseous as well as condensable components). Further, the sensitivity of the filter methods is not low enough for many present day stationary combustion sources, e.g., gas-fired combustion systems and other fuels fired in systems with very high efficiency emission controls (e.g., spray dryer/fabric filters for control of acid gases and PM from coal-fired boilers).

Previous experiments have demonstrated that the iced impinger test methods can artificially produce inorganic condensable matter (Filadelfia and McDannel, 1996; Corio and Sherwell, 2000; Wien *et al.*, 2001). Sulfur dioxide ( $\text{SO}_2$ ) and molecular oxygen ( $\text{O}_2$ ) both are soluble in water. The dissolved  $\text{SO}_2$  can form hydrated  $\text{SO}_2$  ( $\text{SO}_2 \cdot \text{water} (\text{H}_2\text{O})$ ), bisulfite ion ( $\text{HSO}_3^-$ ) and sulfite ion ( $\text{SO}_3^{=}$ ) in aqueous solution. At the potential of hydrogen (pH) range of interest, (pH = 2 to 7),  $\text{HSO}_3^-$  is the preferred state. The individual dissociations are very fast, so aqueous-phase equilibria are established instantaneously. The dissociation of dissolved  $\text{SO}_2$  enhances its aqueous solubility so that the total amount of dissolved sulfate always exceeds that predicted by Henry's Law for  $\text{SO}_2$  alone. There are several pathways for sulfate formation by reaction of these ions with dissolved  $\text{O}_2$ , ozone ( $\text{O}_3$ ) and hydrogen peroxide ( $\text{H}_2\text{O}_2$ ), which can be catalyzed by many substances such as iron (Fe) and manganese (Mn) (Seinfeld and Pandis, 1998). Free  $\text{NH}_3$  in the samples can increase the amount of dissolved  $\text{SO}_2$ , and thereby increase artifact sulfate formation, since it instantly reacts in aqueous solution forming ammonium sulfite/bisulfite ions and additional  $\text{SO}_2$  must dissolve to maintain equilibrium.

EPA Methods 202 and 8 implicitly acknowledge the potential for conversion of  $\text{SO}_2$  to sulfate ion ( $\text{SO}_4^{=}$ ) by requiring a post-test purge of the impingers immediately following the test to purge the impinger solutions of dissolved  $\text{SO}_2$ . Method 8 requires a 15-minute purge with air

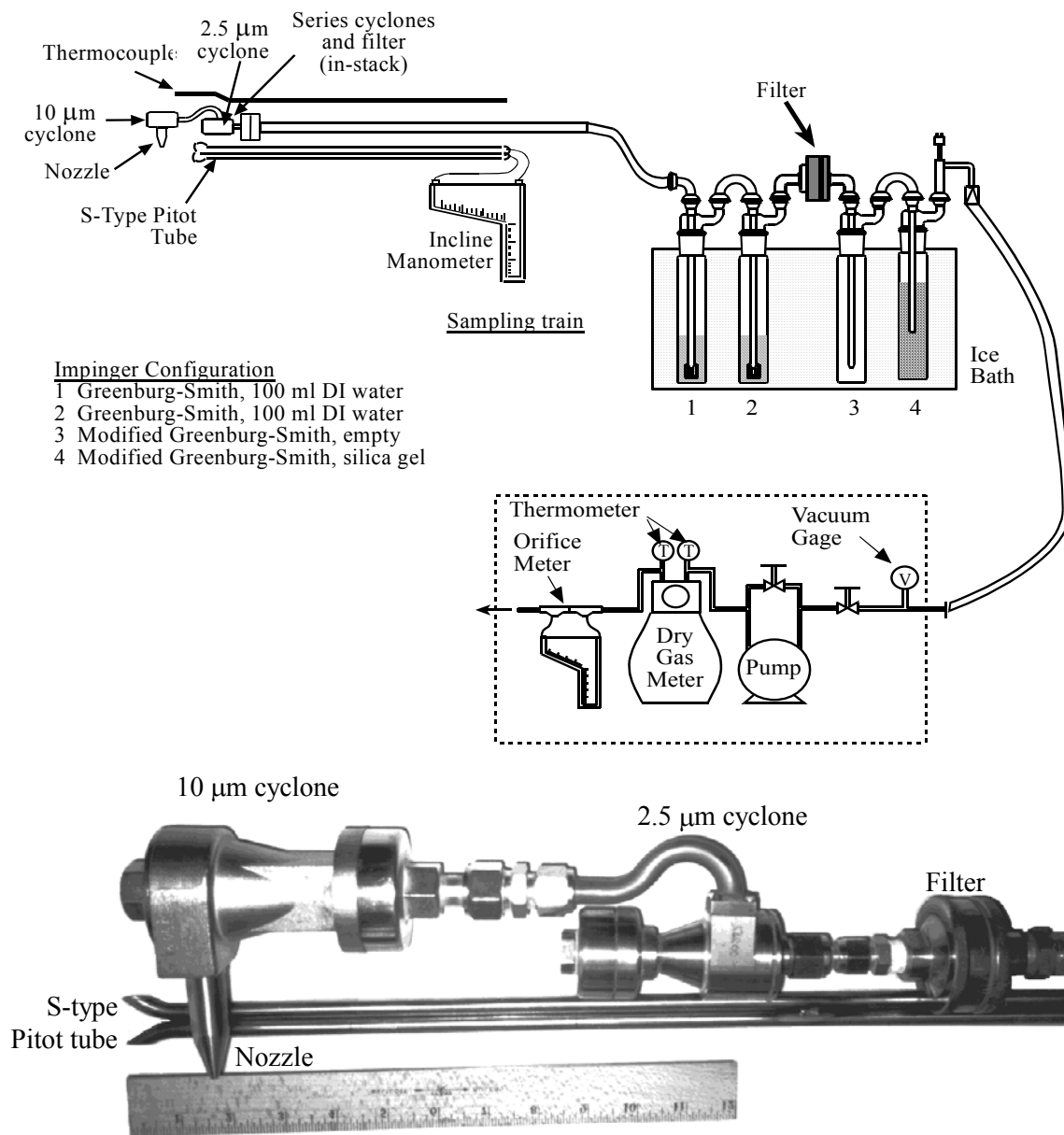


Figure 1-1. U.S. EPA Method PRE-004/202 Sampling Train.

immediately following the test. Method 202 recommends purging the impingers with nitrogen (air also is permitted by the method) for one hour immediately following sample collection. Method 202 provides the option of omitting the post-test purge if the pH of the impingers is above 4.5. The significance of the  $\text{SO}_2\text{-to-SO}_4^-$  artifact in the iced impinger methods is

documented in the literature for high SO<sub>2</sub> concentrations (DeWees et al, 1989; U.S. EPA, 1996; Filadelfia and McDannel, 1996). Earlier studies of systems having SO<sub>2</sub> levels of approximately 2000 parts per million (ppm) showed that the SO<sub>2</sub>-to-SO<sub>4</sub><sup>=</sup> artifact occurs in spite of post-test purging and that it can account for up to 42 percent of the measured CPM (Filadelfia and McDaniel, 1996).

Wien et al. (2001) evaluated the SO<sub>2</sub>-to-SO<sub>4</sub><sup>=</sup> artifact in the laboratory at low SO<sub>2</sub> concentrations typical of gas combustion by passing pure compressed gas mixtures with representative amounts of O<sub>2</sub>, carbon dioxide (CO<sub>2</sub>), nitrogen gas (N<sub>2</sub>), nitric oxide (NO) and SO<sub>2</sub> through two sets of paired Method 202 impinger trains. No particulate or condensable substances were added. Tests were performed for 1-hour and 6-hour sampling runs with mixtures containing 0, 1, and 10 ppm SO<sub>2</sub>. One pair of trains was purged with nitrogen for one hour immediately following the tests, while the other was not. The samples were stored at 4 degrees Celsius (°C) for approximately 2 weeks prior to analysis. Significant amounts of SO<sub>4</sub><sup>=</sup>, approximately proportional to the SO<sub>2</sub> concentration in the gas, were present in impingers regardless of the post-test purge. While the post-test purge clearly reduced SO<sub>4</sub><sup>=</sup> concentration in the impingers, significant SO<sub>4</sub><sup>=</sup> still remained. Purging was less efficient at reducing SO<sub>4</sub><sup>=</sup> for the 6-hour runs than for the 1-hour runs, indicating that much of the SO<sub>2</sub> oxidation occurs within this period. Wien compared the laboratory data to field results from a gas-fired refinery boiler using unpurged sample trains and concluded that approximately 50 to 100 percent of the SO<sub>4</sub><sup>=</sup> in the field samples, which comprised more than 80 percent of the CPM in that field test, could be attributed to the SO<sub>2</sub>-to-SO<sub>4</sub><sup>=</sup> artifact.

Chemical speciation of primary particles in total or in size fractions is essential information for conducting source apportionment analysis. The range of chemical speciation by traditional methods is limited, and the methods are quite different from those used to determine particle speciation in ambient air. For example, elements are frequently determined by methods similar to U.S. EPA Method 29, which captures elements on a Teflon impregnated quartz fiber filter and in aqueous impingers containing strong absorbing solutions. The samples are analyzed by a complex sample preparation and digestion procedure followed by injection into an inductively coupled argon plasma (ICAP) analyzer, sometimes using mass spectrometer detector for improved sensitivity and selectivity. The method is validated only for 12 elements, but others

are frequently determined by modifying the analytical protocol *ad hoc*. In contrast, ambient air samples for elemental analysis are simply collected on a Teflon membrane filter, which is subsequently placed directly into an X-ray fluorescence analyzer for determination of more than 40 elements. No studies directly comparing the two methods were found during an exhaustive literature search, however it is not too difficult to imagine that they might produce quite different results. Measurements of other substances have similar differences. For reliable source apportionment analysis, it is key to have comparability of methods for the source emission and ambient air measurements.

Thus, hot filter/iced impinger methods have significant limitations for determining PM<sub>10</sub> and PM<sub>2.5</sub> emissions from many types of stationary sources. These limitations provide incentive to develop other methods that are not subject to the SO<sub>2</sub> conversion and similar artifacts, and which have improved sensitivity for measuring low concentrations.

#### Formation of Aerosols and Sampling Conditions

Exhaust gases emitted from stationary or mobile sources cool as they mix with the atmosphere. As this natural dilution occurs, particles present at stack temperature tend to grow larger as agglomeration, coagulation and condensation/adsorption on the surface of existing particles occur (together these are referred to as accumulation mechanisms). Also, new particles may form through homogeneous and heterogeneous nucleation of vapor species. These processes, especially condensation and nucleation, are very sensitive to the time-temperature-concentration history of the gases, which can vary significantly with sampling conditions.

Depending on conditions, both accumulation and nucleation mechanisms may be evident in the size distributions of particles in combustion exhaust. For example, Figure 1-2 illustrates a snapshot in time of hypothetical particle size distribution in combustion exhaust with strong size modes characteristic of nucleation (typically 0.005 to 0.05  $\mu\text{m}$ ), accumulation (typically 0.05 to 1.0  $\mu\text{m}$ ). Most of the particles are in the nucleation mode, while most of the particle mass is accounted for by the accumulation and coarse modes. As the aerosol ages, the number of particles in the nucleation mode decreases due to accumulation, and particles in the accumulation size mode increase both in number and in size, while the overall mass both modes stays the

same. Thus, sampling conditions that affect these processes can be important depending on which size fractions are being studied.

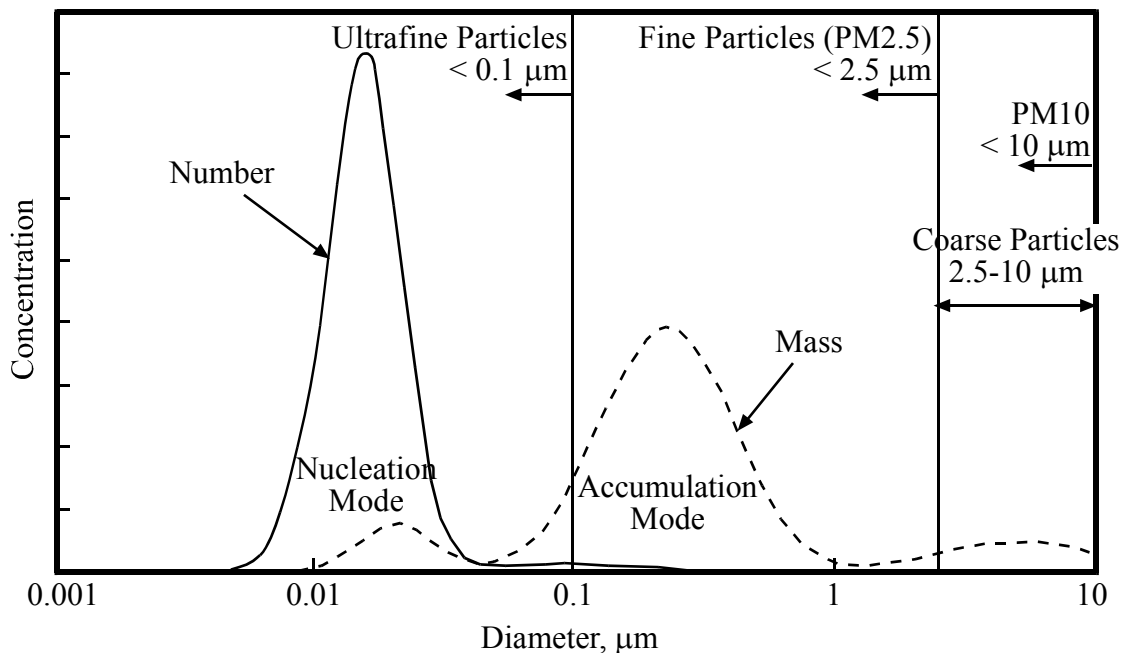


Figure 1-2. Typical Particle Size Distribution in Combustion Exhaust.

The saturation ratio (i.e., the ratio of the vapor pressure of a species to its saturated vapor pressure) is the driving force for condensation and nucleation. In the simplest systems, condensation occurs when the saturation ratio exceeds 1.0. Homogenous nucleation generally occurs at saturation ratios well above 1.0 (supersaturation), creating new nuclei that form ultrafine particles smaller than 50 nanometers (nm) (nanoparticles). This is most likely to occur in stationary source exhaust plumes when few existing particles are present, or when temperature quench rates are rapid creating high local saturation ratios (greater than approximately 3). Once formed, the particles continue to interact and grow through accumulation (agglomeration and coagulation), ultimately creating a distribution of particle sizes. Condensation also occurs on the surfaces existing particles, resulting in coarser particles, and may be suppressed by adsorption and absorption of condensable vapors on existing particles.

Figure 1-3 illustrates the theoretical variation in saturation ratio for a hot exhaust sample that is cooled with and without adiabatic dilution. The saturated vapor pressure of  $H_2SO_4$  in air was

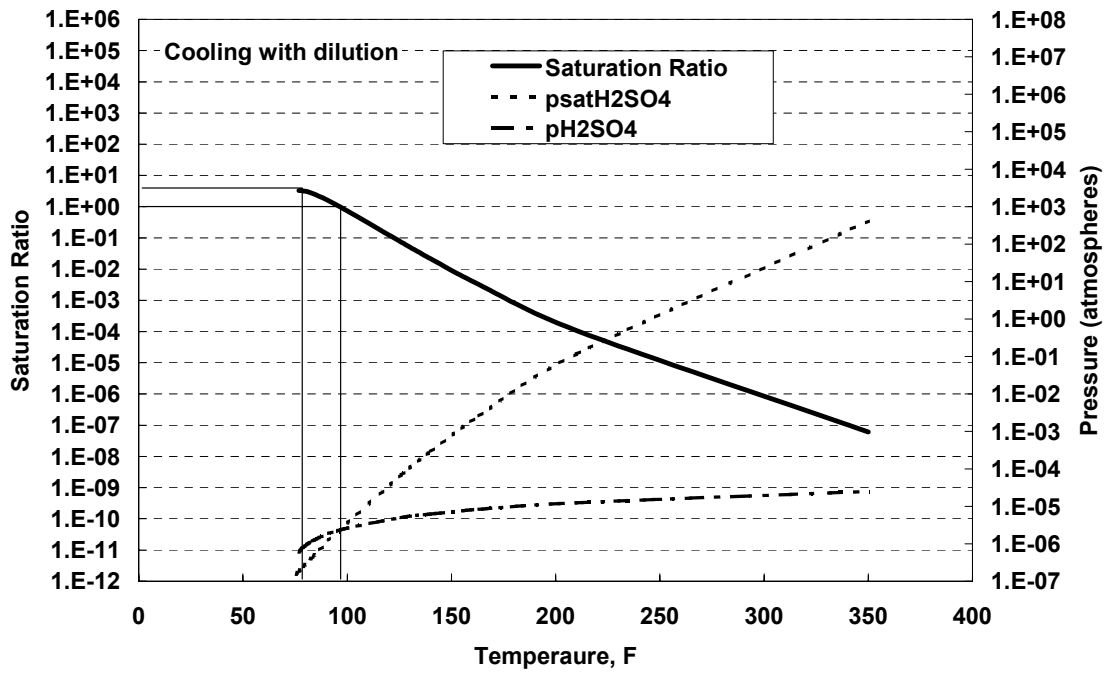
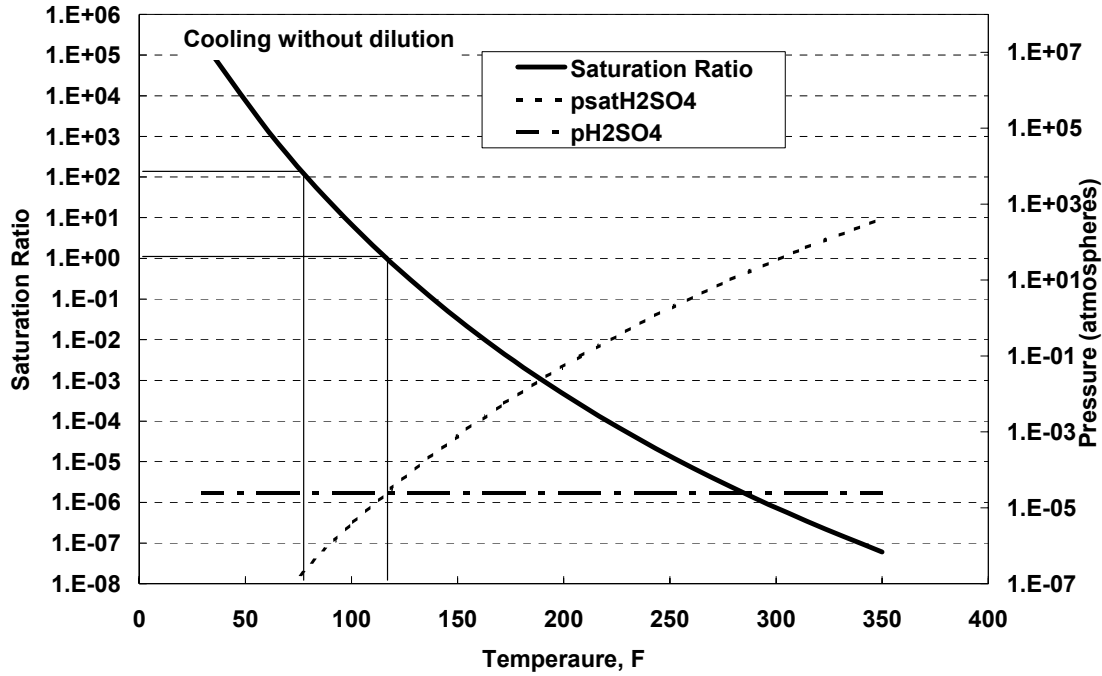


Figure 1-3. Theoretical effect of cooling with and without dilution on saturation ratio for 35 ppm H<sub>2</sub>SO<sub>4</sub> in air.

calculated using the empirical correlation developed by Kulmala and Laaksonen (1990) as a function of temperature, and compared to the partial pressure of H<sub>2</sub>SO<sub>4</sub> in a sample starting at 35 ppm H<sub>2</sub>SO<sub>4</sub> and 400 degrees Fahrenheit (°F). As temperature decreases in the undiluted sample,



the partial pressure of H<sub>2</sub>SO<sub>4</sub> remains constant, the saturated vapor pressure decreases, and thus the saturation ratio increases. As temperature decreases with increasing dilution in the diluted sample, the saturated vapor pressure follows the same relationship with temperature in the undiluted sample, but the partial pressure of H<sub>2</sub>SO<sub>4</sub> also decreases. Therefore, saturation ratio increases much less with decreasing temperature in the diluted case compared to the undiluted case. By the time the sample is diluted to near ambient temperatures (e.g., 75 °F), saturation ratio – the driving force for condensation – is approximately 100 times greater in the undiluted sample compared to the diluted sample. Saturation ratio of 1.0 is reached earlier – at higher temperature – in the undiluted sample. Further, if there are few existing particles or the temperature quench rate is rapid, the saturation ratio can rise significantly above 1.0 (supersaturation) and homogeneous nucleation becomes likely. The calculation shows that the amount of condensed material is likely to be much greater in an undiluted sample compared to that which occurs in diluted samples simulating real exhaust plumes. Therefore, collection of samples in iced impingers (without dilution) is highly unlikely to produce a representative sample of primary aerosols present in the stack plume.

### Dilution Sampling Methods

Dilution sampling methods are widely used to simulate the cooling and dilution processes that occur as combustion exhaust mixes with the atmosphere. Exhaust dilution sampling has been used as the regulatory reference method (e.g., International Organization for Standardization (ISO) 8178, 1996) for mobile source sampling. In contrast, it has been used only in research applications for stationary sources. In exhaust dilution sampling, a sample is extracted from the stack through probe and a heated sampling line, then mixed with a diluent gas, typically filtered ambient air. Mobile source methods do not require it, but the fully diluted sample subsequently may be aged to permit the particles to coagulate and grow by condensation prior to collection on filters for mass and chemical analysis, as they were in this project.

Dilution sampling offers several distinct advantages over iced impinger methods for representative collection of primary condensed aerosols. The sample can be extracted and cooled, without gas-to-particle conversion and excessive condensation sampling artifacts, to present a sample for collection that is representative of the exhaust plume immediately

downstream of the stack discharge. After diluting the sample to ambient temperature, ambient air sample collection and analysis methods can be applied which offers significantly improved comparability with ambient air measurements. A variety of different dilution sampler designs have been employed in recent research programs (England *et al.*, 1998), encompassing a range of sample-dilution air mixing rates, dilution ratios, residence times, materials, etc. Hildemann et al (1989) conservatively estimated an aging time of 80-90 seconds for organic species to condense on particles with dilution air ratios greater than 27. However, large dilution air ratios and long aging times require a large aging chamber that is impractical for the limited space available in many stack-testing situations. In addition, prolonged aging times may result in excessive diffusive wall losses for small particles.

Lipsky et al (2002) investigated how particle size distributions and mass emissions from a pilot-scale pulverized coal combustor changed by varying the dilution air ratio (15, 70, and 150) and aging time (0, 1.5, and 12 minutes). The results suggested that dilution air ratio and aging time did not change the total mass of particles emitted. Particle number decreased and particle size increased with longer aging times, consistent with coagulation theory. Higher number counts and smaller particle sizes were found for higher dilution air ratios over a given aging time, consistent with lower probabilities of particle collisions. The high ash content in coal provided a large surface area on which smaller particles could collide and gases could condense. The results may differ for other fuels and for combustion exhausts that do not produce an abundance of the primary particles typical of coal.

Kittleson et al. (1999) observed that in diesel engine exhaust the formation of nanoparticles is strongly dependent on dilution conditions – dilution ratio, dilution rate, humidity, temperature, relative concentration ratios of condensable and absorbing species - for short residence times (under 10 seconds). Hildemann (1989) recommended a minimum ratio of dilution air to sample of 20:1 and an aging time of 80 to 120 seconds for determining fine particle mass and species from oil- and gas-fired stationary sources. The Hildemann design recently was adopted, with a number of engineering improvements, by Desert Research Institute (DRI) for several recent studies (e.g., Watson et al., 2001; API, 2001a, 2001b, 2001c, 2002; Chow et al., 2003). It is this sampler that was used throughout this program to represent the benchmark Hildemann design, and is referred to at the “DRI design” throughout this report. The long residence time is a

distinguishing feature of the Hildemann design and considered essential for characterization of organic aerosols.

Dilution sampling technology was selected as the basis for the new test method developed under this program because:

- It is widely accepted in the scientific literature for assessing source contributions to ambient PM<sub>2.5</sub>;
- For decades it has been the internationally-accepted regulatory reference test method for mobile reciprocating internal combustion engines;
- It offers measurements free from significant artifacts associated with current stationary source particulate test methods;
- It provides conditions that are nearly identical to important conditions in the stack plume that control PM<sub>2.5</sub> entering the atmosphere, providing a more representative measurement for purposes of PM<sub>2.5</sub> source apportionment and human health risk assessments;
- Compared to current stationary source test methods based on hot filters and impingers, it enables a broader range of chemical and physical characterization and better comparability to ambient PM<sub>2.5</sub> measurements through the application of ambient air sample collection and analysis methods.

In particular, the Hildemann dilution sampler concept was selected because of its most unique design feature – a long residence time for aging the aerosol after dilution - for characterizing organic aerosols. While the Hildemann design has been successfully applied to a limited number of stationary sources, its large physical size and weight make it impractical for the limited space and access available for most stationary source testing situations. Although a variety of designs have been developed for specific applications, the limiting design parameters and operating conditions of dilution samplers - e.g., mixing rate, residence time, dilution ratio, geometry, humidity, etc. – needed to produce representative samples for different fuels and stationary processes are not well established. Hence, a new dilution sampler was designed and tested that addressed the shortcomings of the Hildemann research instrument.

## 2. DILUTION SAMPLER CHARACTERIZATION APPROACH AND METHODS

### TEST OBJECTIVES

The Hildemann dilution sampler design and its derivatives have been successfully applied to several stationary sources; however, improvements need to address the following limitations before the technology can be widely applied:

- Large physical size and weight, which precludes application on many stationary sources due to a lack of sufficiently large or robust sampling platforms on the exhaust stack;
- Costly and time-consuming to setup and operate at stationary source sites;
- Losses of particles within the sampler that are difficult and time consuming to recover.
- Complex operation requiring highly skilled and experienced personnel.

Therefore, the overall goal of the pilot-scale evaluation was to experimentally understand and quantify design criteria for a more compact and easier-to-use dilution sampler that preserves key PM<sub>2.5</sub> characteristics. Also, supplementary tests and engineering analysis were undertaken to understand the characteristics of the Hildemann dilution tunnel performance to aid in interpreting pilot-scale test results.

The specific objectives of these tests were:

- Quantify PM<sub>2.5</sub> mass and ultrafine particle number size distributions via dilution sampling in combustion products of natural gas, No. 6 fuel oil and coal;
- Determine effect of residence time and dilution ratio on PM<sub>2.5</sub> mass and ultrafine particle number distributions over the range of 10:1 to 50:1 dilution and 2 to 80 seconds residence time;
- Determine the minimum residence time and dilution ratio for stable mass and size distributions for different exhaust conditions and matrices.
- Determine the effect of stack temperature on PM<sub>2.5</sub> mass.

- Evaluate particle losses in the dilution sampler over a range of solid and condensable particle concentrations.

## PILOT-SCALE COMBUSTOR

A pilot-scale combustion rig (Figure 2-1) was used to generate a range of exhaust gas matrices and conditions for evaluating dilution sampling parameters. The Fuels Evaluation Facility (FEF) is a vertically down-fired research combustor designed for a nominal fuel heat input of 234 kilowatts (kW). The design simulates flame conditions, furnace gas composition, and residence time-temperature profile found in full-scale boilers from the furnace through the exit of the radiant heat transfer sections. A multi-fuel, variable swirl burner is located at the top of the down-fired furnace. The cylindrical furnace section is constructed of six modular refractory-lined sections with an inside diameter of 56 centimeters and has numerous ports for cooling panels and sampling probes. The exhaust from the furnace passes through a refractory lined convection section with air-cooled tubes that simulate radiant superheater tube sections in a

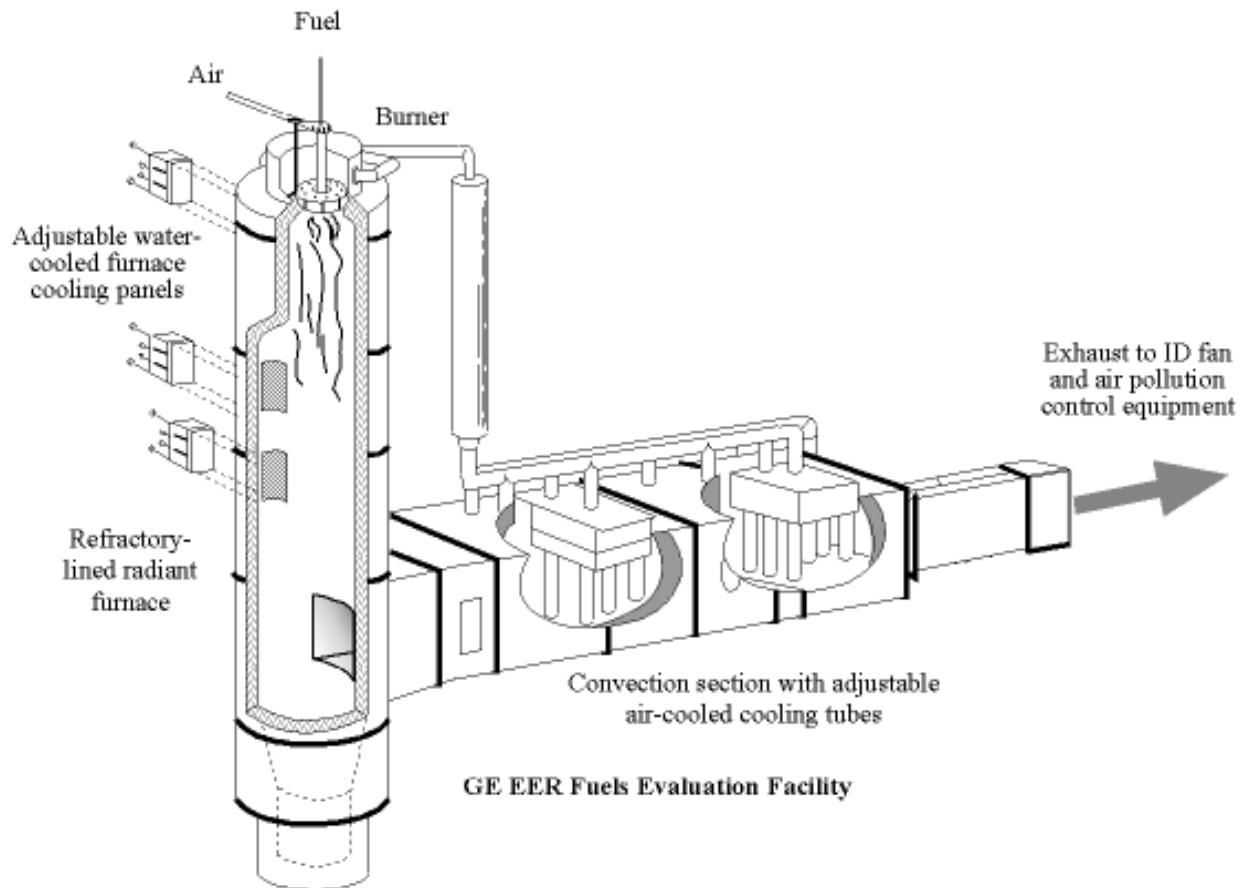


Figure 2-1. Pilot-Scale Combustion Facility.

typical large boiler. The configuration of cooling panels in the furnace and tube sections in the convection section can be varied to adjust time-temperature profile.

The flue gases leaving the FEF convection section passed through an air-cooled stainless steel cooling and sampling section, designed for these tests, for final trim of the exhaust temperature and measurement access (Figure 2-2). After an air-cooled shell section, the flue gases then continue through an un-cooled stainless steel section containing numerous sample ports for measurements before exhausting to atmosphere via a fabric filter for particulate emissions control. For these tests, the furnace was operated at a fuel firing rate of approximately 160 kW to achieve target flue gas temperature conditions at the sampling locations. Firing rate, excess oxygen and heat transfer panels were adjusted slightly to achieve the target exhaust temperatures.

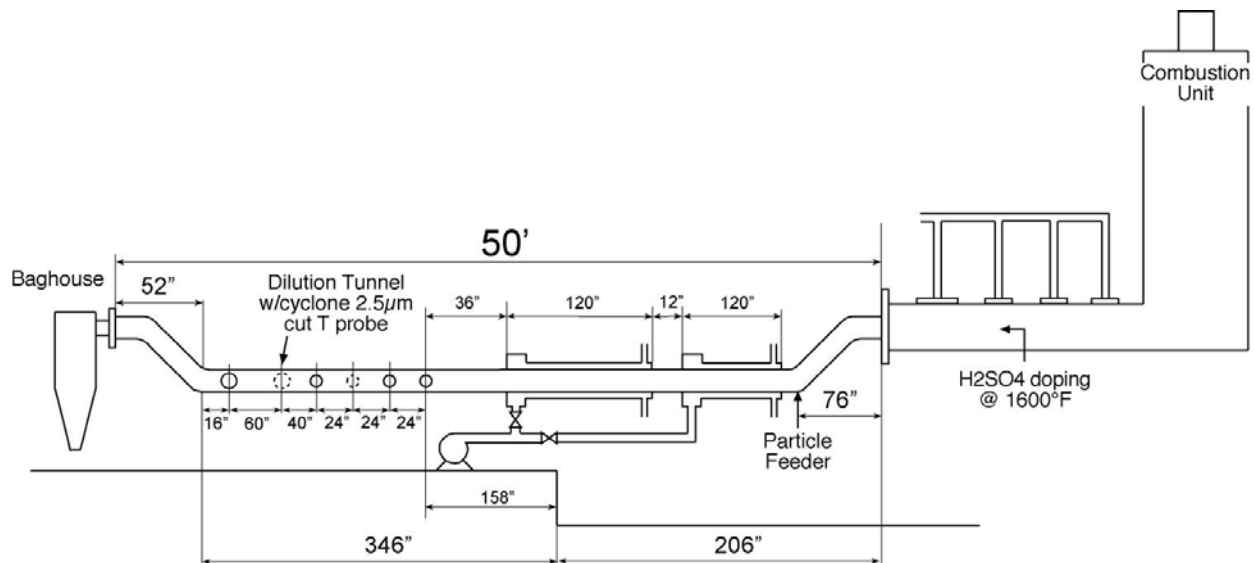


Figure 2-2. FEF exhaust cooling and sampling section.

For selected tests, dilute  $H_2SO_4$  was injected via a spray atomizer into the convection section at a gas temperature of approximately  $870\text{ }^\circ\text{C}$  to produce a known amount of condensable vapor in the flue gas downstream. This injection temperature was chosen because it is high enough to ensure that  $H_2SO_4$  decomposes to sulfur trioxide ( $SO_3$ ), but below the temperature at which  $SO_2$  formation would occur, and high enough to ensure that the spray evaporates and mixes completely before the flue gas reaches the sampling location. The  $H_2SO_4$  solution was metered

using a variable speed pump and the reservoir was weighed before and after each test to determine the average flow rate.

A series of tests on natural gas also was planned to simulate known solid particle loading in the furnace by injecting of solid zinc oxide (ZnO) powder into the furnace just downstream of the exit of the refractory convection section. The dry feeding system consisted of an Acrison variable speed screw feeder to meter the powder, a cyclone particle separator to remove particles larger than 2.5  $\mu\text{m}$  and a pneumatic conveying line. However, the system could not maintain a stable feed rate due to the fineness of the powder. The problem was traced to the cyclone separator. Based on the manufacturers specifications, the geometric mean particle size of the powder was 2.0  $\mu\text{m}$ . This was considered close enough to the desired size, so the cyclone separator was removed from the system. Reasonably stable powder flow rates were achieved with this configuration.

## FUELS

Tests were conducted with three fuels: natural gas, No. 6 Fuel Oil, and Kitanning Coal (Table 2-1). Natural gas was typical pipeline gas from the Southern California region. The No. 6 fuel oil is a high sulfur residual oil. Kitanning Coal is a medium sulfur bituminous coal from the western Appalachian region.

## TEST MATRIX

The tests were conducted in 3 phases:

- Phase 1 – Initial Assessment. Phase 1 was designed to collect data and assess the feasibility of using the scanning mobility particle sizer (SMPS) to determine aerosol characteristics. The DRI dilution sampler was used throughout this phase.
- Phase 2 – Detailed Assessment. Phase 2 continued the assessment test matrix after a pause to analyze Phase 1 samples, review results and validate the experimental approach. The DRI dilution sampler was used throughout this phase.
- Phase 3 – Comparison Tests. Tests comparing results obtained with the DRI and new compact dilution samplers were conducted in Phase 3.

Table 2-1. Fuel Characteristics for Pilot-Scale Tests.

Parameter	Units	Kittanning coal	No. 6 fuel oil	Natural Gas
Gross Heating Value	Btu/scf	--	--	1,020
Gross Heating Value	Btu/lb	12,390	18,236	23,331
C	% wt.	72.4	85.4	72.8
H	% wt.	4.2	10.47	23.6
N	% wt.	1.21	0.56	0.9
S	% wt.	1.22	1.53	0.0003
O	% wt.	7.02	1.35	2.6
Ash	% wt.	10.85	0.04	--
Moisture	% wt.	3.1	0.65	0
Volatile Matter	% wt.	29.07	--	--
Fixed Carbon	% wt.	56.98	--	--
Specific Gravity	vol/vol	--	0.9974	0.586
API Gravity	degrees	--	10.4	--
Hydrogen sulfide (as S)	grains/100scf	--	--	0.01
Mercaptans (as S)	grains/100scf	--	--	0.04
Total sulfur (as S)	grains/100scf	--	--	0.08
N <sub>2</sub>	% mol	--	--	0.55
O <sub>2</sub>	% mol	--	--	0.15
CO <sub>2</sub>	% mol	--	--	1.25
CH <sub>4</sub>	% mol	--	--	95.41
C <sub>2</sub> H <sub>6</sub>	% mol	--	--	2.12
C <sub>3</sub> H <sub>8</sub>	% mol	--	--	0.39
I-C <sub>4</sub> H <sub>10</sub>	% mol	--	--	0.04
n-C <sub>4</sub> H <sub>10</sub>	% mol	--	--	0.06
I-C <sub>5</sub> H <sub>12</sub>	% mol	--	--	0.01
n-C <sub>5</sub> H <sub>12</sub>	% mol	--	--	0.01
C <sub>6</sub> +	% mol	--	--	0.01
Total	% mol	--	--	100
Ash Elemental Analysis				
SiO <sub>2</sub>	% wt.	57.81	42.1	--
Al <sub>2</sub> O <sub>3</sub>	% wt.	26.38	10.5	--
TiO <sub>2</sub>	% wt.	1.33	--	--
Fe <sub>2</sub> O <sub>3</sub>	% wt.	7.38	4.1	--
CaO	% wt.	1.47	27.3	--
MgO	% wt.	0.62	8.6	--
K <sub>2</sub> O	% wt.	2.81	2.7	--
Na <sub>2</sub> O	% wt.	0.33	3.2	--
SO <sub>3</sub>	% wt.	0.61	0.8	--
P <sub>2</sub> O <sub>5</sub>	% wt.	0.4	0.5	--
SrO	% wt.	0.2	--	--
BaO	% wt.	0	--	--
Mn <sub>3</sub> O <sub>4</sub>	% wt.	0	--	--
V <sub>2</sub> O <sub>5</sub>	% wt.	--	0.2	--
Undetermined	% wt.	0.66	--	--



## Phases 1 and 2 Tests – Design Development

The tests included controlled variation of exhaust gas conditions and dilution sampler operation while making measurements and collecting samples from various locations to characterize aerosols in the dilution sampler. The overall experimental approach was to evaluate the effect of dilution conditions on aerosol size, mass and composition for a range of solid and condensable particulate concentrations (Table 2-2). Tests were performed with natural gas, a high sulfur No. 6 fuel oil, and an Appalachian medium sulfur bituminous coal (Kitanning seam). The furnace was operated with a nominal heat input rate of 160 kW and 3 percent excess oxygen. Selected tests with natural gas combustion and H<sub>2</sub>SO<sub>4</sub> doping were performed to establish elevated condensable aerosol concentrations in the absence of solid particles. Tests were conducted at two nominal flue gas temperatures, 450±10 Kelvin (K) and 645±10 K, by adjusting the FEF cooling sections and firing rate.

Table 2-2. Phase 1 and 2 Test Matrix.

Dilution Ratio		10:1			20:1,30:1	50:1		
Residence Time		2 sec (L1)	10 sec (L3)	80 sec (L4)	80 sec (L4)	2 sec (L2)	10 sec (L3)	80 sec (L4)
Natural Gas	450 K	A,B,C,D	A,B,C,D,E	A,B,C,D,E,G	E	A,B,C,D,E	A,B,C,D,E	A,B,C,D,E,G
	645 K	E	E	E		--	--	--
Natural Gas + H <sub>2</sub> SO <sub>4</sub>	450 K	E	E	E		E	E	E
	645 K	--	--	--		--	--	--
Natural Gas + ZnO	450 K			E				
	645 K							
Coal	450 K	A,B,C,D,E	A,B,C,D,E	A,B,C,D,E,G		A,B,C,D,E	A,B,C,D,E	A,B,C,D,E,G,H
	645 K	E	E	E,G		E	E	E,G,H
No. 6 Fuel Oil	450 K	A,B,C,D	A,B,C,D	A,B,C,D,E,G		A,B,C,D,E	A,B,C,D,E	A,B,C,D,E
	650 K					E	E	E,G,H

A - TMF/Gravimetric (mass concentration)

B - TMF/XRF (Element mass concentrations)

C - QFF/IC (Ion mass concentrations)

D - QFF/TOR (OC/EC mass concentrations)

E - SMPS (Size, number concentration)

F - MOUDI (Size, mass concentration)

G - MOUDI/XRF (Size, mass concentration, element mass concentrations)

H - Laser photometer (volume concentration)

Residence time is one of the factors most influencing the physical size of the dilution sampler. Hildemann previously defined the residence time necessary for particle condensational growth to be 80-90 seconds (Hildemann et al., 1989). To explore the sensitivity of measurements to

residence time, aerosol characteristics at locations in the dilution sampler corresponding to residence times of 2, 10 and 80 seconds were evaluated. Dilution air ratios were varied from 10:1 to 50:1. Sample flow rate was held constant while the dilution air flow rate was varied.

### Phase 3 Tests – Design Validation

The results of the Phase 1 and 2 tests were used to design and construct a new bench prototype dilution sampler. The goals of Phase 3 was to characterize the new sampler to determine if the design performance specifications were met, and to compare results obtained with the new and old samplers. The key objectives of the sampler characterization were:

- Determine the effectiveness of the rapid mixing design in achieving complete mixing between the dilution air and the sample prior to aging;
- Quantify particle losses in the various sections of the new sampler over a range of solid and condensable particle concentrations;
- Compare results obtained with the new sampler, the original DRI sampler and traditional EPA methods for a range of solid and condensable particle concentrations.

These tests were conducted in August 2002. The overall scope of the Phase 3 tests is summarized in Table 2-3. Tests were conducted firing natural gas, No. 6 oil, and natural gas doped with H<sub>2</sub>SO<sub>4</sub>. Measurements of filterable and condensable particulate matter using traditional hot filter/iced impinger methods (EPA Methods PRE-4 and 202) were made in the exhaust duct approximately two feet downstream of the dilution sampler. Flue gas temperature at dilution sampler location was maintained at 350±20 °F throughout the tests. Diluted exhaust was sampled with filter packs for particulate mass, elements, ions, organic carbon (OC) and elemental carbon (EC).

## MEASUREMENTS

### DRI Dilution Sampler

The DRI dilution sampler (Figure 2-3) was used to collect the flue gas samples. The sample was mixed with the dilution air in a 15-centimeter (cm) diameter tunnel that is U-shaped. A high-

volume blower located at the exit of the tunnel was used to draw the dilution air and sample through the tunnel. The high-volume blower speed and the dilution air slide gate at the entrance of the dilution tunnel were adjusted to set the target sample flow rate and dilution air ratio. At the end of the tunnel, a portion of the diluted sample was extracted into a chamber that provides additional residence time for sample aging. The aged sample was withdrawn through ports at the exit of the chamber.

Table 2-3. Phase 3 Test Matrix

Test Objectives	Type of test	Particle losses	Mixing		Condensable H2SO4			#6 heating oil	Operator
		Tunnel Characterization	Ambient	#6 heating oil	Tunnel Blank	Gas Fired + H2SO4	Tunnel Blank		
Numbers of tests			2	2	1	5	1	3	
Days needed		2	2	2	1	3	1	2	
Flue Gas / FEF condition	Flue Gas Temp (F)	Ambient/CO	350	350	350	350	350	350	FEF
	Excess O2 (%)	Ambient/CO	3	3	3	3	3	3	FEF
	Dilution Ratio of X		20-25	20-25	20-25	20-25	20-25	20-25	Oliver
	H2SO4 Feeding concentration					30 ppm			FEF
	Other factors								FEF
	Manual Method		M201A/202	M201A/202		CCS		M201A/202	Bob Z.
Time Integrated	47 mm PTFE at 10 sec	No	No	No					Oliver
	47 mm Quartz, 10 sec	No	No	No					Oliver
Physicochemical analysis	Gravimetric on 47 mm PTFE filters	No	No	No					DRI
	XRF on 47 mm PTFE filters	No	No	No					DRI
	IC, EC/OC on 47 mm Quartz filters	No	No	No					DRI
Semi Continuous Monitor	CLIMET at Ambient				No	No	No	No	Oliver
	CLIMET at 2 sec				No	No	No	No	Oliver
	CLIMET at 10 sec				No	No	No	No	Oliver
	DRI dilution sampler							Yes	TBD
	Sample collection interval	N.A.	6	6	6	2-3	6	2	Oliver
	Tunnel Cleaning/ FEF shakedown time (day)	No	No	No	No	Yes	No	No	

The dilution sampler drew the flue gas sample at a rate of approximately 25 liters per minute (L/min) from the center of the 6-inch diameter horizontal exhaust section through an in-situ cyclone ( $d_{50}=2.5 \mu\text{m}$ ) attached to a 316 stainless steel probe. The sample flow rate through the probe was monitored using a venturi flow meter. The venturi velocity head was measured with a diaphragm gauge (Dwyer Magnahelic®) and the venturi temperature was measured with a thermocouple. The pressure drop across a calibrated orifice in the high-volume blower housing, determined using a differential pressure transducer, was measured to determine the diluted sample flow leaving the system. The thermocouples and pressure transducers were connected to a laptop computer data acquisition system. Dilution ratio was calculated using the sample venturi flow rate, high-volume blower flow rate, and sample collection media flow rate, defined as follows:

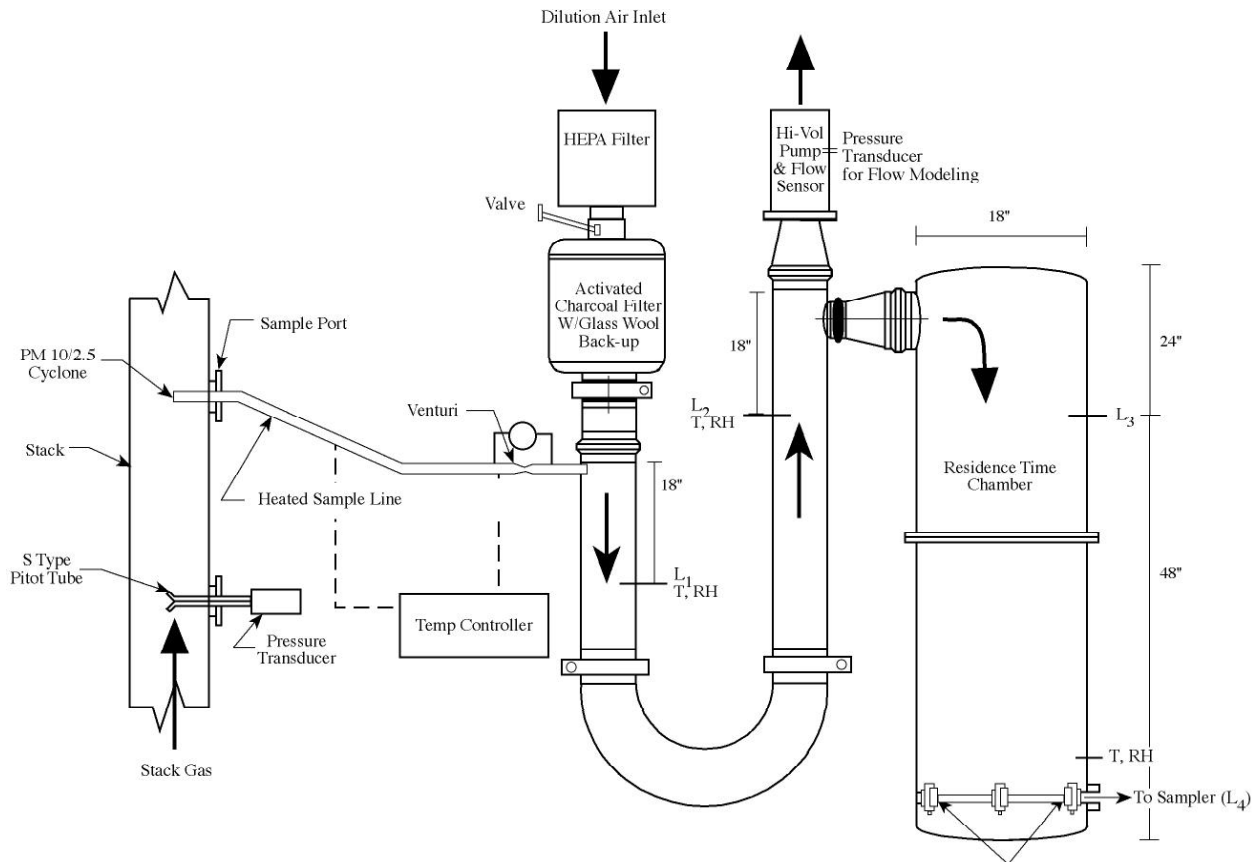


Figure 2-3. DRI Dilution Sampler Setup and the Sampling Locations Corresponding to Different Residence Times in the Sampler.

$$DilutionRatio = \frac{(Q_{HiVolPump} + Q_{SampleMedia}) - Q_{Sample}}{Q_{Sample}}$$

The bulk mean gas residence time at the exit of the residence time chamber (L4 in Figure 2-3) under the conditions of these tests was constant at approximately 80 seconds. Additional sampling ports were installed in the upper portion of the residence time chamber (L3) and in the dilution tunnel (L1 and L2) to enable access at points corresponding to 2 and 10 seconds bulk mean gas residence time. Diluted samples were extracted from a single point at each cross-sectional plane. At 10:1 dilution ratio, locations L1, L2, and L4 correspond to 2, 10 and 80 seconds residence time, respectively. At 50:1 dilution ratio, locations L2, L3, L4 correspond to 2, 10 and 80 seconds residence time, respectively. Note, the bypass flow rate through the Hi-Vol pump varies with dilution ratio while the flow rate through the residence time chamber stays constant with sample media flow rate.

## GE Energy and Environmental Research Corporation (GE EER) Dilution Sampler

Figure 2-4 shows a schematic arrangement of the GE EER sampler. The key design differences compared to the DRI sampler are:

- The heated sample transfer line between the probe and venturi was removed;
- The mixing section was shortened by adding a mixing plate to produce more rapid mixing between the dilution air and the sample gas;
- The size of the residence time chamber was reduced by reducing bulk mean gas residence time to approximately 10 to 15 seconds and reducing the sample flow rate through the aging section; and
- The sample path through the dilution sampler is linear rather than convoluted to minimize inertial particle losses in the system and facilitate traversing from conventional stack monorails.

Key design specifications of the DRI and GE EER samplers are compared in Table 2-4.

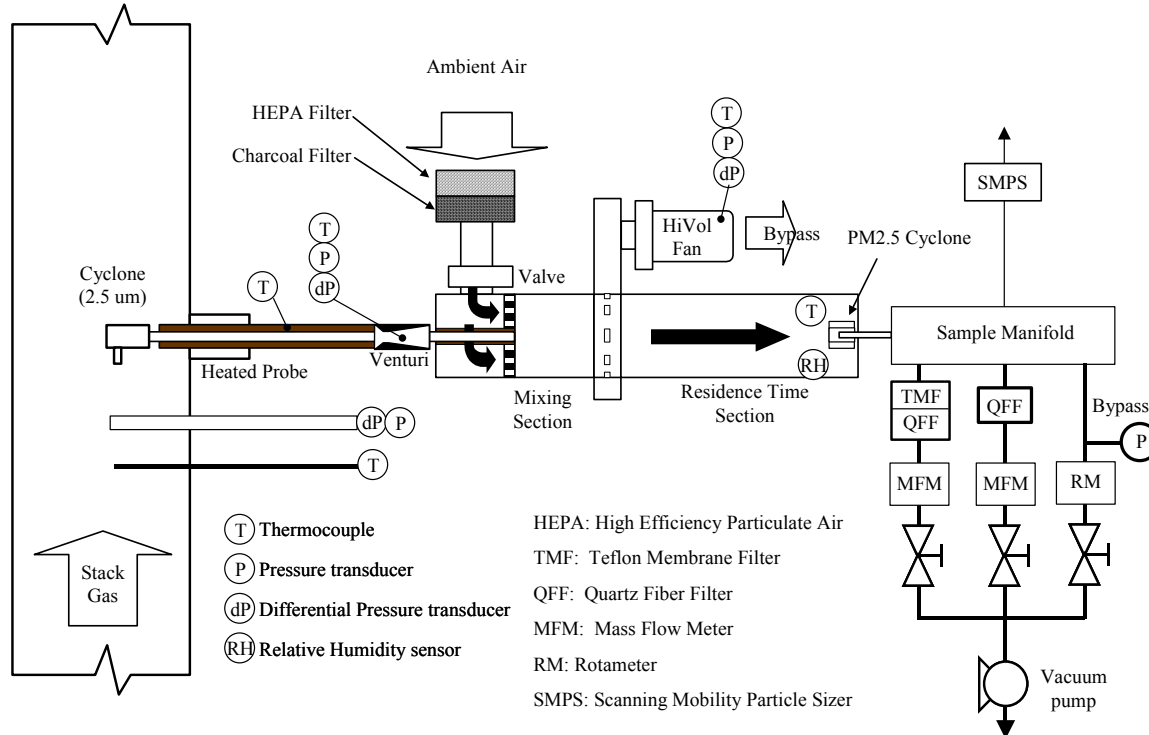


Figure 2-4. Compact (GE EER) Dilution Sampler.

Table 2-4. Design Specification Comparison for DRI and GE EER Dilution Samplers

Parameter	DRI Design	EER Design
Raw Sample Flow Rate	25 L/min	25 L/min
Dilution ratio (nominal)	40:1	20:1
Dilution ratio (range)	25:1 to 50:1	10:1 to 40:1
Mixing Section diameter	15 cm	20 cm
Effective mixing length	18 diameters	1.4 diameters
Mixing section type	1-step, single cross-jet	1-step, multiple parallel jets
Mixing section Reynolds number*	9,000	6000
Bypass prior to aging*	799 L/min	412 L/min
Aging section diameter	46 cm	20 cm
Aging Section Flow Rate*	226 L/min	113 L/min
Aging section residence time*	80 sec	10 sec
Aging section Reynolds number*	1000	800
PM2.5 cyclone after aging	Yes	Yes
Materials	Stainless steel	Stainless steel
Relative Humidity	Uncontrolled**	Uncontrolled**
Sample Temperature	Ambient + (<~10 °C)	Ambient + (<~10 °C)
Sample Flowmeter	Venturi	Venturi

\*At nominal dilution ratio.

\*\*Provided that relative humidity of diluted sample is less than 70 percent.

### Sample Collection Methods

Various media were used to collect samples from the dilution sampler (Table 2-5). At each residence time sampling port, a total of 30 L/min was drawn through a 3/8-inch tube and split to two parallel 47millimeter (mm) filter holders (one pre-weighed polytetrafluoroethylene (PTFE) filter and one pre-baked 47mm quartz filter) at 15 L/min each. The two filters were sampled for 2-6 hours, depending on the nature of test and fuel type, to obtain sufficient filter loading for analysis. Samples were subsequently analyzed for mass, elements, ions and/or carbon, depending on the test. The filter results were paired and normalized to determine particle growth and potential particle losses in dilution sampler.

A laser photometer (DustTrak model 8520, Thermo Scientific Incorporated (TSI)) and was used to provide a real-time indication of particle concentration to minimize run times for acceptable filter loadings. The laser photometer employs a laser diode directed at a sample stream. Light scattered at 90° to the light beam is measured with a photodetector. The intensity of the scattered light is a function of the particle size and mass concentration, but ignoring the particle size effect provides a qualitative indication of particle mass. Samples for the laser photometer were

extracted at 1.7 L/min through a cyclone ( $d_{50}=2.5 \mu\text{m}$ ) connected to the 80 second residence time sampling port at the residence time chamber outlet with a four foot length of 9.5 mm plastic tubing. The data displayed on the instrument readout were manually recorded during the test.

Table 2-5. Sample Collection Media, Analysis, and Location.

Sample collection	Sample analysis
Quartz filters	TOR (EC and OC) IC (nitrate, ammonia, chloride)
47mm PTFE filters	Gravimetric (mass concentration) XRF (metals and elements)
Scanning Mobility Particle Sizer (SMPS)	Ultrafine (0.01-0.4 $\mu\text{m}$ ) particle size distribution
Laser photometer	Particle concentration
Micro-Orifice Uniform Deposit Impactor	Size segregated mass, elements and metals in size range <0.32, 0.32-2.5 $\mu\text{m}$
Optical Particle Counter	Particle number concentration in 16 size bins between 0.3 and >10 $\mu\text{m}$

An SMPS was used for characterizing particle number distribution over the 0.01-0.4  $\mu\text{m}$  size range. The SMPS consisted of two components: a TSI Model 3071 differential mobility analyzer (DMA), which classifies particles according to size; and a TSI Model 3025 condensation particle counter (CPC), which counts particles leaving the DMA. The DMA included a radioactive Kr-85 charge neutralizer, which produces bipolar ions that apply an equilibrium charge distribution to the aerosol. The DMA extracts particles according to their electrical mobility, which is inversely related to particle size. The classified particles entered the CPC, where supersaturated butyl alcohol vapor condensed onto the particles, causing them to grow larger. The particles were detected and counted by a simple diode laser light source and photodetector. By continuously varying the electrical field in the DMA, the particle size leaving the DMA was varied in a known manner enabling the particle size distribution to be determined. SMPS samples were withdrawn from the dilution sampler at 5-minute average intervals from each sampling locations. The SMPS measurements were repeated several times for each test and the average results were calculated for each test condition. To minimize the effect of temporal changes, the SMPS samples were performed sequentially at the three sampling locations, then repeat tests were performed by going back to the previous locations. The effects of residence

time were evaluated by comparing results at consecutive sampling locations, evaluating whether the observed effect was consistent among the repeat tests, and then averaging the results of the repeat tests. Several replicate measurements were made at each dilution ratio and residence time. Some tests were as long as 6 hours. The SMPS results were reduced using an inversion routine and are expressed as  $dN/d(\log dp)$  as a function of  $dp$  for each series of measurements, where  $N$  is the number concentration and  $dp$  is the electrical mobility diameter

A modified Micro-Orifice Uniform Deposit Impactor (MOUDI; Marple, 1991) with stages for particles smaller than  $0.32 \mu\text{m}$  and  $0.32$  to  $2.5 \mu\text{m}$  at  $30 \text{ L/min}$  sampling rate was used at the outlet of dilution sampler (corresponding to 80 seconds residence time) to characterize particles less than  $0.32 \mu\text{m}$  and in accumulation modes ( $0.32$ - $2.5 \mu\text{m}$ ) for mass and elements.

Aerosol size and concentration at different locations within the new dilution sampler was measured to evaluate mixing uniformity and particle losses. An optical particle counter (Model SPECTRO 0.3, CLIMET Instruments, Redlands, CA) was used to measure aerosol size and concentration in 16 size bins between  $0.3$  to  $>10 \mu\text{m}$ . The optical particle counter determines the size of a sampled particle by the quantity of monochromatic light scattered and focused onto a photodetector using a system of mirrors. The light source is a laser diode. Since the amount of light scattered from a particle is a strong function of its size, precise and repeatable sizing of particles is possible. Particle concentrations are kept low enough within the measuring volume of the instrument to ensure only one particle is measured at a time. The optical particle counter sampled at  $1 \text{ L/min}$ . The instrument also measured sample temperature and relative humidity. Radial traverses were conducted through a cross-sectional plane located between the mixing and residence time sections in the new dilution sampler (see Figure 2-4). Several replicate measurements were made each traverse point.



### 3. DESIGN DEVELOPMENT TEST RESULTS

#### DILUTION SAMPLER FLOW FIELD CHARACTERIZATION

To determine if measurements at the different sampling locations in the dilution sampler are comparable, the degree of mixing between the flue gas sample with dilution air was characterized. Methane ( $\text{CH}_4$ ) was doped into the probe and  $\text{CH}_4$  concentration profile measured at L1, L2 and L3.  $\text{CH}_4$  concentration was measured using a sample probe, pump and non-dispersive infrared analyzer.  $\text{CH}_4$  concentration profiles at L1 (i.e., mean residence time of 2 second at dilution air ratio of 10:1) show that the sample and dilution air were not fully mixed at this point. For overall dilution ratio of 50:1, the  $\text{CH}_4$  concentration is highest on the probe side of the tunnel, and decreases towards the opposite wall (Figure 3-1). The opposite profile was observed for overall dilution ratio of 10:1. The unmixedness indicates that the local dilution ratio at L1 ranges from approximately 6 to 13 for 10:1 overall dilution, with the local dilution ratio matching the overall dilution ratio at a point slightly off-center in the tunnel. The local residence time is much more difficult to estimate. The flat  $\text{CH}_4$  concentration profiles measured at L2 (i.e., residence time of 10 seconds for dilution air ratio of 10:1 and 2 seconds for dilution ratio of 50:1) indicate the sample and dilution air are fully mixed by this point.

The geometry of the dilution sampler and experimental flow characterization tests suggest that samples taken from a single point at L1, L2 and L3 may not be representative of the entire flow at that point under all conditions. Subsequent to the experiments described later in this section of the report, the characteristics of the flow field in the sampler were evaluated using a computational fluid dynamics (CFD) model of the sampler. Figure 3-2 shows the dilution sampler geometry and reference points used in the CFD model. Temperature, velocity, and gas concentration profiles were calculated for dilution ratios of 10:1 and 50:1. Using the temperature field as an indication of gas mixing, results show that mixing is incomplete at L1 but substantially complete by the end of the tunnel section at L2 (Figure 3-3). The temperature profile also shows that the incoming sample jet impinges on the far wall of the tunnel at 10:1 dilution ratio. Similarly, at 50:1 dilution ratio the sample jet is deflected to the near wall of the tunnel. Examining the velocity profiles (Figure 3-4) reveals that this is due to the relative

velocity of the incoming sample jet and the dilution air. The concentration and velocity profiles are consistent with the CH<sub>4</sub> concentration profiles presented in Figure 3-1.

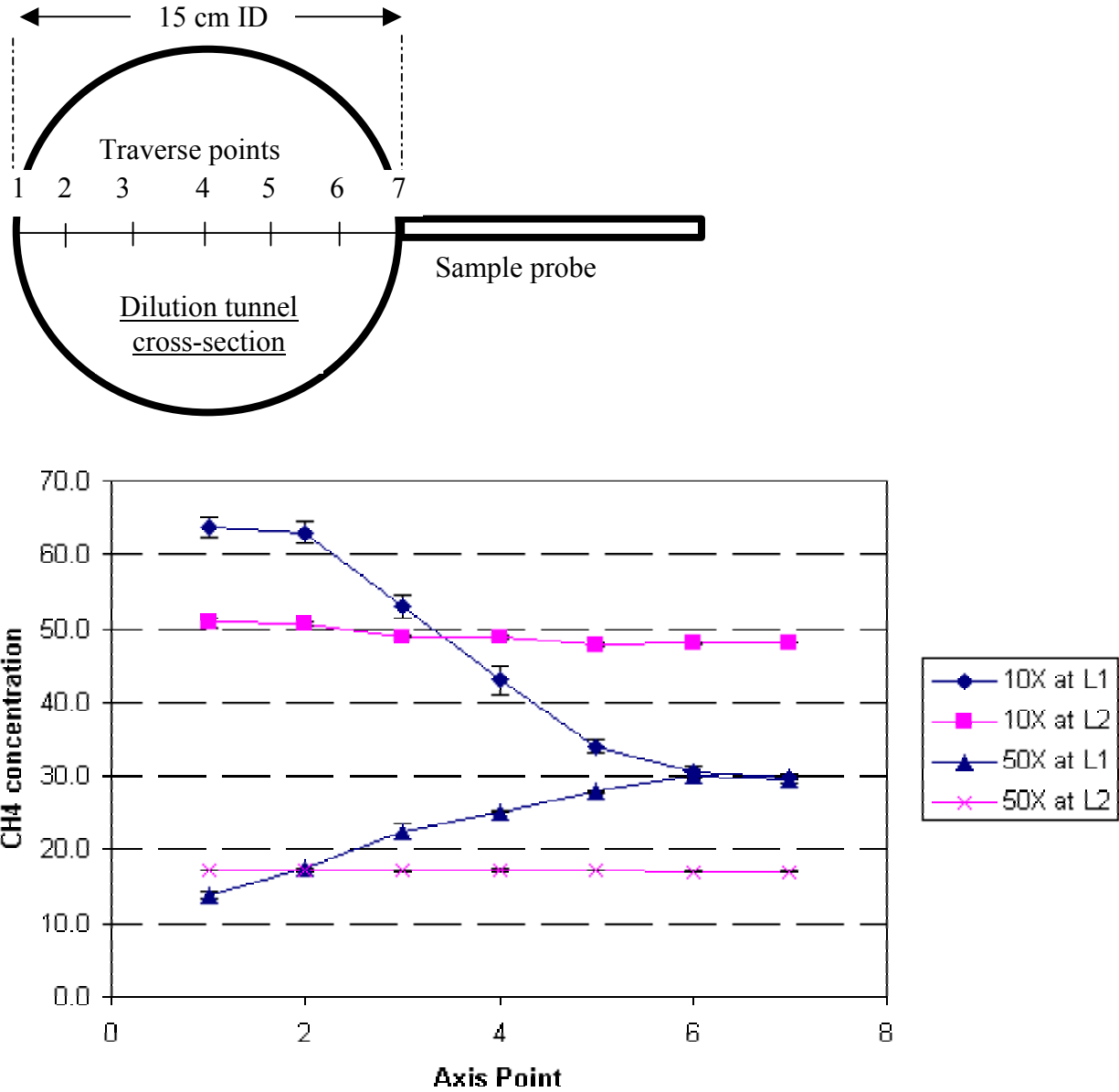


Figure 3-1. Concentration profiles at different cross-sectional planes in the DRI dilution sampler.

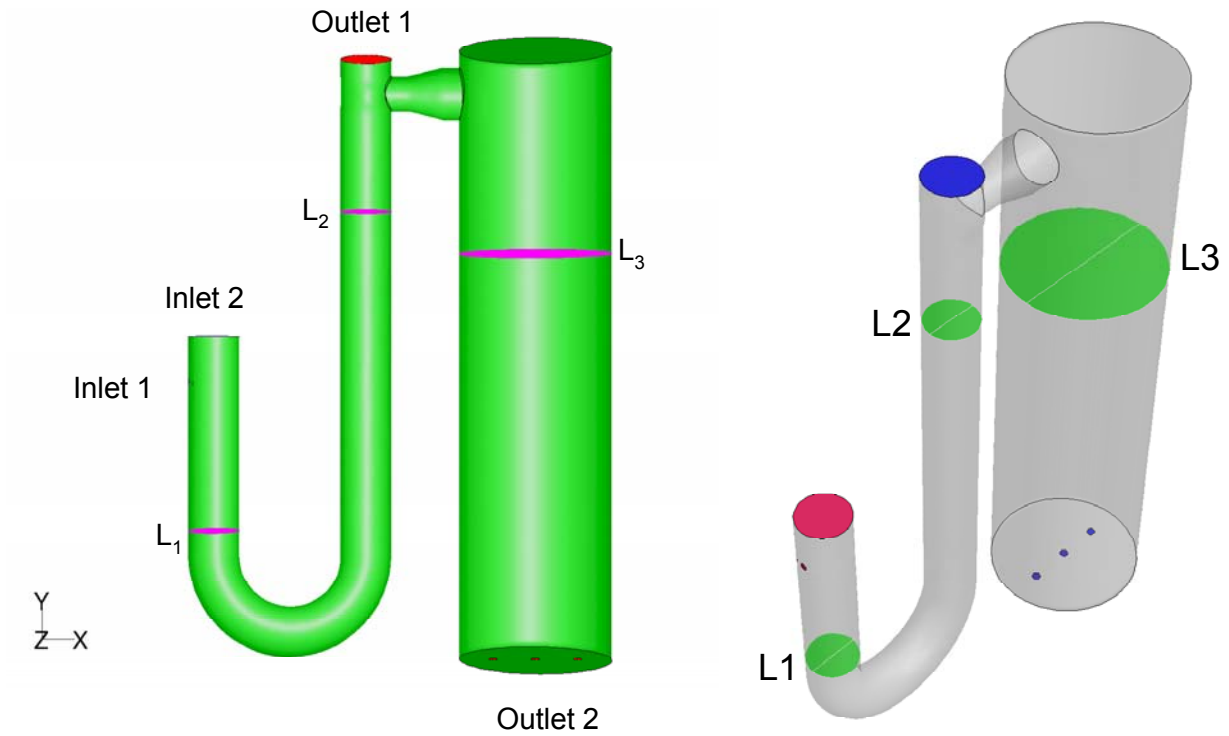


Figure 3-2. Dilution sampler geometry and reference locations for computational simulation.

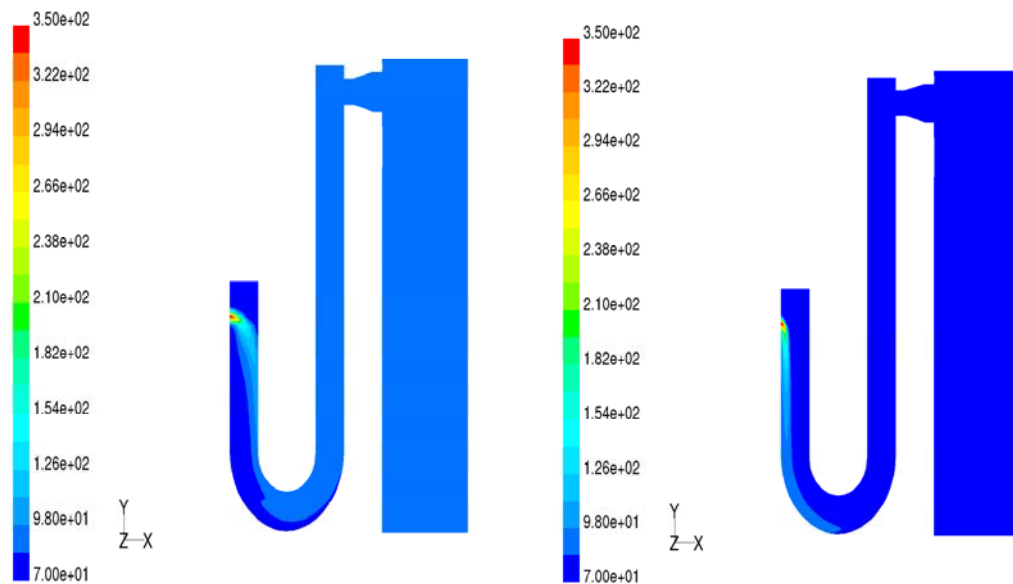


Figure 3-3. Calculated temperature profile predicted by CFD simulation showing mixing between sample and dilution air in dilution tunnel for dilution ratio of 10:1 (left) and 50:1 (right).

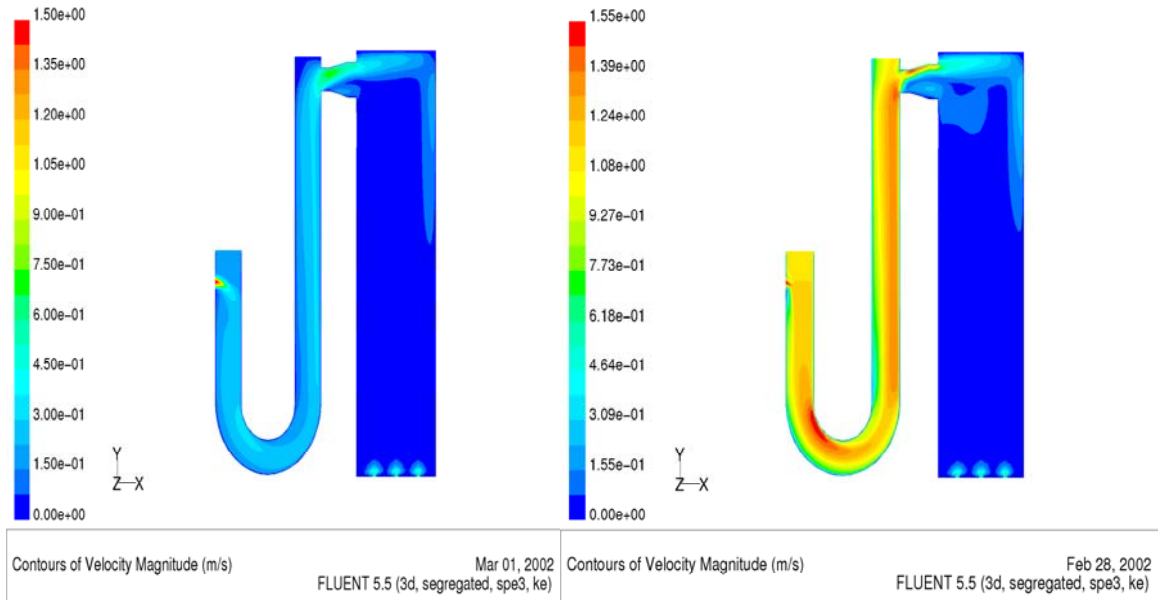


Figure 3-4. Velocity profiles in dilution tunnel sampler by CFD: left 10:1 and right 50:1.

The velocity profiles in the residence time chamber suggest that the flow field is more of a stirred character rather than plug flow. In a perfectly stirred reactor, gas residence time is the same throughout the reactor and decays in time when the inlet concentration is changed, whereas in a plug flow reactor gas residence time is equal across all cross sections and increases monotonically along the axis of the reactor. Therefore, in a stirred reactor there is a significant distribution of residence times about the bulk mean gas residence time, whereas in a plug flow reactor all gas elements reside for the same amount of time equal to the bulk mean residence time. Table 3-1 shows calculated mean residence times and standard deviations for 1 and 5  $\mu\text{m}$  particles through the plane L3 at 10:1 and 50:1 dilution. To better characterize the gas flow characteristics, particle coagulation and growth were neglected and total re-bounce when colliding on the wall was assumed (no wall losses). Flow regime is turbulent in the mixing (U-tube) section and laminar in the residence time chamber. 1  $\mu\text{m}$  particles are expected to follow the gas flow very well and hence the mean residence time is very close to the calculated bulk mean gas residence time (approximately 10 seconds at L3 for 50:1 dilution ratio). The standard deviation for 1  $\mu\text{m}$  particles at L3 is 2 seconds, or approximately 20 percent, for 50:1 dilution ratio. At 10:1, the standard deviation at this location is nearly 100 percent of the mean residence time. Results for 5  $\mu\text{m}$  particles show an even greater distribution of residence times; however, the results for 5  $\mu\text{m}$  particles are suspect since the CFD model was not set up to account for all gas-

particle interactions. The results show that particles experience a wide distribution of aging times due to the geometry of the residence time chamber.

Table 3-1. Calculated Mean Residence Times and Standard Deviations for 1  $\mu\text{m}$  Particles in the Residence Time Chamber at 10:1 and 50:1 Dilution.

	10:1 dilution		50:1 dilution	
	Mean (seconds)	Standard deviation (seconds)	Mean (seconds)	Standard deviation (seconds)
1 $\mu\text{m}$	57.2	50.6	9.7	2.0
5 $\mu\text{m}$	91	86	38	68

The main significance of the CFD study was to characterize the flow fields within the benchmark sampler to better understand the characterization test results and apply that understanding to the new design. The CFD results helped in the interpretation of radial concentration profiles measurements in the mixing section and residence time chamber. The CFD study showed two major areas for improvement in the new design: minimize the dependence of dilution ratio on mixing between the sample and dilution air; and achieve better utilization of the volume within the residence time chamber, and therefore more uniform aging of the aerosol, by avoiding large recirculation zones.

#### PARTICLE CONCENTRATION TRENDS

Preliminary tests were conducted with coal combustion and a flue gas temperature of 645 K to establish how long it would take to obtain repeatable measurements. The laser photometer was used to monitor PM concentration trend over a one-and-a-half hour period with coal combustion. PM gradually increased by approximately 20 percent over this period (Figure 3-5). At the end of this period, the sample inlet was blocked and only filtered dilution air was passed through the dilution sampler. The laser photometer response returned to the background level after a period of approximately 30 minutes. Similar trends were observed with natural gas and No. 6 oil. The results show that the time constant for residence time decay is fairly long, which is consistent with the CFD results. Based on these results, it was decided to collect several replicate

measurements on different days and to make several replicate scans for each test run. In most tests, the sampler was allowed to purge for at least 30 minutes after changing test conditions.

#### ULTRAFINE PARTICLE SIZE DISTRIBUTION AND CONCENTRATION

Continuous size distributions of particles measured by SMPS are presented as  $dN/d\log(dp)$ . The results are also presented as density plots in Appendix A. The particle number concentrations measured in the diluted sampler are converted to in-stack concentrations by multiplying the measured particle number concentration by the dilution factor (dilution factor = 1 + dilution ratio). These measurements under different conditions were averaged and the potential impact on particle size distribution due to both measurement and process variation is expressed as the standard deviation from the mean.

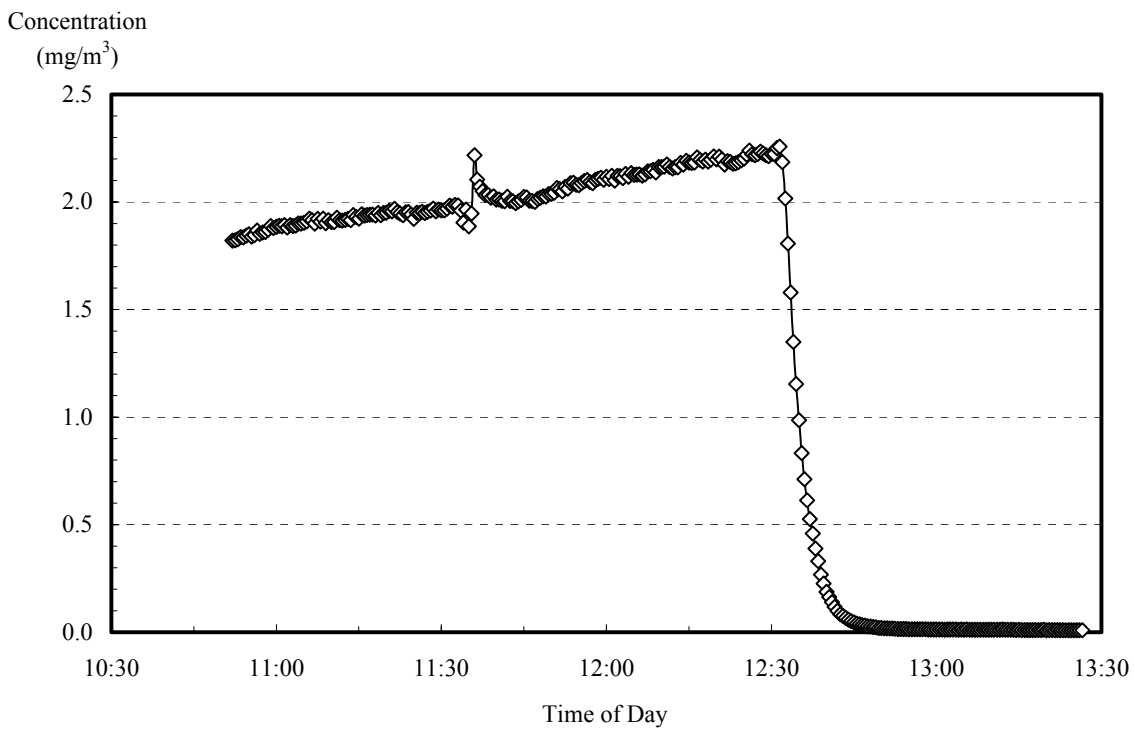


Figure 3-5. PM concentration trend from coal combustion measured from dilution sampler with 50:1 dilution ratio and flue gas temperature of 645 K

## Effects of Dilution Ratio

Figures 3-6 to 3-8 shows ultrafine particle size distributions and total number concentrations for coal, oil, and gas at combustion exhaust temperature of 450 K and for different dilution ratios at an aging time of 80 seconds. Error bars indicate one standard deviation from the mean value (typically more than 3 replicate SMPS scans) for each size bin. Those plots without error bars generally represent data sets with only 3 or 5 SMPS scans and hence the standard deviation is not considered representative of the true distribution. In the legend on these and following figures, the variable of interest (e.g. dilution ratio, temperature, residence time, fuel) and total particle number concentration integrated over the measured size range are given. Following the No. 6 fuel oil tests, minor leaks in the sampling system were found, which invalidated measurements for particles larger than 200 nm; therefore, only SMPS results with a size bin range of 10-193 nm were used.

The particle size distributions show modes at 40 to 50 nm with coal (Figure 3-6), 70 to 100 nm with No. 6 Fuel Oil (Figure 3-7), and 15-25 nm with natural gas (Figure 3-8). The particle size modes are insensitive to dilution ratio for coal and No. 6 fuel oil, but increase slightly for natural gas as the dilution air ratio decreases from 20:1 to 10:1. For coal and No. 6 fuel oil, particle number concentrations with a dilution air ratio of 50:1 are twice those measured at a dilution air ratio of 10:1. The increase in particle number concentrations as dilution air ratio increases observed with coal and No. 6 fuel oil is consistent with results reported by Lipsky et al. (2002).

Particle size distribution and total particle number concentrations for natural gas (Figure 3-8) remain approximately constant as dilution ratio decreases from 50:1 and 20:1 but change sharply with further decrease in dilution ratio from 20:1 to 10:1. Although the 10:1 dilution test was not repeated on a different day to confirm the results, the data set includes 6 scans over a 1-hour period. The size mode was very repeatable between 20 to 30 nm, and the peak number concentration had a standard deviation of approximately 6 percent. In general, other results with natural gas were found to be repeatable within this same approximate range. Therefore, there is fairly high confidence in the results. The natural gas results imply that a minimum dilution ratio of 20:1 is required to achieve stable aerosol characteristics under these conditions.

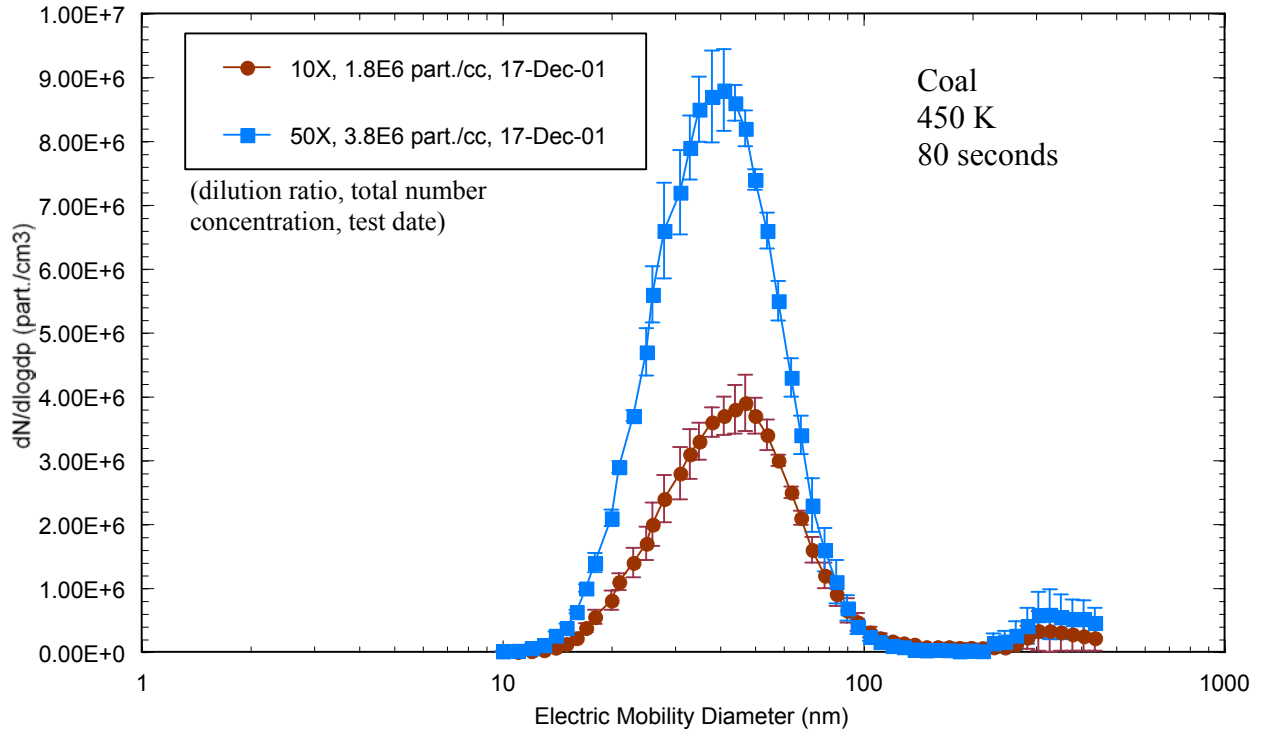


Figure 3-6. Effect Of Dilution Ratio On Ultrafine Particle Size Distribution And Number Concentration (Coal, Sample Temperature 450 K, Residence Time 80 Seconds).

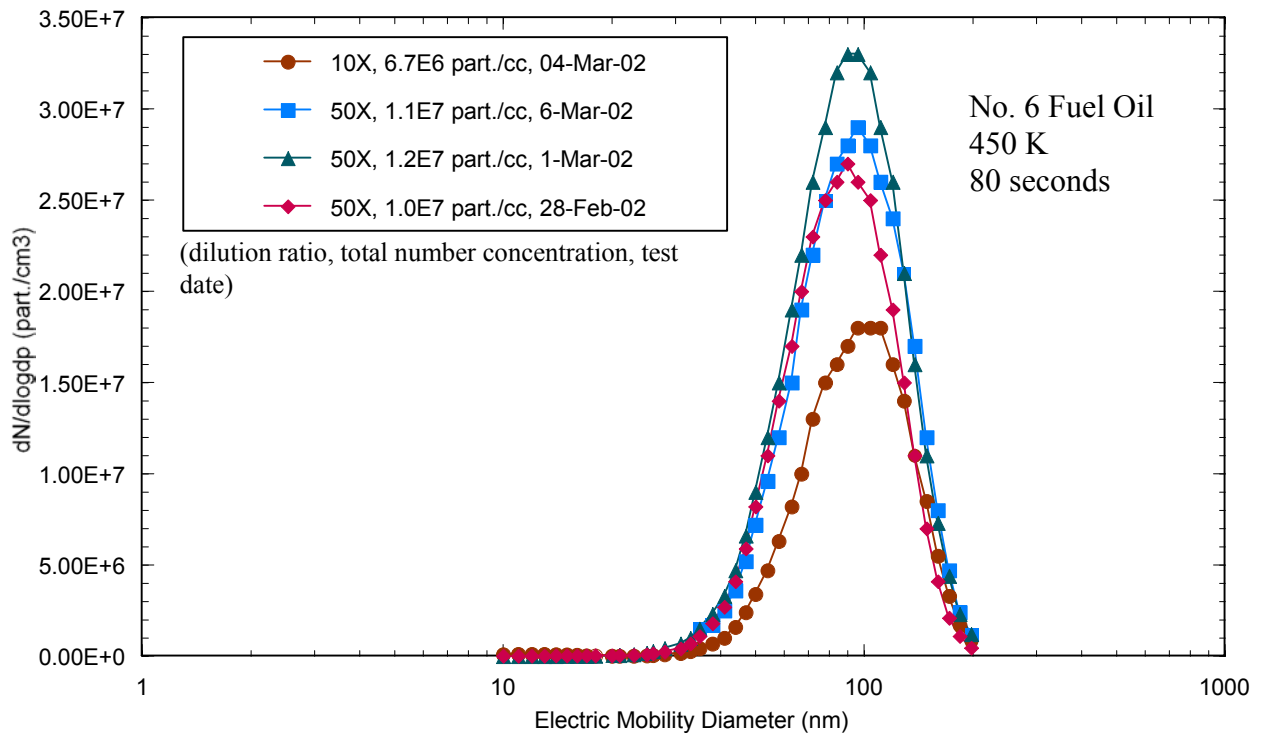


Figure 3-7. Effect Of Dilution Ratio On Ultrafine Particle Size Distribution And Number Concentration (No. 6 Fuel Oil, Sample Temperature 450 K, Residence Time 80 Seconds).



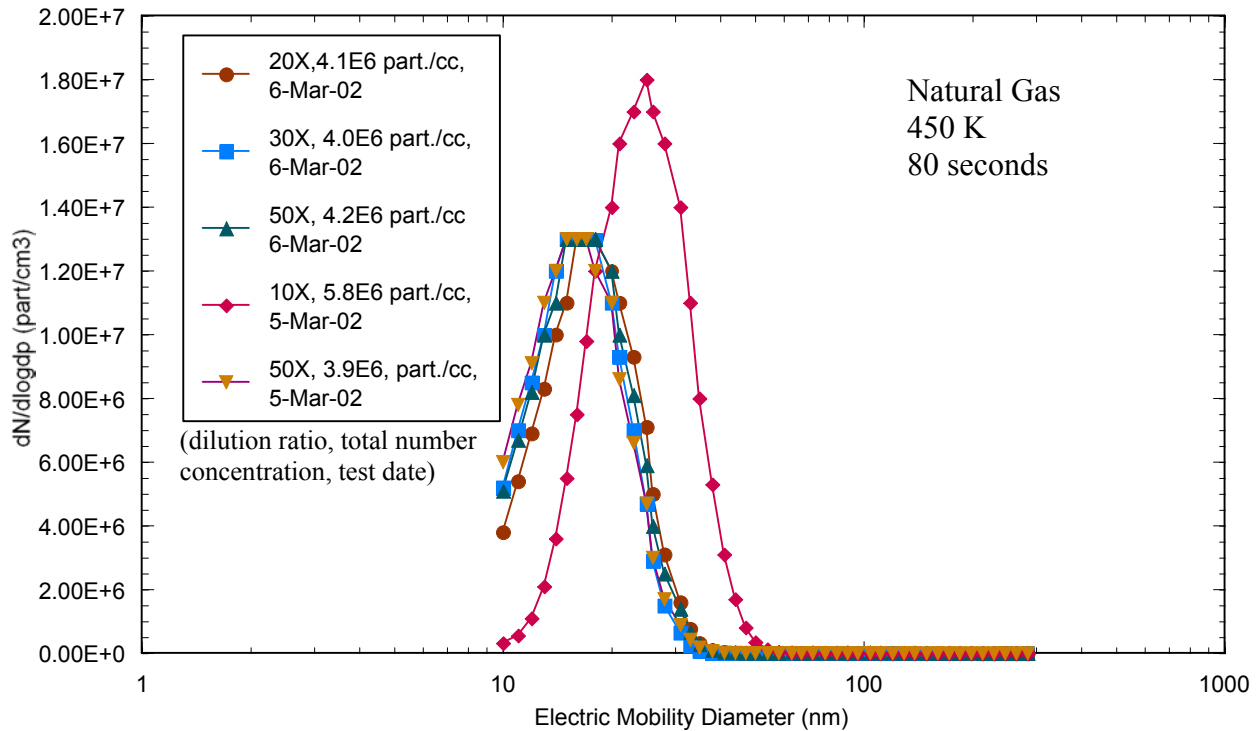


Figure 3-8. Effect Of Dilution Ratio On Ultrafine Particle Size Distribution And Number Concentration (Natural Gas, Exhaust Temperature 450 K, Residence Time 80 Seconds).

The difference in the effects of dilution ratio and residence time on particle number concentrations for natural gas compared to No. 6 fuel oil and coal can be explained by differences in solid particle (soot, fly ash, etc.) concentration and saturation ratio of vapor species during the dilution process. The solid particle mass concentrations from natural gas exhaust are much lower in contrast to those with high fly ash content for coal and No. 6 fuel oil. Therefore, particle nucleation occurs due to the supersaturation of vapor species and the lack of available primary particle surface area on which to condense when they are rapidly cooled and diluted. Ultrafine particle number concentrations for diluted natural gas exhaust increased as dilution air ratio was decreased from 20:1 to 10:1 and the particle distribution shifted slightly to a larger size, which is indicative of coagulation and or condensational growth. For coal, a higher rate of particle coagulation at a dilution air ratio of 10:1 could explain the apparent decrease in the smallest particles. The high particle concentration in coal exhaust also provided a larger surface area for condensable species to condense on, rather than undergo nucleation. For No. 6 fuel oil, in addition to the coagulation of particles, the higher fraction of condensable species—

such as sulfate and carbonaceous organic species—condensed on and grew ultrafine particles to the particle modes of 70-100 nm (Figure 3-7), which are larger than those for coal.

### Effects of Residence Time

Particle number concentrations at dilution ratio of 50:1 as a function of aging time for coal, oil, and gas are shown in Figures 3-9, 3-10, and 3-11, respectively. Number concentrations are highest for an aging time of 2 seconds for No. 6 fuel oil, and are virtually the same from 10 seconds to 80 seconds for all three fuels. Figure 3-9 shows a shift to larger sizes as the aging time increased from 2 seconds to 10 seconds for coal, but the size distribution stayed the same for aging times larger than 10 seconds. This shift is probably due to condensational growth. For natural gas (Figure 3-11), particle size distribution was similar with aging, but for No. 6 residual oil (Figure 3-10), the number concentration decreased as the aging time increased. Differences in number concentration between 2 and 10 seconds for No. 6 fuel oil are due to particle transformation by condensational growth and coagulation. Particle coagulation and condensational growth rates are highest when combustion exhaust mixes with dilution air, slowing with the decrease in number concentration (coagulation) and depletion of vapor species (condensational growth). The similarities in particle size distributions between 10-second and 80-second aging times show that particle transformation occurs very rapidly in the first 10 seconds. These results show that a total particle aging time of slightly more than 10 seconds after the exhaust is fully mixed should be sufficient for a dilution sampler to provide a representative sample for analysis.

Note, because of incomplete mixing between the sample and dilution air at sampling location L1 with a dilution ratio of 10:1, no valid results were obtained for residence times of 2 seconds at this dilution ratio.

### H<sub>2</sub>SO<sub>4</sub> and ZnO Doping Results

To simulate a combustion source exhaust with high condensable vapor concentration but low solid particle concentration, natural gas was doped with H<sub>2</sub>SO<sub>4</sub>. H<sub>2</sub>SO<sub>4</sub> was atomized into the FEF at a location in the convective heat transfer section where the combustion exhaust

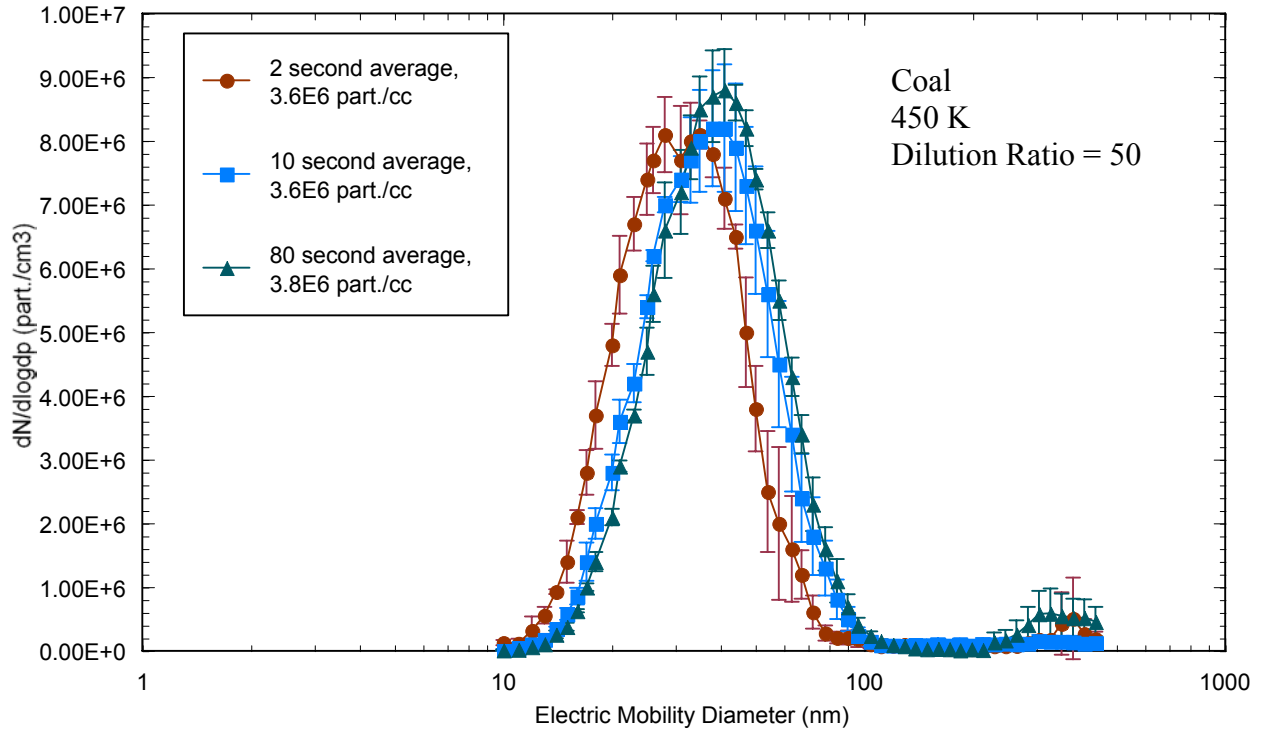


Figure 3-9. Effect Of Residence Time On Ultrafine Particle Size Distribution And Number Concentration (Coal, Exhaust Temperature 450 K, Dilution Ratio 50:1).

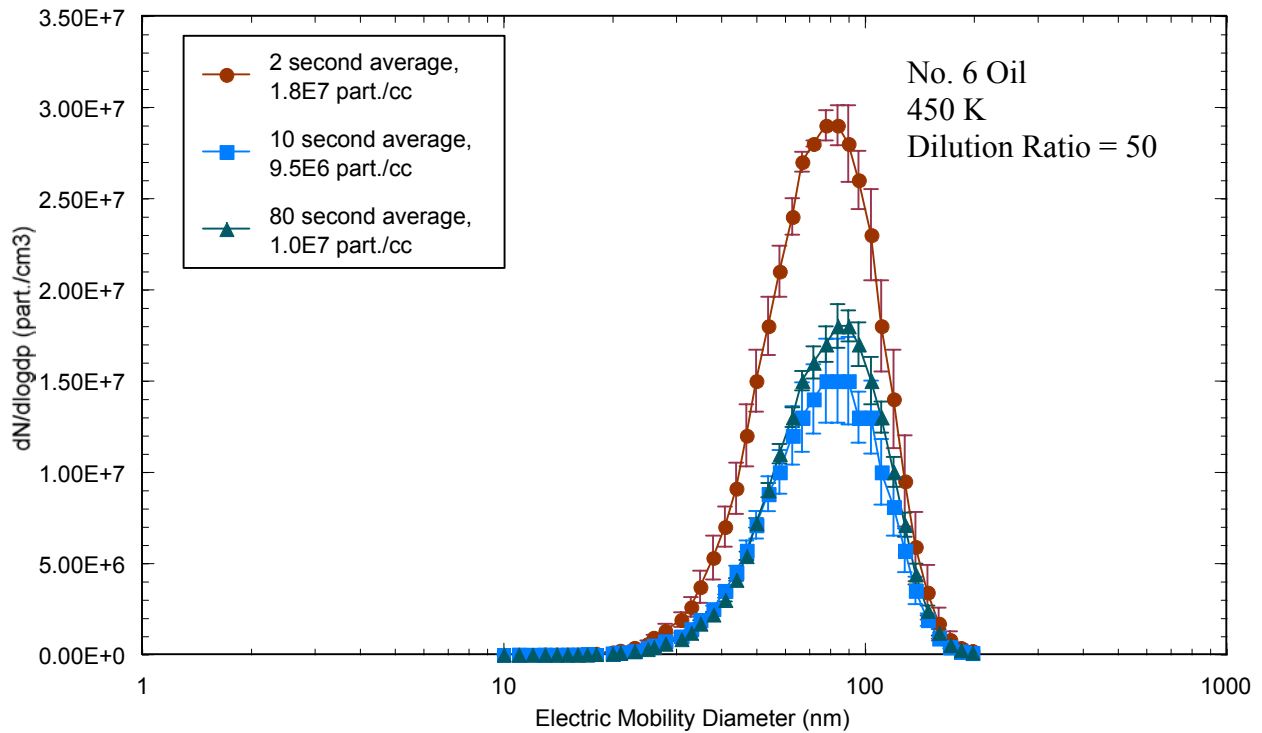


Figure 3-10. Effect Of Residence Time On Ultrafine Particle Size Distribution And Number Concentration (No. 6 Fuel Oil, Exhaust Temperature 450 K, Dilution Ratio 50:1).

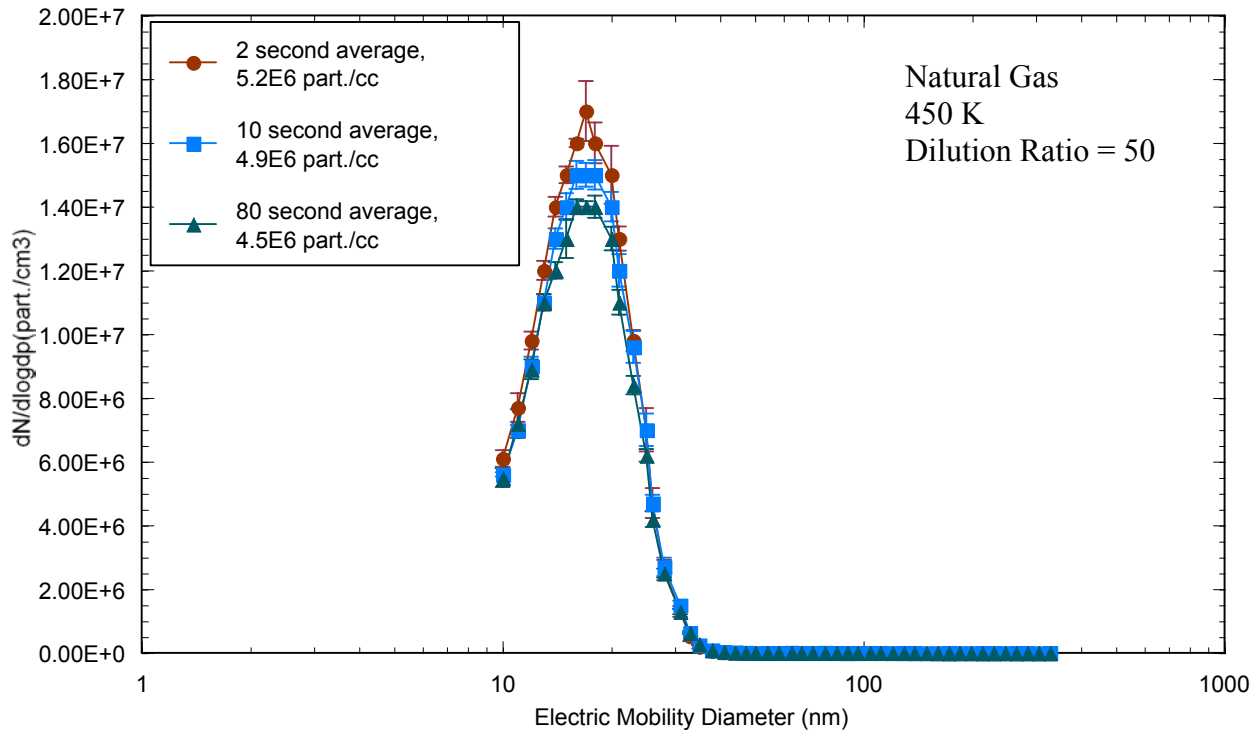


Figure 3-11. Effect Of Residence Time On Ultrafine Particle Size Distribution And Number Concentration (Natural Gas, Exhaust Temperature 450 K, Dilution Ratio 50:1).

temperature was 1,145 K. This assured complete evaporation of the droplets and conversion of  $\text{H}_2\text{SO}_4$  to  $\text{SO}_3$  rather than  $\text{SO}_2$ . As the flue gases rapidly cool beyond the injection point, moisture in the flue gas reacts with  $\text{SO}_3$  and  $\text{H}_2\text{SO}_4$  forms. The vapor becomes supersaturated, favoring aerosol formation by nucleation followed by condensational growth. The injection rate was adjusted to produce a fully mixed concentration in the flue gas stream of 30 ppm  $\text{SO}_3/\text{H}_2\text{SO}_4$ . Comparing results at dilution ratio of 50:1 without  $\text{H}_2\text{SO}_4$  (Figure 3-11) to those with  $\text{H}_2\text{SO}_4$  (Figure 3-12), addition of  $\text{H}_2\text{SO}_4$  increases the peak number concentration at 2 seconds from  $1.7\text{E}+7$  to  $6.8\text{E}+7$  particles/ $\text{cm}^3$  and increases the particle size mode from approximately 18 to 40 nm. Particle number concentration initially decreases rapidly from  $6.8\text{E}+7$  to  $4.0\text{E}+7$  particles/cubic centimeter ( $\text{cm}^3$ ), presumably due to coagulation, between 2 and 10 seconds aging time, then decreases more slowly between 10 and 80 seconds. The particle size mode with  $\text{H}_2\text{SO}_4$  (Figure 3-12) increases slightly with aging time between 2 and 80 seconds, which can be explained by condensational growth. Particle size mode at 80 seconds aging time increases slightly from approximately 50 nm to 70 nm with decreasing dilution ratio between 50:1 (Figure 3-12) and 10:1 (Figure 3-13). This can be explained by a higher

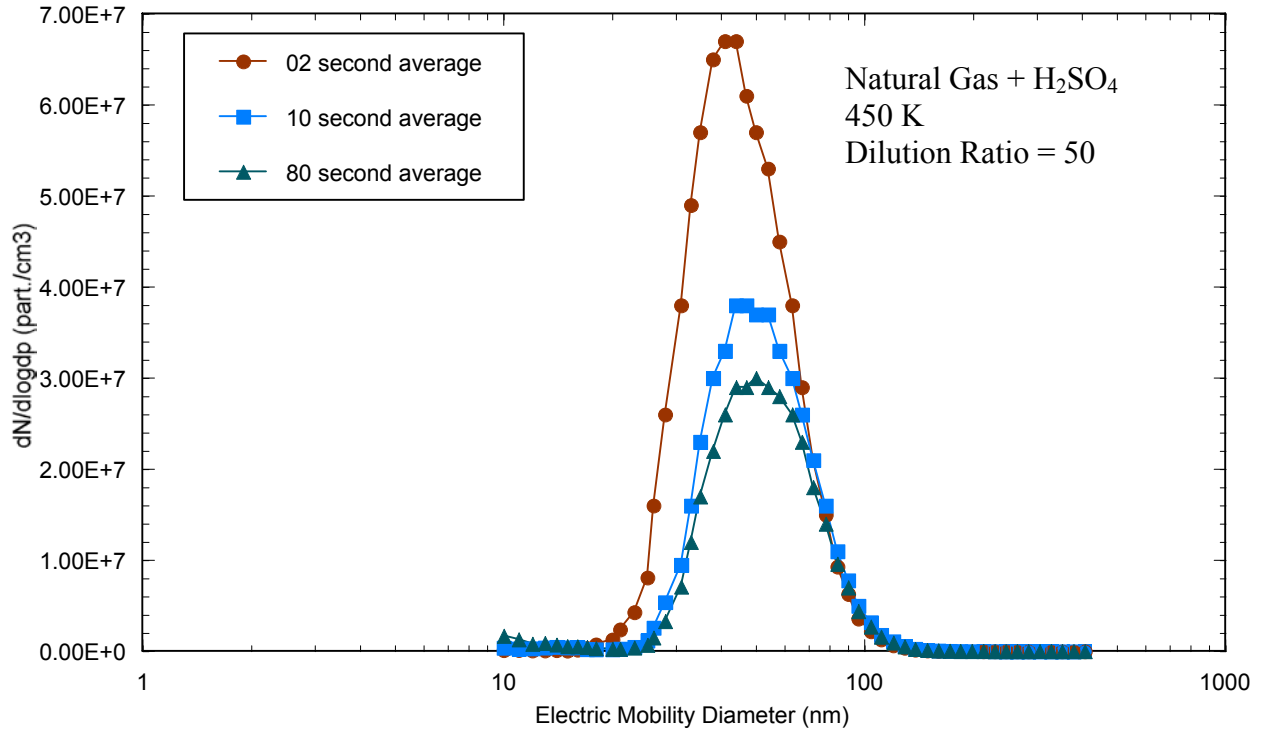


Figure 3-12. Effect Of Residence Time On Ultrafine Particle Size Distribution And Number Concentration (Natural Gas + 30 ppm H<sub>2</sub>SO<sub>4</sub>, Exhaust Temperature 450 K, Dilution Ratio 50:1).

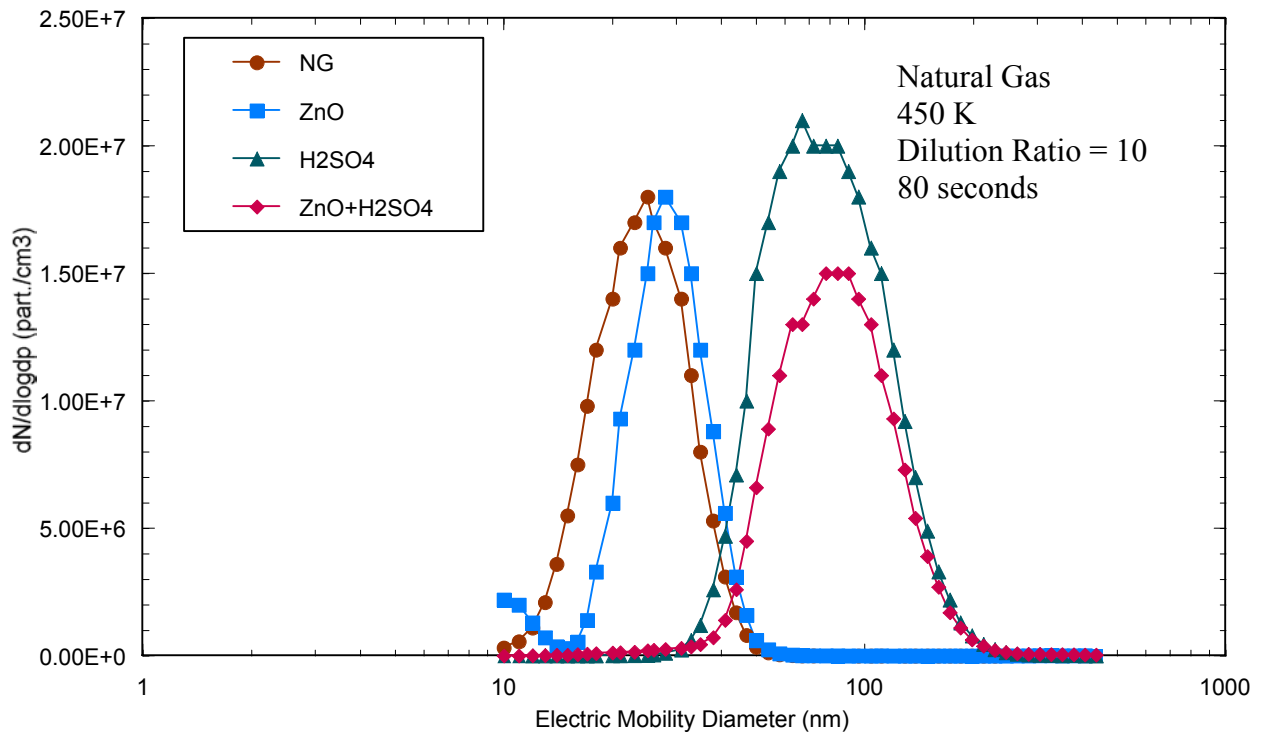


Figure 3-13. Effect Of Solid and Liquid Aerosol Doping On Ultrafine Particle Size Distribution And Number Concentration (Natural Gas, Exhaust Temperature 450 K, Dilution Ratio 10:1, Residence Time 80 Seconds).

supersaturation ratio and therefore higher nucleation rate of condensable species at the lower dilution ratio. This behavior agrees with the results shown in Figure 3-8 for pure natural gas, where very low concentrations of primary particles were present in the exhaust.

To evaluate aerosol dynamics with both solid particles and condensable vapors present, ZnO powder with a geometric mean diameter of 2  $\mu\text{m}$  was injected into natural gas combustion exhaust, with and without  $\text{H}_2\text{SO}_4$  doping. Dilution sampler measurements were made with a dilution ratio of 10:1 at 80 seconds residence time (Figure 3-13). Since the ZnO powder has a geometric mean size of 2  $\mu\text{m}$  (2000 nm), it is not expected to contribute significantly to ultrafine particles. When ZnO powder alone is injected into the natural gas exhaust, there is little effect on the measured particle size and number concentration. When  $\text{H}_2\text{SO}_4$  alone is added, an increase in both the particle size mode (from approximately 30-40 nm to approximately 90-100 nm) and number concentration is observed, presumably a result of  $\text{H}_2\text{SO}_4$  condensation by nucleation and subsequent coagulation. When ZnO powder and  $\text{H}_2\text{SO}_4$  are injected together, the particle size mode is similar to natural gas with  $\text{H}_2\text{SO}_4$  alone, but the number concentration is much lower. This is consistent with depletion of condensable vapor by condensation on the surface of the larger particles, reducing the amount available to condense as nuclei in the ultrafine size range. The effects evident in Figure 3-13 provide an explanation for the differences in the No.6 fuel oil (high condensable vapor, low solid particle concentrations) and coal (high condensable vapor, high solid particle concentrations) results observed in Figures 3-6 and 3-7.

### Effect of Exhaust Temperature

Figures 3-14 to 3-17 show the effects of dilution ratio and aging time at high exhaust temperature. The change in number concentration between 2 and 10 seconds is much greater than the change between 10 and 80 seconds for coal and No. 6 fuel oil (Figures 3-14 and 3-15, respectively). The large decrease in number concentration for coal between 2 and 10 seconds is in stark contrast to the results at 450 K (Figure 3-9), where almost no change was observed. For No. 6 fuel oil, the effect of aging time for exhaust temperature of 645 K (Figure 3-15) is much less pronounced compared to results for 450 K (Figure 3-10). For both coal and oil, the number concentrations at 645 K are greater than at 450 K. More rapid quenching of the exhaust sample

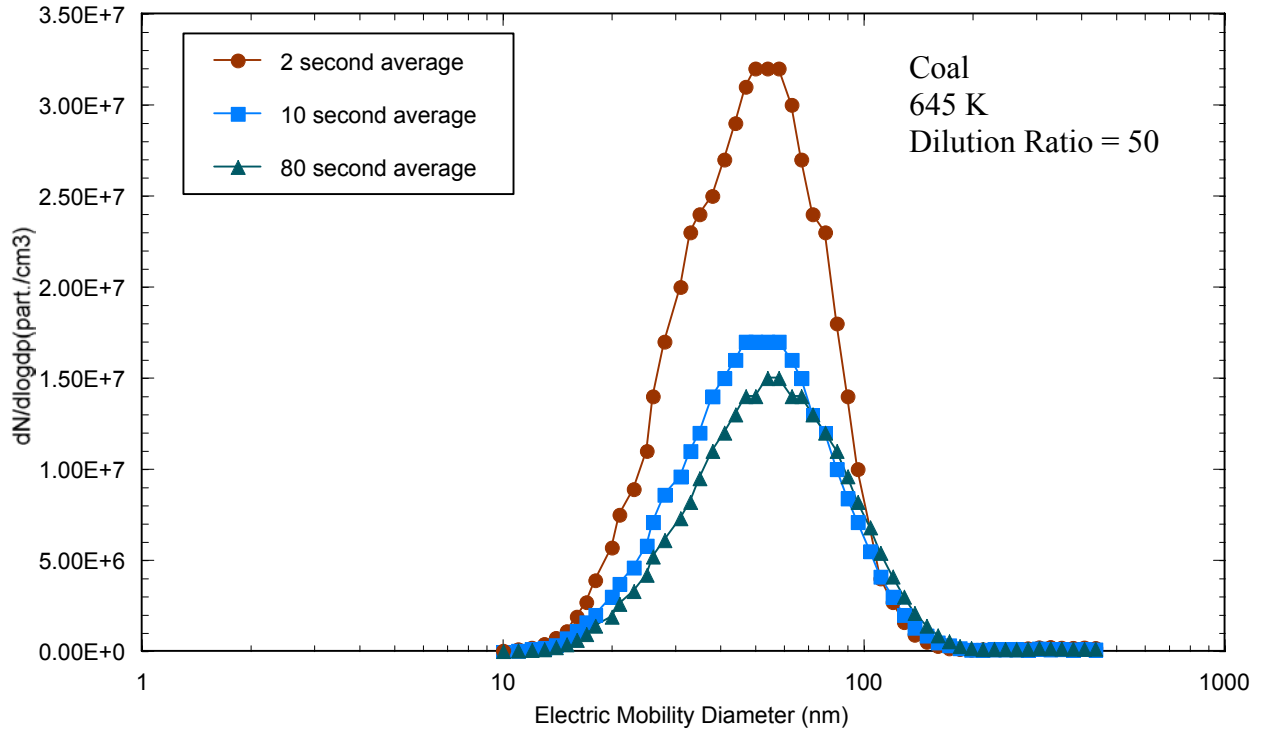


Figure 3-14. Effect Of Residence Time On Ultrafine Particle Size Distributions (Coal, Exhaust Temperature 645 K, Dilution Ratio 50:1).

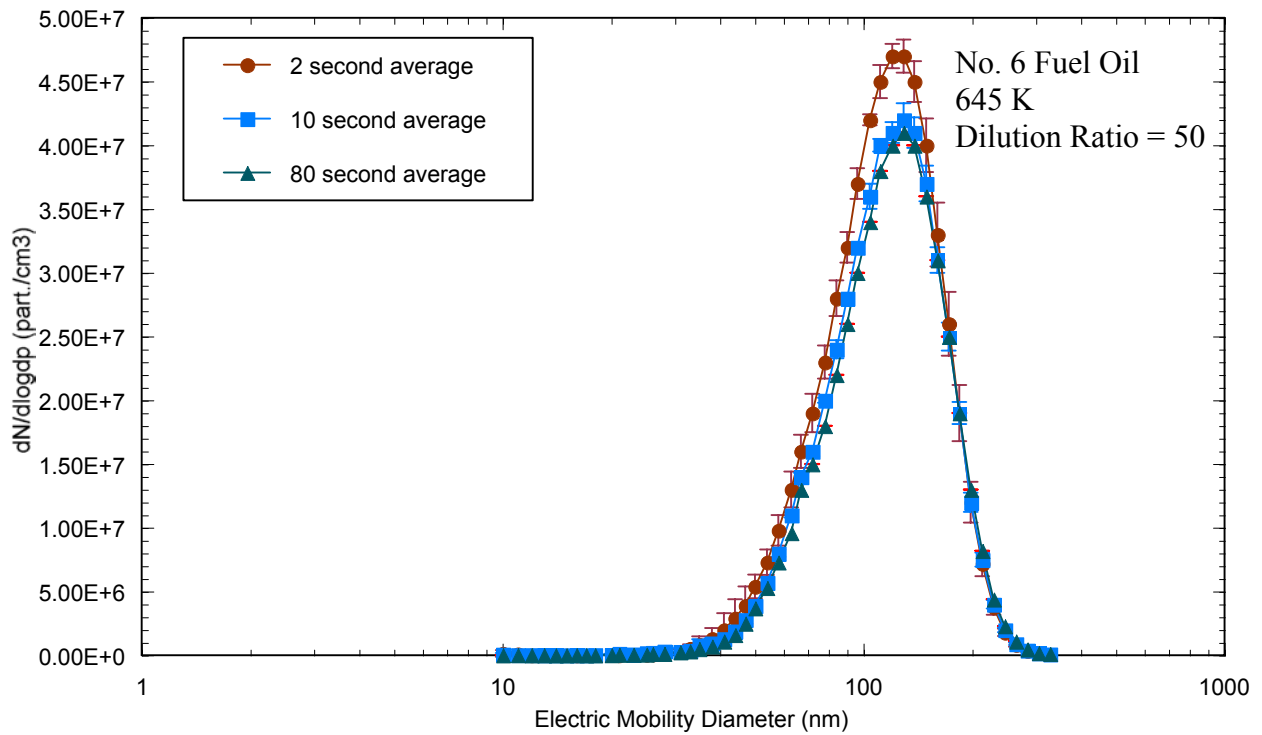


Figure 3-15. Effect Of Residence Time On Ultrafine Particle Size Distributions (No. 6 Fuel Oil, Exhaust Temperature 645 K, Dilution Ratio 50:1).

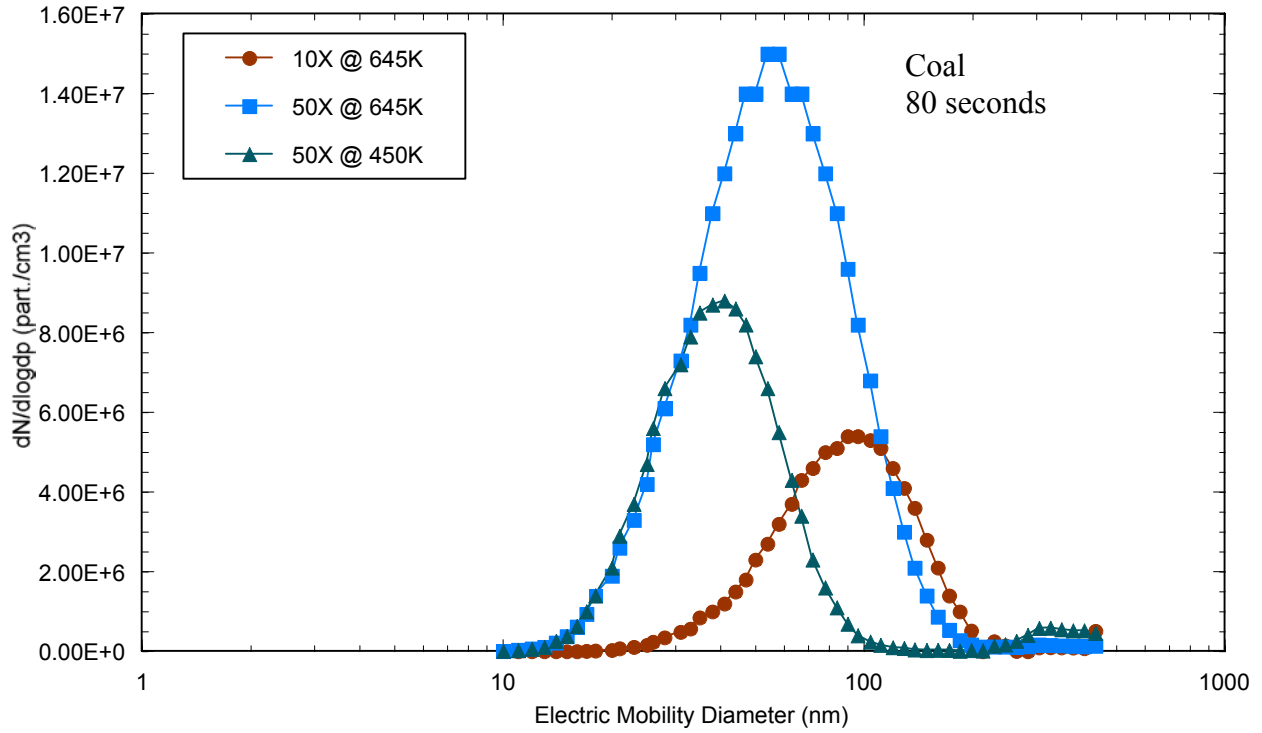


Figure 3-16. Effect Of Dilution Ratio And Exhaust Temperature On Ultrafine Particle Size Distributions (Coal, Residence Time 80 Seconds).

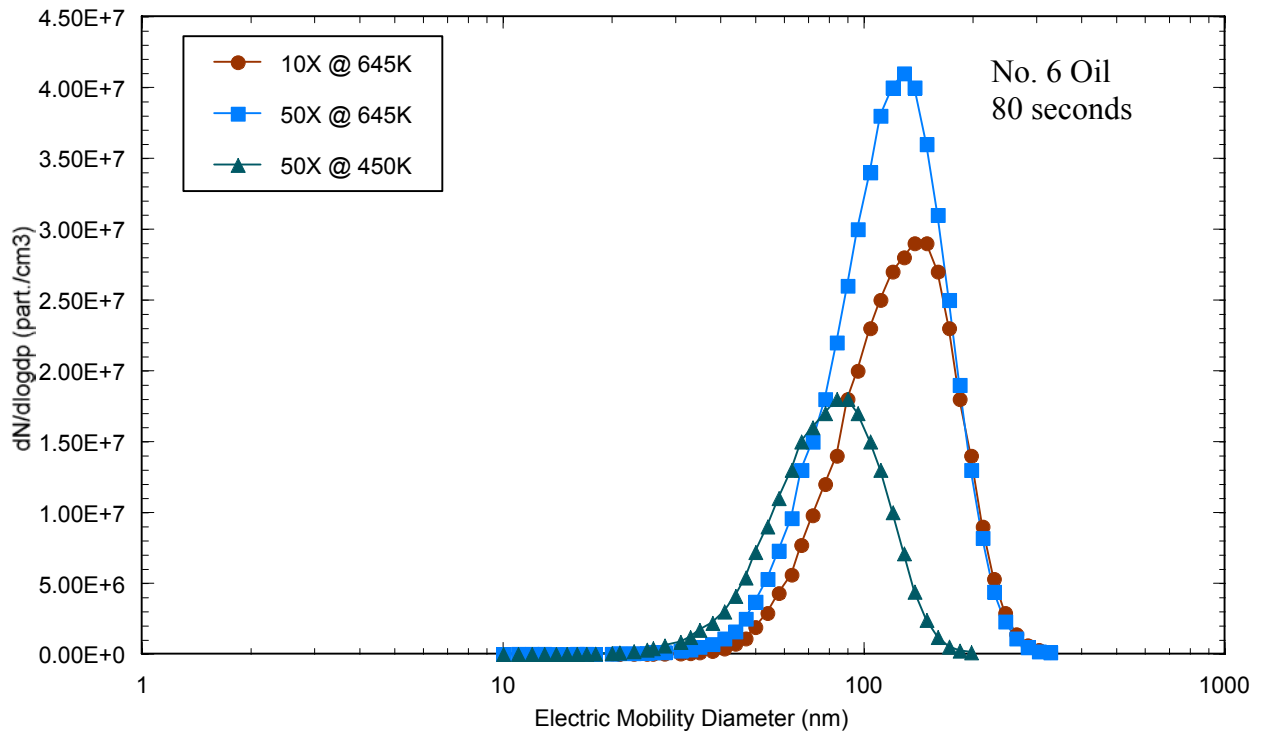


Figure 3-17. Effect Of Dilution Ratio And Exhaust Temperature On Ultrafine Particle Size Distributions (No. 6 Oil, Residence Time 80 Seconds).



at the higher exhaust temperature (i.e., a greater temperature differential between sample and dilution chamber in approximately the same amount of time), forcing higher H<sub>2</sub>SO<sub>4</sub> supersaturation and more condensation in the ultrafine size range, can at least partially explain these differences.

At a dilution air ratio of 50:1, increasing the exhaust temperature increases both particle number concentrations and size mode at 80 seconds for both coal and oil (Figures 3-16, 3-17). The particle number concentration at 645 K is 2 to 3 times greater than at 450 K, and the particle size mode increased from 90 to 130 nm for No. 6 fuel oil and from 45 nm to 65 nm for coal. This is probably due to higher concentrations of condensable species available at the higher combustion exhaust temperature and a higher temperature gradient between exhaust and dilution air. This favors both greater nucleation rate and more condensational growth. Particle number concentrations increase as the dilution air ratio increases for oil and coal, similar to results at the lower combustion exhaust temperature (Figures 3-6 and 3-7).

#### Particle Losses

Measurements were made at the centerline of the tunnel and residence time chamber for all of the results presented above. To assess the potential for particle losses on the walls of the residence time chamber, measurements also were made near the wall on the assumption that any significant particle losses on the wall should create an observable radial concentration gradient. Measurements near the wall near the exit (80 seconds) of the residence time chamber showed a slight decrease in particle number concentration compared to centerline (Figures 3-18, 3-19, and 3-20). The results at the wall are not conclusive evidence of diffusive losses because they appear to be within the scatter of replicate centerline measurements.

#### Ambient Air

To provide a reference level for the furnace exhaust measurements, a few measurements of the ambient air aerosol size distribution were made during the initial series of pilot-scale tests. Ultrafine particle concentrations in the ambient air are significantly lower than the in combustion exhaust samples, with relatively low number concentrations typically below 10,000 particles/cm<sup>3</sup> (Figure 3-21). Samples collected on two different days gave widely varying results. A bimodal

Coal, 350F, 10:1, 80 seconds (Dec 17-18, 2001)  
Wall versus Centerline

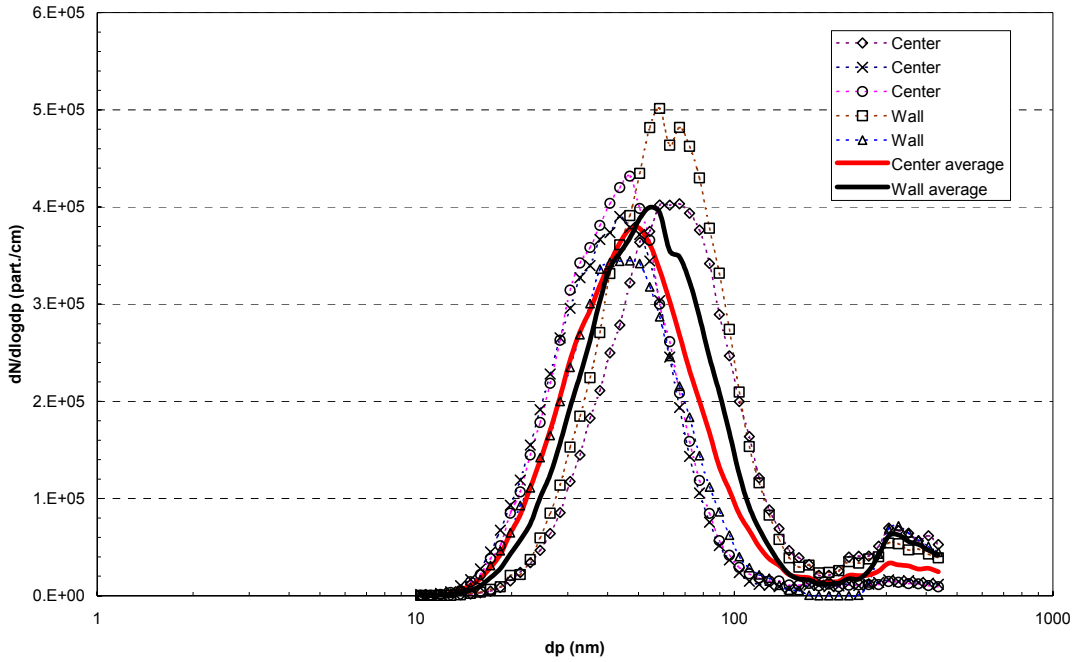


Figure 3-18. Size distributions of number concentration ( $\#/cm^3/mm$ ) measured from the center aligned sampling port and the sampling port on the wall using a SMPS for the coal combustion with a ten times dilution ratio.

Coal, 700F, 50:1, 80 seconds  
centerline vs. wall

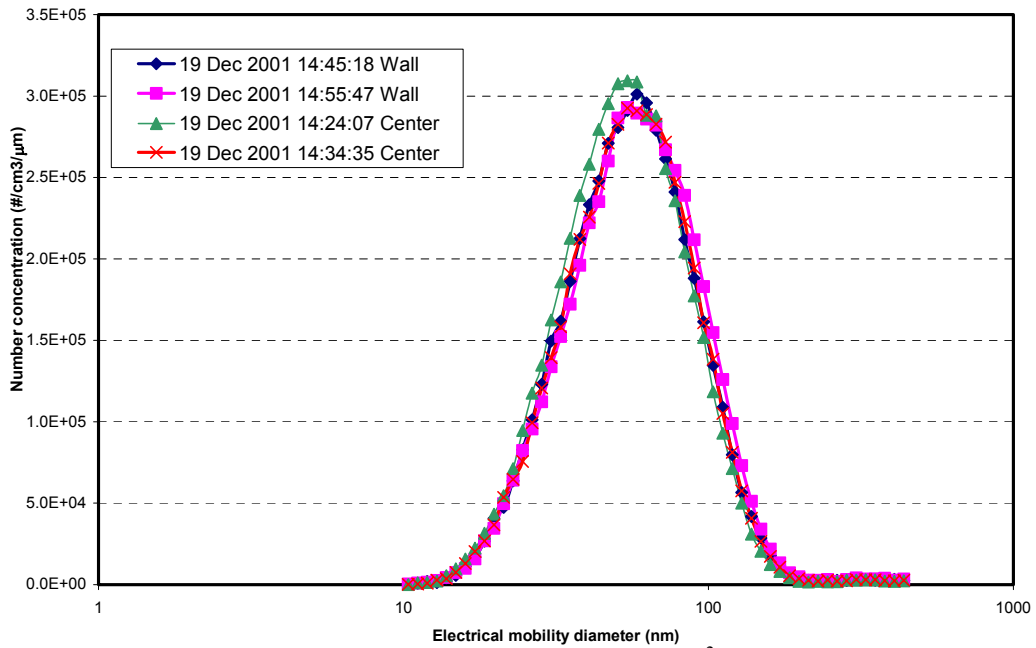


Figure 3-19. Size distributions of number concentration ( $\#/cm^3/um$ ) measured from the center aligned sampling port and the sampling port on the wall using a SMPS for the coal combustion with 50:1 dilution ratio.

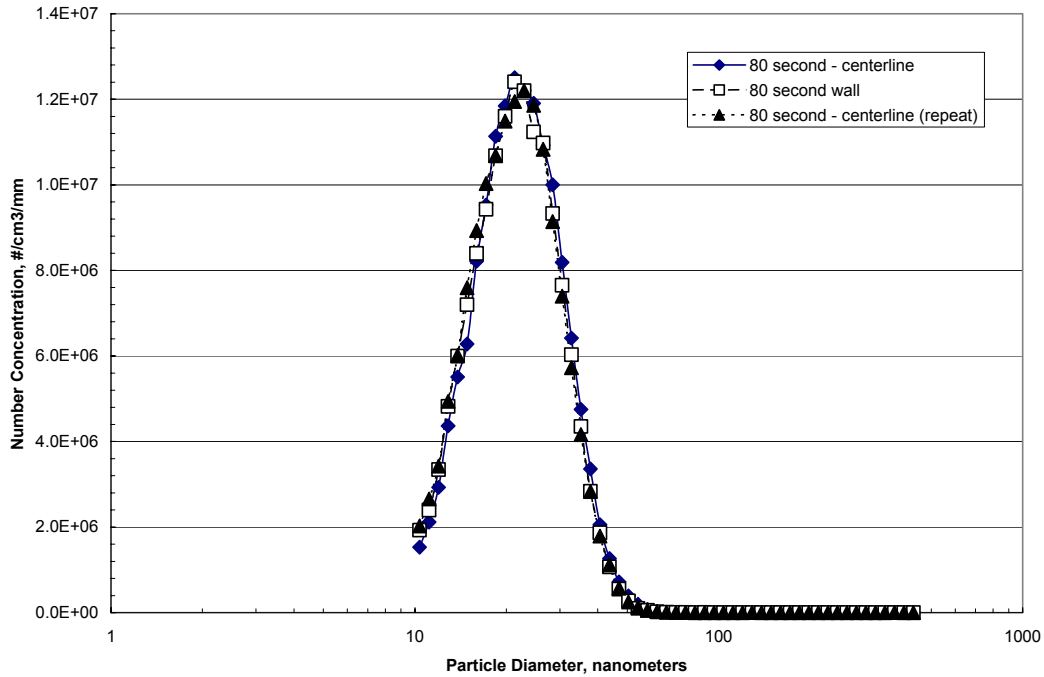


Figure 3-20. Ultrafine particle size and number concentration measured at the centerline and near the wall of the aging chamber exit (natural gas, 645 K, dilution ratio 10:1).

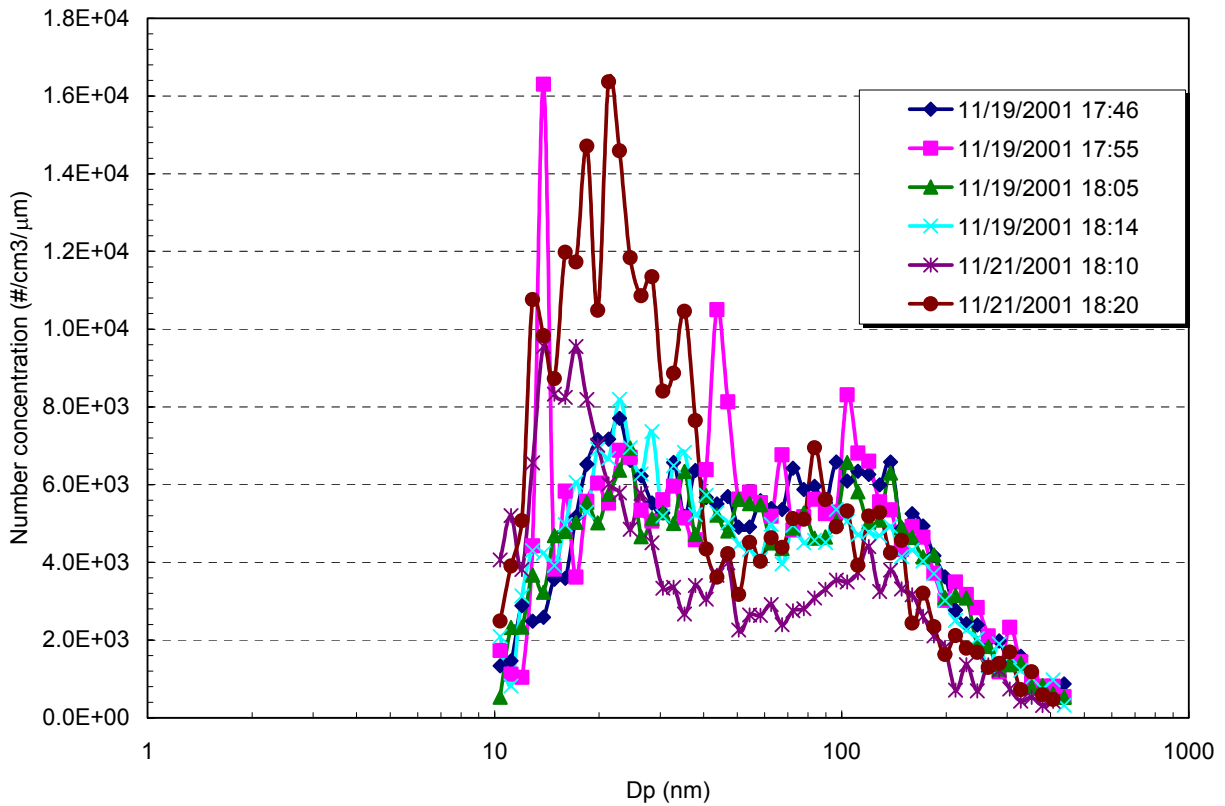


Figure 3-21. Ambient Air Aerosol Concentrations During Pilot-Scale Tests.

size distribution is evident in most of the results collected on 11/19/01, with modes at approximately 20 to 30 nm and 100 to 110 nm and number concentrations in the range of 1,000 to 6,000 particles/cm<sup>3</sup>. On 11/21/01, the size distributions also are bimodal, but the mode at 20-30 nm is more pronounced with peak number concentrations in the range of 10,000 to 16,000 particles/cm<sup>3</sup>.

## GRAVIMETRIC AND CHEMICAL ANALYSIS RESULTS

The MOUDI impactor was configured to provide samples of particles in two size fractions: less than 0.32 µm (PM0.32) and 0.32 to 2.5 µm. The samples were analyzed for mass and elements. For natural gas combustion, the low concentrations in the samples are near analytical detection limits; therefore, the results are considered qualitative. While 80 percent of the PM2.5 µm mass from natural gas combustion is found in the PM0.32 fraction, 75 to 85 percent of aluminum (Al), selenium (Si), potassium (K), calcium (Ca), iron (Fe), and zinc (Zn) are found in the 0.32 to 2.5 µm size fraction (Table 3-2). More than 80 percent of the PM2.5 mass and elements from coal combustion also is in the PM0.32 fraction.

Table 3-2. Fraction of PM2.5 Mass and Elements Smaller Than 0.32 µm.

Fuel	Natural Gas		Coal			
Exhaust Temperature	350	350	350	350	700	700
Dilution Ratio	50:1	10:1	50:1	10:1	50:1	10:1
Mass	nv	82.3	78.6	53.7	92.5	79.5
Al	38.5	18.1	93.6	74.6	99.6	78.4
Si	8.3	20.8	92	70.7	99.7	80.8
P	67	70	82	79	100	72
S	3.9	34.7	91.5	77.3	100	93.2
K	2.1	30	87.8	59.7	99.8	75.4
Ca	20.3	15.1	89.3	62.3	99.9	82.4
Cr	nv	nv	81.7	51.3	96.2	76
Mn	25.1	nv	88.5	57.5	100	74.1
Fe	5.5	23.7	85.9	55	99.3	75.7
Co	77.4	44.3	85	60.1	93.3	68.5
Ni	1.1	16.9	85.5	59.5	75.5	81.5
Cu	6	8.6	87.2	60.8	99	88.5
Zn	16	7.7	87.2	56.7	95.6	76.1
Pb	21	7	90	54	97	83

nv = not valid; net filter weight was negative.

Filter samples (without size selective inlets) were collected from different locations within the dilution sampler to evaluate total mass, ions, OC, EC and elements as a function of residence time. Figures 3-22 and 3-23 compare the concentrations of selected species collected at 2, 10 and 80 seconds residence time with a dilution air ratio of 50:1 for natural gas combustion, on two different test days. Total concentration of some elements tends to decrease as residence time increases. However, results for soluble K, sodium (Na), chloride, sulfate, EC and OC show increasing concentrations with increasing residence time. The low concentrations of elements and ions for natural gas combustion present in these tests make it difficult to draw any firm conclusions about dilution sampler performance from these results.

The composition of PM<sub>2.5</sub> at 2 and 10 seconds with 50:1 dilution is compared to that at 80 seconds in Figures 3-24 and 3-25, respectively. Overall, the concentrations of various species at shorter residence times correlate well with that at 80 seconds (correlation coefficients of 0.97 and 0.99 at 2 and 10 seconds, respectively). Species concentrations are lower at 2 seconds compared to 80 seconds (slope = 0.78), while they are nearly equal at 10 seconds (slope = 0.94). This suggests that, for natural gas combustion, significant condensation and agglomeration-coagulation occurs between 2 and 10 seconds, but by 10 seconds the rate has become very slow.

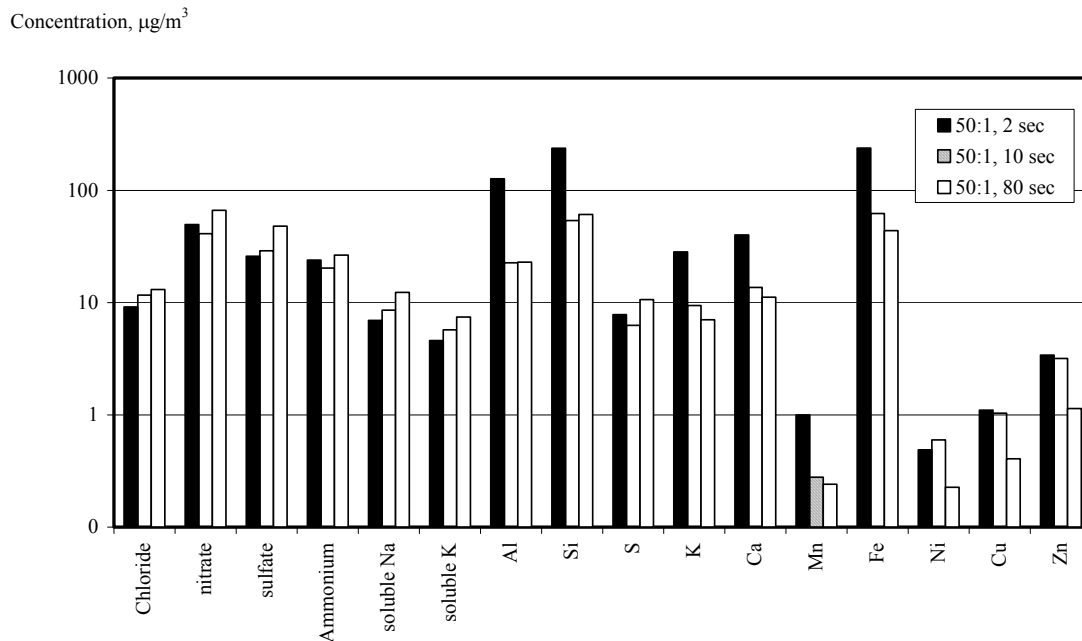


Figure 3-22. Species Concentrations at Different Residence Times in the Dilution Sampler (Natural Gas, 50:1 Dilution Ratio, Exhaust Gas Temperature 445 K, February 4, 2002).

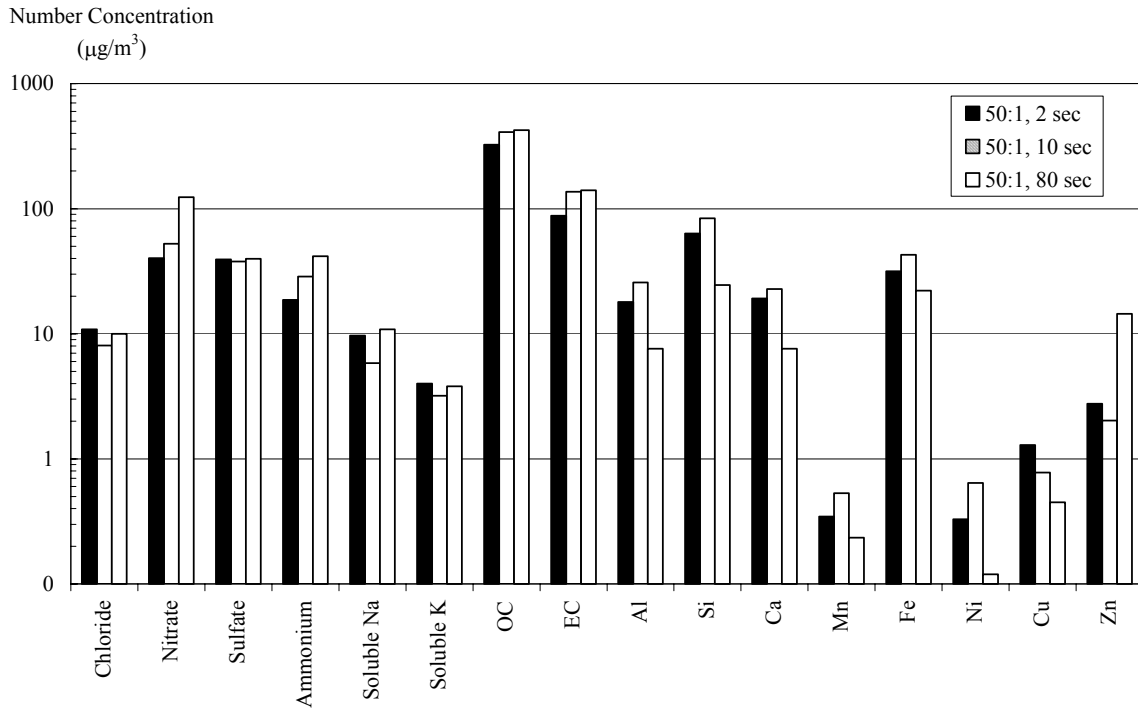


Figure 3-23. Species Concentrations at Different Residence Times in the Dilution Sampler (Natural Gas, 50:1 Dilution Ratio, Exhaust Gas Temperature 445 K, February 5, 2002).

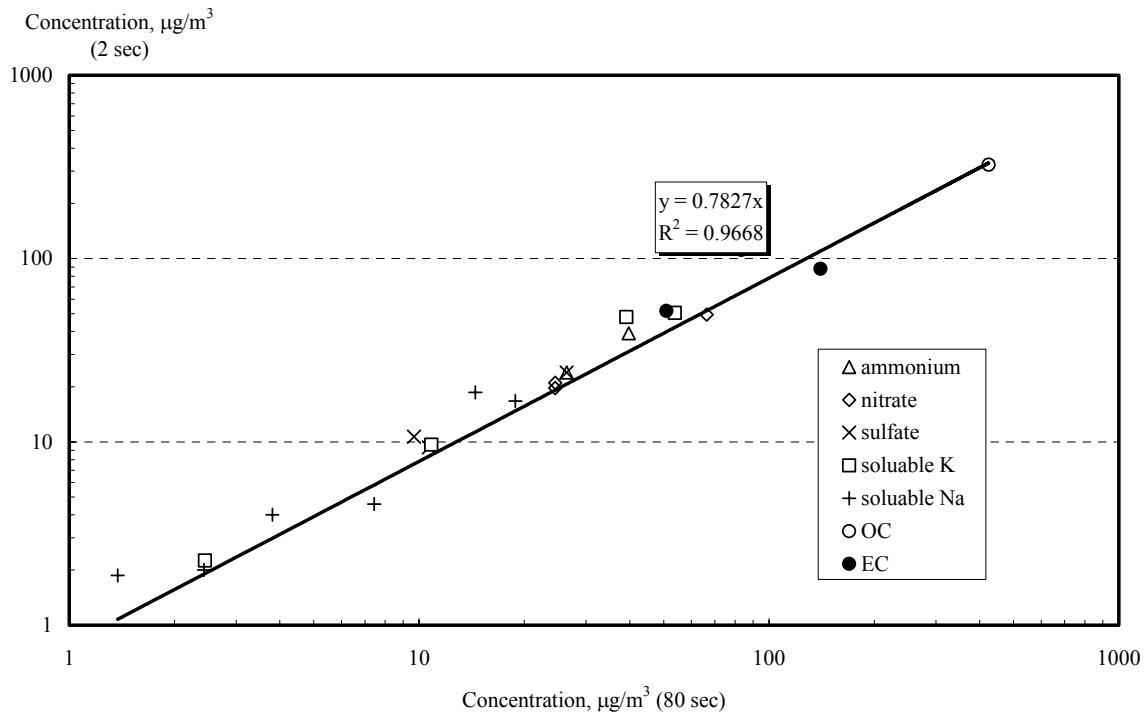


Figure 3-24. Concentrations of aerosol species at 2 and 80 seconds residence time, expressed as in-stack concentration (natural gas, 50:1 dilution ratio, exhaust gas temperature 445 K).

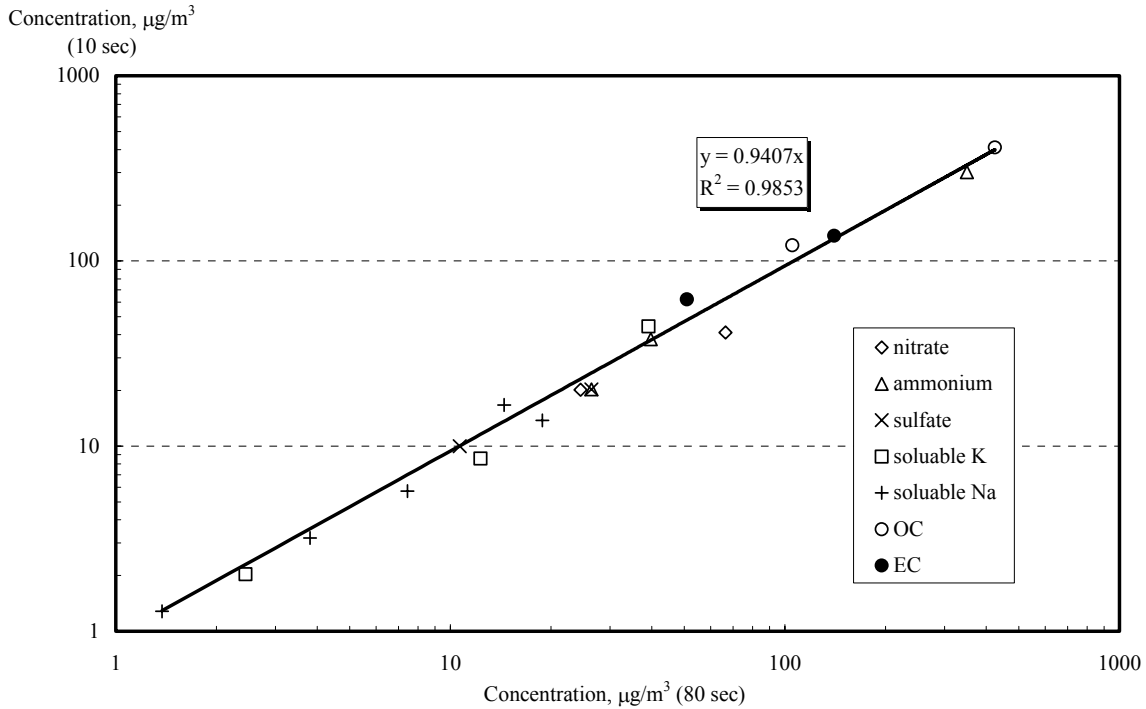


Figure 3-25. Concentrations of aerosol species at 10 and 80 seconds residence time, expressed as in-stack concentration (natural gas, 50:1 dilution ratio, exhaust gas temperature 445 K).

Similar results comparing species concentrations at 2 and 10 seconds to those at 80 seconds for coal combustion are presented in Figures 3-26 and 3-27, respectively. Overall, species concentrations at 2 and 10 seconds correlate very well with that at 80 seconds (correlation coefficients of 0.95 and 0.95, respectively). Species concentrations at 2 seconds are approximately 11 percent higher than at 80 seconds (slope = 1.11). The difference between 2 and 80 seconds may be indicative of particle losses in the dilution sampler, possibly due to condensational growth and increased particle inertial impaction and/or settling within the sampler. Concentrations at 10 seconds are very similar to those at 80 seconds (slope = 1.03). The results imply that particle condensational growth and coagulation reaches equilibrium within a few seconds for high particulate matter mass concentrations present with coal combustion.

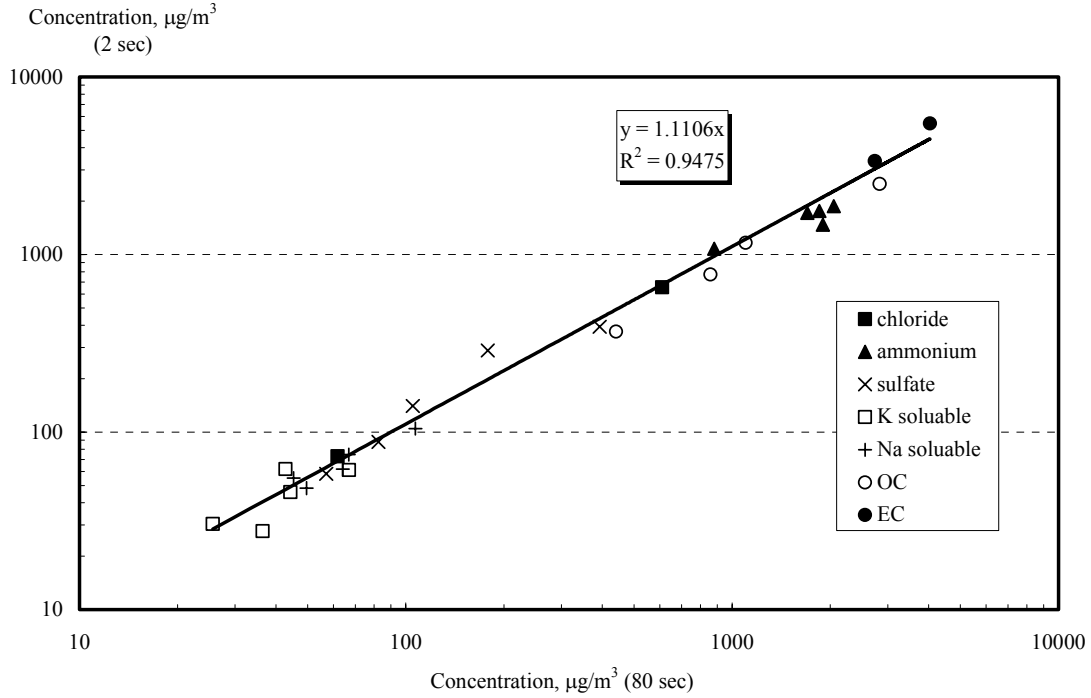


Figure 3-26. Concentrations of aerosol species at 2 seconds and 80 seconds residence time, expressed as in-stack concentration (coal, 50:1 dilution ratio, exhaust gas temperature 445 K).

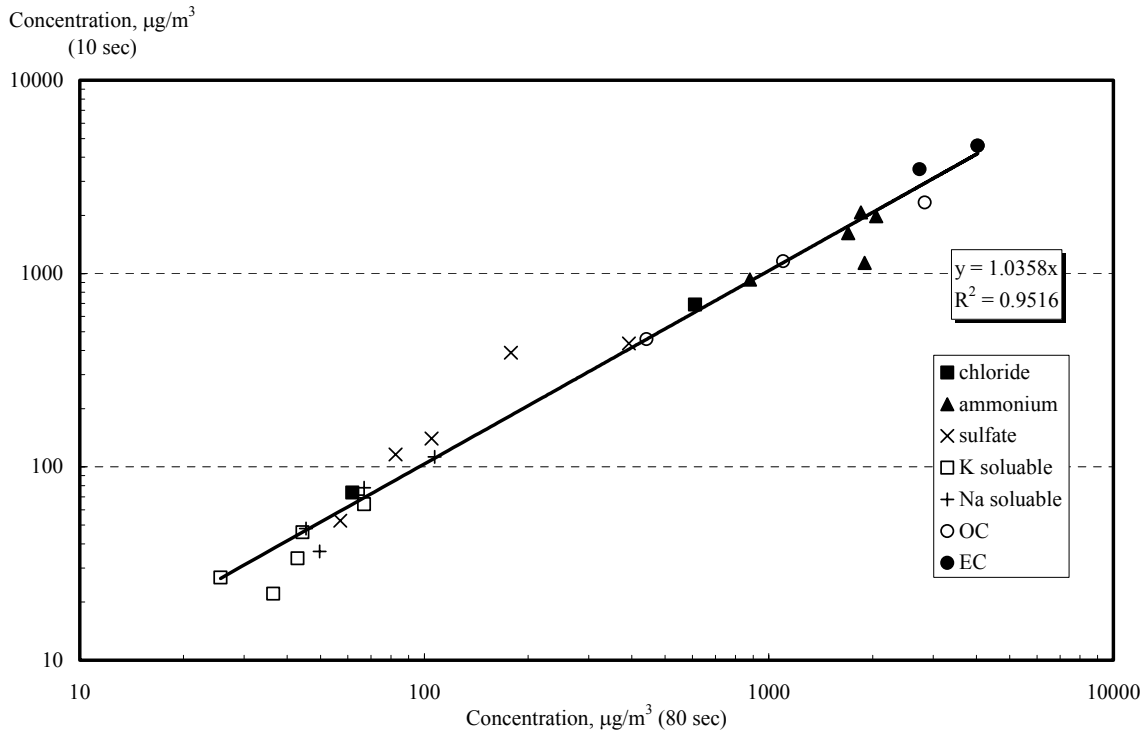


Figure 3-27. Concentrations of aerosol species at 10 seconds and 80 seconds residence time, expressed as in-stack concentration (coal, 50:1 dilution ratio, exhaust gas temperature 445 K).



Wipe-tests were performed after the coal combustion tests to gain a qualitative assessment of particle losses. Samples were collected on laboratory tissue paper and examined under a microscope. Most visible particles (>90 percent) collected from the dilution sampler wall were in the size range of 5-15  $\mu\text{m}$ . Since a relatively small number of large particles can account for a large fraction of the total mass, this suggests that the particle losses indicated by the filter measurements may be due largely to particles larger than 2.5  $\mu\text{m}$ . This is consistent with the SMPS results, which indicated no significant losses of 15 to 400 nm particles. The presence of these larger particles is most likely an indication of the sample probe PM<sub>2.5</sub> cyclone size cut-off characteristics.

## 4. DESIGN VALIDATION TEST RESULTS

After the design development tests were completed and analyzed, the new bench prototype dilution sampler was designed and constructed (see Section 2 for details). A series of tests was conducted to characterize the sampler and develop preliminary results comparing the new and old sampler designs.

### DILUTION SAMPLER CHARACTERIZATION

#### CO Tracer Profiles

Cold flow tests were performed to determine the completeness of mixing between the dilution air and the sample within the short (1.5 diameters) 8-inch diameter mixing section of the new sampler. The dilution sampler was horizontally oriented as shown earlier in Figure 2-4. Carbon monoxide (CO) was introduced into the axial sample stream as a tracer for the sample gas, and radial profiles of CO concentration were measured by extracting samples with a small probe at the cross-sectional planes at the exit of the mixing section (12 inches downstream of the mixing plate immediately before the diluted sample bypass ports, see Figure 2-4) and at a point after the sample bypass ports (7 inches or 0.9 diameters downstream of the ports). Four replicate traverses were performed and average results calculated for each traverse point. The fully mixed CO concentration was determined by measuring CO in the exhaust of the residence time chamber for each radial point measurement. The normalized CO concentration shows mixing is better than 90 percent complete on average at the mixing zone exit (Figure 4-1). A reading slightly exceeding the design tolerance (+/- 10 percent) near the wall indicates a degree of local unmixedness. The variation among the 4 replicate points is greatest at this point also. Flow visualization tests in an acrylic physical model of the sampler showed a high degree of turbulence in this region, and a slight tendency for the partially diluted sample flow to periodically favor the lower portion of the chamber consistent with the CO tracer results. While this low degree of unmixedness is considered acceptable and validates the parallel jet mixing design, it does indicate the potential for further optimization of the design.

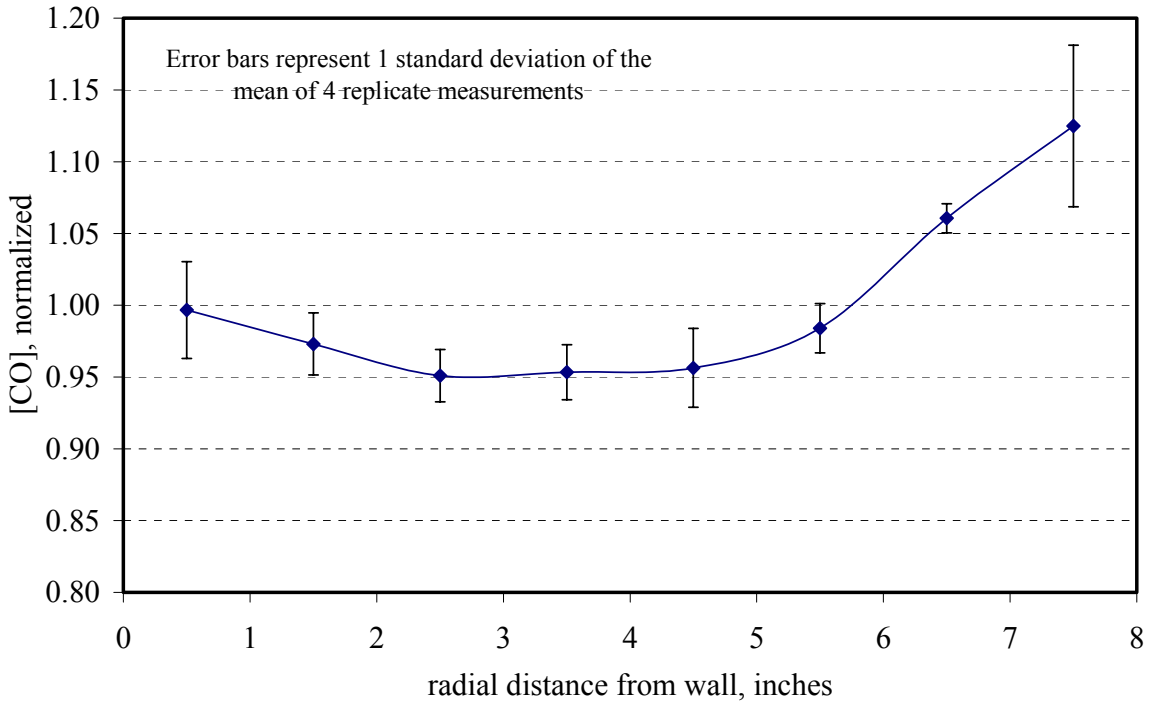


Figure 4-1. Sample gas concentration profile in the cross-sectional plane 12 inches downstream of the mixing plate (end of the mixing zone).

Figure 4-2 shows the normalized CO profile measured at a cross section downstream of the sample bypass ports, approximately 18 inches downstream of the mixing plate. The CO profile at this plane is very flat, with less than 5 percent variation from fully mixed concentrations.

### Particulate Concentration Profiles

As another means of characterizing the performance of the parallel jet mixing design, aerosol concentration profiles were measured within the sampler. The optical particle counter was used to measure radial aerosol concentration profiles in various geometric size fractions at the cross-sectional plane 12 inches downstream of the mixing plate (end of the mixing section) during natural gas combustion (Figure 4-3). Radial concentration profiles of particles 0.45  $\mu\text{m}$  and smaller show some variation across the plane, with highest concentrations at the point furthest from the wall (similar to the cold flow characterization results). Little variation in concentration is seen for particles 0.51  $\mu\text{m}$  and larger. In general, the variation across the plane is below 10 percent of the mean concentration.

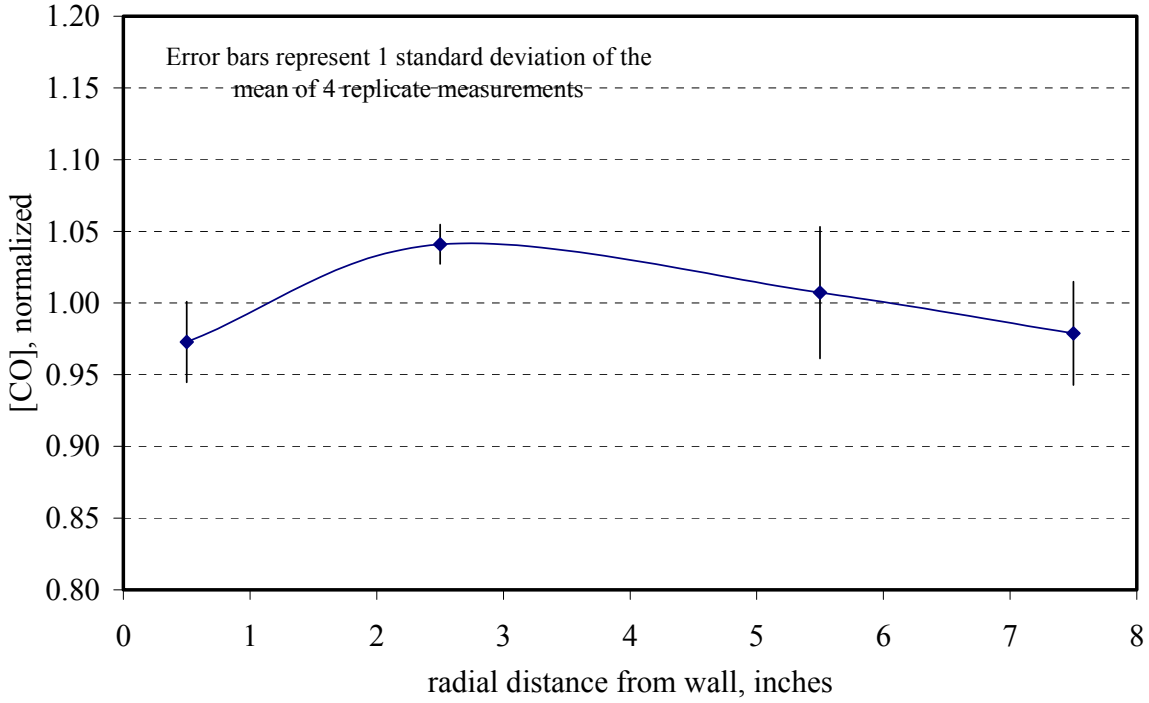


Figure 4-2. Sample gas concentration profile in the cross-sectional plane 18 inches downstream of the mixing plate.

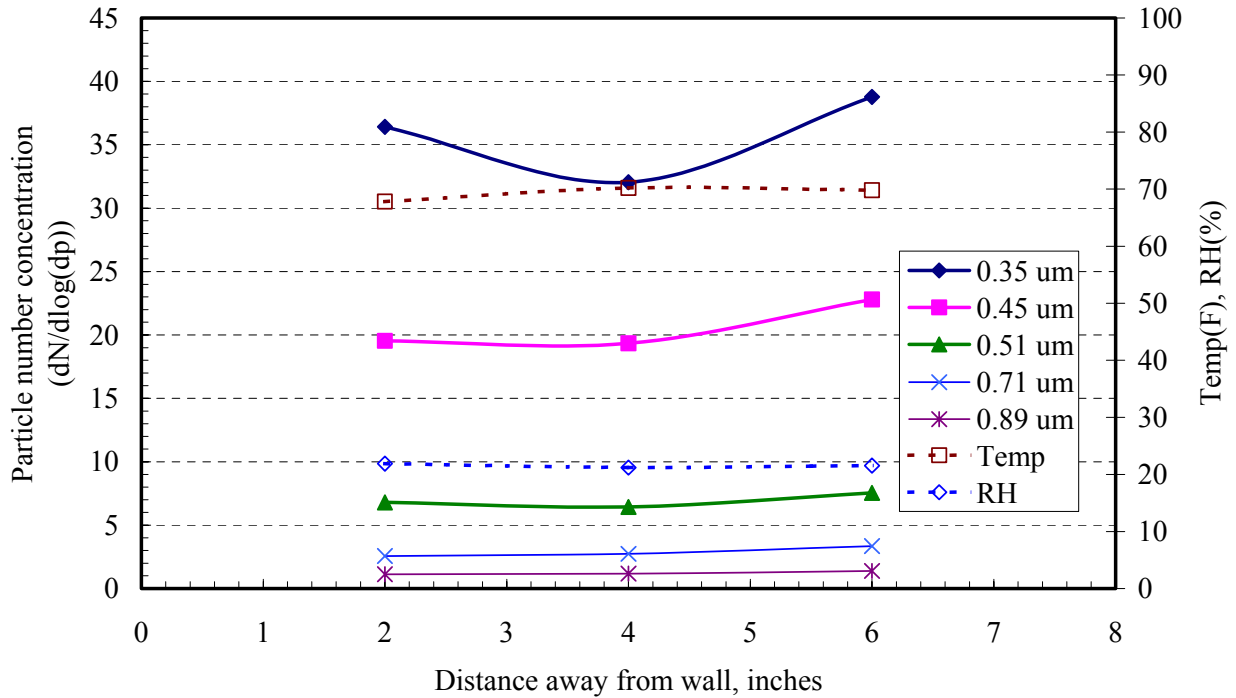


Figure 4-3. Radial particle number concentration profiles at the cross-sectional plane 12 inches downstream of the mixing plate (end of mixing zone, natural gas, exhaust temperature 450 K, 20:1 dilution ratio).

Residence time effects were briefly explored using the optical particle counter with natural gas combustion. Duplicate axial measurements of particle number concentrations were made at three distances downstream of the mixing plate, the first at 12 inches (end of mixing zone), the second at 18 inches (a few inches downstream of the bypass) and the third at approximately 36 inches (near end of residence time section). Concentrations of particles 0.32  $\mu\text{m}$  and larger are very similar at all three locations (Figure 4-4), implying negligible loss of particles between 0.3 and 1.0  $\mu\text{m}$ .

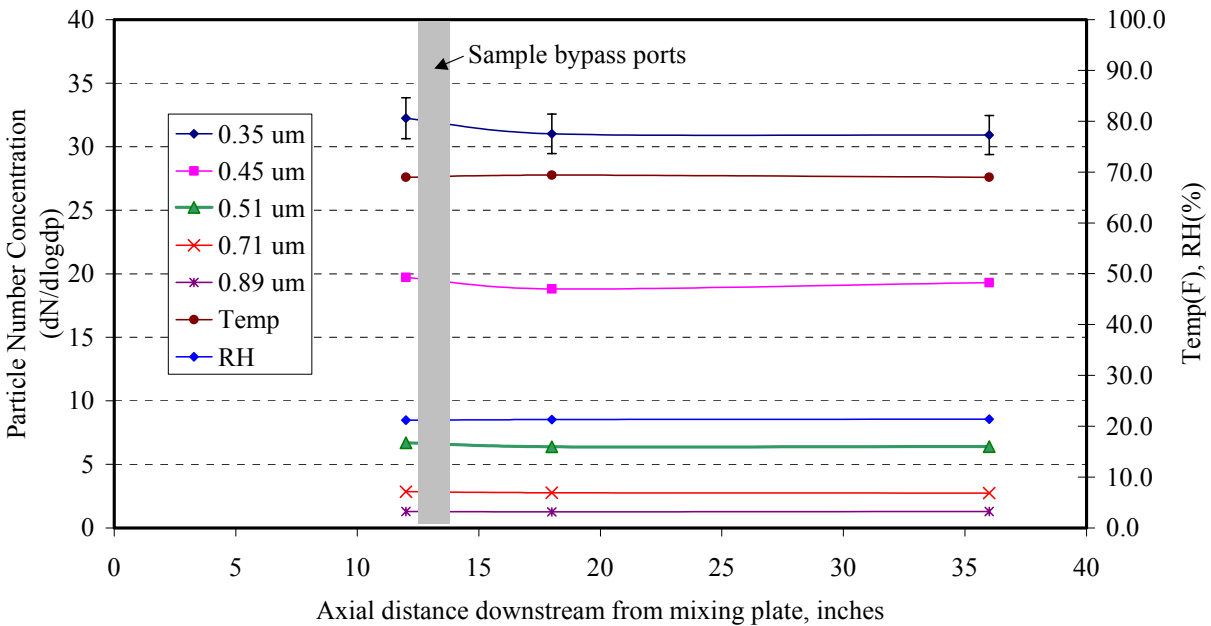


Figure 4-4. Axial particle concentration profile at centerline of dilution sampler (natural gas, exhaust temperature 450 K, 20:1 dilution ratio).

## COMBUSTION TESTS

### Natural Gas Tests

Concurrent measurements were made using the new dilution sampler and EPA Method PRE-004 (in-stack cyclones and filter) with natural gas combustion and 450 K exhaust gas temperature. The dilution sampler was operated at a dilution ratio of 18 to 22. Average PM<sub>2.5</sub> mass concentration measured by the dilution sampler is approximately 55 percent of that measured by EPA Method PRE-004/202 (including filterable and condensable PM<sub>2.5</sub> as defined by the test

methods). It should be noted that the filterable PM<sub>2.5</sub> results from EPA Method PRE-004 are dominated by the acetone rinses, which have a fairly high blank correction typically exceeding the maximum correction (20 percent) technically allowed in the method. All the net filter weights are slightly negative and counted as zero in the sum. Thus, the filterable particulate results are highly uncertain and likely below the lower limit of quantification for the test method. Previous field tests revealed that the majority of condensable PM measured in Method 202 samples is accounted for by sulfates. Wien et al. (2001) showed that much of the sulfate in Method 202 samples collected for gas combustion can be accounted for by conversion of SO<sub>2</sub> to solid residue during sampling and storage prior to analysis. The Method 202 samples (for condensable PM) were analyzed without the optional sodium hydroxide (NaOH) titration procedure for preservation of H<sub>2</sub>SO<sub>4</sub>; therefore, the results are probably biased low due to loss of H<sub>2</sub>SO<sub>4</sub> during analysis (Eckard, 2004). Despite these difficulties with the EPA methods, the difference between dilution and traditional method results is striking and consistent with prior field test results.

Table 4-1. Comparison of PM<sub>2.5</sub> Mass Concentrations Measured by New Dilution Sampler and EPA Methods 201A/202 (Natural Gas, Exhaust Temperature 450 K).

	EER Dilution Sampler		EPA Method 201A/202		
	Dilution Factor*	PM <sub>2.5</sub> mass (in-stack, mg/dscm)	Filterable PM <sub>2.5</sub> (mg/dscm)	CPM (mg/dscm)	Total PM <sub>2.5</sub> (mg/dscm)
Run 1	22.8	0.72	0.09	0.69	0.78
Run 2	17.4	0.24	0.24	0.49	0.73
Run 3	15.6	0.39	0.51	0.22	0.73
Run 4	16.3	0.39	0.21	0.65	0.85
Average	18.0	0.43	0.26	0.51	0.77
RSD	18%	47%	67%	41%	8%

\*=1+dilution ratio

### No. 6 Oil Tests

Concurrent measurements using the new dilution sampler, the old DRI dilution sampler and EPA Methods PRE-004/202 were made while firing No. 6 fuel oil. Three 120-minute test runs were planned; however, Run 3 was terminated at 53 minutes because the fuel atomizer clogged creating poor combustion conditions. Dilution ratio averaged 28:1 in the DRI dilution sampler and 22 in the GE EER dilution sampler. PM<sub>2.5</sub> concentration measured by the GE EER dilution

sampler averaged approximately 82 milligrams per dry standard cubic meter (mg/dscm), including mass collected on the filter and recovered from the probe, venturi and injector (Table 4-2). The results of the three runs are tightly grouped, with a relative standard deviation of only 4 percent. Approximately 96 percent of the total sample is accounted for by the filter catch. The DRI dilution sampler results averaged approximately 23 percent lower. However, the results are uncharacteristically variable and a large fraction (35 percent, on average) of the sample was recovered from the probe, transfer line and venturi. Both the DRI and GE EER dilution sampler PM<sub>2.5</sub> mass results are three to four times higher than the combined EPA Method PRE-004 and 202 results for filterable and condensable particulate matter. As noted earlier, the Method 202 samples (for condensable PM) were analyzed without the optional NaOH titration procedure for preservation of H<sub>2</sub>SO<sub>4</sub> in the sample, which is expected to contribute significantly to the condensable PM catch for sulfur-bearing fuels. Therefore, the condensable PM catch is uncharacteristically small compared to other test results. This probably accounts for most of the difference between the EPA method and dilution sampler results.

The agreement among the two dilution methods is only fair when all samples are considered. The DRI sampler results are unusually variable, with Run 3 substantially lower than the other two runs (Figure 4-5). No errors or other reasons to exclude Run 3 were identified; however, if Run 3 is excluded, the DRI and GE EER dilution sampler results are in much better agreement. It is apparent that deposits in the undiluted sample components are significant for No. 6 oil. The GE EER sampler is designed to minimize inertial losses by virtue of a shorter, linear sample path from the stack into the dilution mixing chamber, and the benefits of this are evident in the much greater recovery of the sample from the filter alone compared to the DRI sampler. The probe/venturi/injector recovery procedures used for the pilot tests did not rigorously adhere to EPA Method 5 procedures. The difference between the DRI and GE EER dilution sampler results is probably due to a combination of the unexpectedly high fraction of losses in the undiluted components of the DRI dilution sampler and the ad hoc recovery procedures used.

Note, the large difference in PM<sub>2.5</sub> measured with the dilution and hot filter/iced impinger method that was observed with gas combustion in previous tests (API 2001a, 2001b, 2001c) is not apparent with No. 6 oil. This is most likely due to the higher concentrations (two orders of

magnitude) of particles with No. 6 oil, due to solid ash particles and condensable H<sub>2</sub>SO<sub>4</sub> vapors arising from the ash and sulfur content of the No. 6 oil.

Table 4-2. Comparison of PM<sub>2.5</sub> Mass Concentrations Measured by DRI Dilution Sampler, EER Dilution Sampler, and EPA Methods PRE-004/202 (No. 6 Oil, Exhaust Temperature 450 K).

	EER Dilution Sampler			DRI Dilution Sampler			EPA Method PRE-004/202		
	Probe, venturi, injector (mg.dscm)	Filter (mg/dscm)	Total PM2.5 mass (mg/dscm)	Probe, venturi, injector (mg.dscm)	Filter (mg/dscm)	Total PM2.5 mass (mg/dscm)	Filterable PM2.5 (mg/dscm)	CPM (mg/dscm)	Total PM2.5 (mg/dscm)
Run 1	1.7	76.8	78.5	54.8	16.2	71.0	16.7	11.5	28.2
Run 2	1.8	82.2	84.0	3.8	91.3	95.1	19.1	2.6	21.7
Run 3*	<u>4.3</u>	<u>80.5</u>	<u>84.8</u>	<u>7.8</u>	<u>17.3</u>	<u>25.1</u>	<u>9.3</u>	<u>3.3</u>	<u>12.5</u>
Average	2.6	79.8	82.4	22.1	41.6	63.8	15.0	5.8	20.8
RSD	57%	3%	4%	128%	103%	56%	34%	86%	38%

\*Run terminated at 53 minutes due to clogged atomizer.

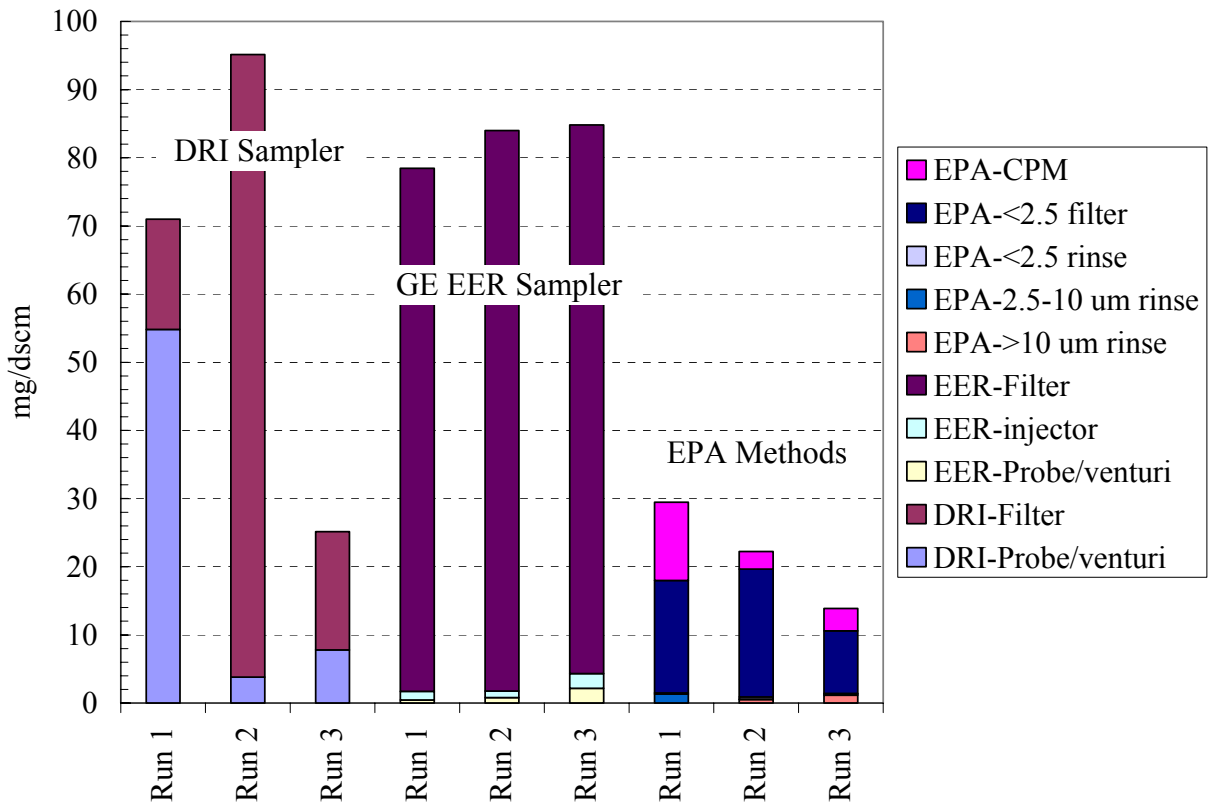


Figure 4-5. Partitioning of particulate to different sample fractions for dilution methods and EPA Methods 201A/202 (No. 6 Fuel Oil, exhaust temperature 450 K).



### Natural Gas H<sub>2</sub>SO<sub>4</sub> Doping

Formation and collection of condensed aerosols can be expected to be sensitive to dilution conditions. To assess the capture of H<sub>2</sub>SO<sub>4</sub> vapor and aerosols in the dilution sampler, concurrent measurements were made using the GE EER dilution sampler and a controlled condensation sampling train. The controlled condensation method directly measures SO<sub>3</sub> and H<sub>2</sub>SO<sub>4</sub> mist. Liquid H<sub>2</sub>SO<sub>4</sub> was atomized into the furnace at high temperature to produce SO<sub>3</sub>/H<sub>2</sub>SO<sub>4</sub> vapor without forming SO<sub>2</sub>, as described earlier in Section 4. The filter packs included a PTFE filter front filter and three backup potassium carbonate (K<sub>2</sub>CO<sub>3</sub>) impregnated filters in series behind it. The three K<sub>2</sub>CO<sub>3</sub> impregnated filters were analyzed separately by ion chromatography (IC) to evaluate potential breakthrough. The PTFE front filters, which collected particulate sulfate, were analyzed for elemental sulfur (S) by x-ray fluorescence (XRF) analysis and the K<sub>2</sub>CO<sub>3</sub> impregnated filters were extracted and analyzed for sulfate ion by IC. Duplicate PTFE filters were used in Run B to assess precision. H<sub>2</sub>SO<sub>4</sub> doping rate was set to produce an approximate target concentration of 5 ppm in the flue gas for Run 1 and approximately 15 ppm for Runs 2, 3 and 4. Overall, the variability in all the results makes the experiment difficult to interpret. The dilution sampler results are approximately two times higher than the controlled condensation results for Run 1 (Table 4-3). However, in Runs 2, 3 and 4 the dilution sampler results are substantially lower than the controlled condensation results. Separate analysis of the K<sub>2</sub>CO<sub>3</sub> filters indicates it is likely that the capacity of the K<sub>2</sub>CO<sub>3</sub> filters was exceeded during the latter test runs, leading to saturation and breakthrough (incomplete capture of H<sub>2</sub>SO<sub>4</sub> vapor). The large variability of the controlled condensation results probably indicates true H<sub>2</sub>SO<sub>4</sub> variation in the exhaust gas due to the relatively short duration of the tests and nonequilibrium losses of H<sub>2</sub>SO<sub>4</sub> on the furnace surfaces. These factors confound a conclusive interpretation of the results. However, it seems clear that improved procedures for collecting H<sub>2</sub>SO<sub>4</sub> vapor, when present at high concentrations, are needed for the dilution sampler.

Table 4-3. Sulfate Results for Dilution Sampler and Controlled Condensation Train.

	Dilution Sampler (mg/dscm)*				Controlled Condensation Train (mg/dscm)*			
	Venturi/ Injector	PTFE	K <sub>2</sub> CO <sub>3</sub>	Total	Probe Wash	Filter	Condenser	Total
Run 1	2.9	9.1	9.1	21	0.9	8.2	3.1	12
Run 2	13	3.3	3.3	20	0.1	0.2	60	61
Run 3	13	10	10	34	0.1	1.2	44	45
Run 4	NA	NA	NA	NA	0.1	0.8	64	65
Average	9.5	7.6	7.6	24.7	0.3	2.6	42.9	45.8
RSD	60%	50%	50%	31%	140%	145%	65%	52%
Run 2 duplicate	--	4.3	--	--				
RPD	--	29%	--	--				

\* Results expressed as SO<sub>4</sub><sup>=</sup>

RSD = relative standard deviation

RPD = relative percent difference

## 5. DISCUSSION AND FINDINGS

The Hildemann dilution sampler design concept is a well documented and characterized benchmark for dilution sampler design. In the development test phase, the effects of key design parameters for dilution sampler were examined using the DRI version of the Hildemann dilution sampler, building on earlier published results (Hildemann et al., 1989). The results of the development test phase provided the basis for a new dilution sampler design intended to be more compact and practical for routine stationary source stack sampling while providing results equivalent to the Hildemann benchmark over a range of solid and condensable particle concentrations. Subsequent tests were conducted to gain a preliminary assessment of the new design. The preliminary test results indicated the new design achieved the main design performance criteria (e.g., completeness of mixing, target dilution ratios, etc.). Comparative tests between the new and old dilution sampler designs were encouraging, but indicated the need for further validation.

The results also show that significant deposits of particulate matter can occur in the undiluted components of the sampler for some conditions. These deposits must be recovered after sampling to achieve accurate results. The linear sample path in the new sampler produced vastly reduced deposits compared to the DRI sampler. Tests indicated the need for improvements in the sample recovery procedures to reduce variability and improve accuracy.

### FINDINGS

The key findings from these tests are:

- SMPS and chemical speciation results at different residence time in dilution sampler suggest that an aging time after dilution of 10 seconds or more is necessary for vapor condensation growth and particle agglomeration. Shorter residence times may be adequate for sampling sources with high aerosol and/or condensable vapor concentrations.
- Preliminary tests of a new, more compact dilution sampler design demonstrated reduced particle losses in the undiluted sample components and more rapid mixing of the dilution

air and sample. Aerosol concentration measurements within the sampler indicate negligible losses of particles within the sampler after dilution.

- A minimum dilution ratio of 20:1 is necessary to obtain representative particle size distributions. The total mass of PM<sub>2.5</sub> was not affected by dilution ratio.
- Particles smaller than 0.1  $\mu\text{m}$  in aerodynamic diameter rapidly accumulate into larger particles (typically less than 10 seconds).
- Deposits of particles in the undiluted portions of the sampling system (i.e., sample nozzle, sample probe, venturi, etc.) can be significant and should be recovered for each sample run. Further development of recovery procedures for these components is needed to reduce imprecision and improve accuracy.
- Further tests are needed to validate the new dilution sampler against the current benchmark Hildemann design for a range of aerosol and condensable vapor concentrations.

## REFERENCES

- API. 2001a. Gas-Fired Boiler – Test Report Site A: Characterization of Fine Particulate Emission Factors and Speciation Profiles from Stationary Petroleum Industry Combustion Sources. Publication No. 4703. American Petroleum Institute, Washington, D.C.
- API. 2001b. Gas-Fired Heater – Test Report Site B: Characterization of Fine Particulate Emission Factors and Speciation Profiles from Stationary Petroleum Industry Combustion Sources. Publication No. 4704. American Petroleum Institute, Washington, D.C.
- API. 2001c. Gas-Fired Steam Generator – Test Report Site C: Characterization of Fine Particulate Emission Factors and Speciation Profiles from Stationary Petroleum Industry Combustion Sources. Publication No. 4712. American Petroleum Institute, Washington, D.C.
- API. 2002. Test Report: Fluidized Catalytic Cracking Unit at a Refinery (Site A): Characterization of Fine Particulate Emission Factors and Speciation Profiles from Stationary Petroleum Industry Combustion Sources. Publication No. 4713. American Petroleum Institute, Washington, D.C.
- Chow, J.C., J.G. Watson, H. Kuhns, V. Etyemezian, D.H. Lowenthal, D. Crow, S.D. Kohl, J.P.Engelbrecht, M.C. Green. 2003. “Source Profiles for Industrial, Mobile and Area Sources in the Big Bend Regional Aerosol Visibility and Observational Study,” *Chemosphere* **54**: 185-208.
- Corio, L.A. and J. Sherwell. 2000. In-stack condensible particulate matter measurements and issues. *J. Air and Waste Management Association*. 50: 207-218.
- DeWees, W.G., S.C. Steinsberger, G.M. Plummer, L.T. Lay, G.D. McAlister and R.T. Shigehara. 1989. Laboratory and Field Evaluation of the EPA Method 5 Impinger Catch for Measuring Condensable Matter from Stationary Sources. *Proceedings of the 1989 EPA/AWMA International Symposium on Measurement of Toxic and Related Air Pollutants*, Air & Waste Management Association, Pittsburgh, PA.
- Eckard, S.J. 2004. "EPA Methods 202 and 5F: Overcorrecting for Sulfates?," presented at 28th Stationary Source Sampling and Analysis for Air Pollutants Conference (March 7 to 12, 2004), Kiawah Island, South Carolina.
- England, G. C., B. Toby, and B. Zielinska. 1998. Critical Review of Source Sampling and Analysis Methodologies for Characterizing Organic Aerosol and Fine Particulate Source Emission Profiles. Publication No. 344, Health and Environmental Affairs Department, American Petroleum Institute, Washington, D.C.
- Filadelfia, E. J. and McDannel, M. D. 1996. Evaluation of False Positive Interferences Associated with the Use of EPA Method 202. Air and Waste Management Association 89th Annual Meeting and Exhibition, Nashville, Tennessee, June 1996.

Hildemann, L.M.; Gass, G.R. and Markowski, G.R. "A Dilution Stack Sampler for Collection of Organic Aerosol Emissions: Design, Characterization and Field Tests"; *Aerosol Sci. &Tech.* **1989** *10*:193-204

International Standard ISO 8178-1, Reciprocating internal combustion engines—Exhaust emission measurement-Part 1: Test-bed measurement of gaseous and particulate exhaust emissions, 1996.

International Standard ISO 8178-1, Reciprocating internal combustion engines—Exhaust emission measurement-Part 2: Measurement of gaseous and particulate exhaust emissions at site, 1996.

Kittelton, D. B., Arnold, M., and Watts, W. F., Jr. 1999. "Review of Diesel Particulate Matter Sampling Methods: Final Report." EPA grant report published on web site: [http://www.me.umn.edu/centers/cdr/Proj\\_EPA.html](http://www.me.umn.edu/centers/cdr/Proj_EPA.html), National Vehicle and Fuels Emission Laboratory, Ann Arbor, MI, January 14, 1999.

Kulmala, M. and Laaksonen, A. 1990. Binary nucleation of water-sulfuric acid system: comparison of classical theories with different H<sub>2</sub>SO<sub>4</sub> saturation vapor pressures, *J. Chem. Phys.*, **93**, 696-701.

Lipsky, E.; Stainer, C.O.; Pandis, S.N; Robinson, A.L. Effects of Sampling Conditions on Size Distribution of Fine Particulate Matter Emitted from a Pilot-Scale Pulverized-Coal Combustor; *Energy & Fuel* 2002, *16*, 302-310.

Marple, V.A., Rubow, K.L., and Behm, S.M. (1991) A Micro-Orifice Uniform Deposit Impactor (MOUDI): Description, Calibration, and Use. *Aerosol Sci. Technol.* *14*: 434-446

Seinfeld, J.H. and Pandis, S.N., 1998. *Atmospheric Chemistry and Physics from Air Pollution to Climate Change*, John Wiley & Sons, New York, NY.

U.S. EPA. 1996. *Method 202 – Determination of Condensable Particulate Emissions from Stationary Sources*. U.S. Environmental Protection Agency. Office of Air Quality Planning and Standards. Research Triangle Park, NC. <http://www.epa.gov/ttnemc01/promgate>.

U.S. EPA. 2003. "Draft Emissions Inventory Guidance for Implementation of Ozone and Particulate Matter National Ambient Air Quality Standards (NAAQS) and Regional Haze Regulations," Office of Air Quality Planning and Standards, U.S. Environmental Protection Agency, Research Triangle Park, NC 27711, June 2003.

Watson, J.G. and J. Chow. 2002. *Considerations in Identifying and Compiling PM and VOC Source Profiles for the SPECIATE Data Base*. SPECIATE Expert Panel Meeting, Charlotte, NC. October 10, 2002. [http://www.epa.gov/ttn/chief/software/speciate/panel\\_minutes.zip](http://www.epa.gov/ttn/chief/software/speciate/panel_minutes.zip).

Wien, S.E., G.C. England, K.R. Loos, K. Ritter. 2001. Investigation of Artifacts in Condensable Particulate Measurements for Stationary Combustion Sources. Paper #536. Air and Waste Management Association, 94th Annual Conference and Exhibition, Orlando, Florida, 25-27 June 2001.

## APPENDIX A LIST OF ABBREVIATIONS

°C	degrees Celsius
°F	degrees Fahrenheit
µm	micrometers
Al	aluminum
API	American Petroleum Institute
Ca	calcium
CEC	California Energy Commission
CFD	computational fluid dynamics
CH <sub>4</sub>	methane
cm <sup>3</sup>	cubic centimeter
cm	centimeter
CO <sub>2</sub>	carbon dioxide
CO	carbon monoxide
CPM	condensable particulate matter
CPC	condensation particle counter
DMA	differential mobility analyzer
DOE/NETL	United States Department of Energy National Energy Technology Laboratory
dp	electrical mobility diameter
DRI	Desert Research Institute
EC	elemental carbon
EPA	Environmental Protection Agency
Fe	iron
FEF	fuels evaluation facility
FPM	filterable particulate matter
GE	General Electric
GE EER	General Electric Energy and Environmental Research Corporation
GRI	Gas Research Institute
H <sub>2</sub> O	water
H <sub>2</sub> O <sub>2</sub>	hydrogen peroxide
H <sub>2</sub> SO <sub>4</sub>	sulfuric acid
HCl	hydrochloric acid
HSO <sub>3</sub> <sup>-</sup>	bisulfite ion
IC	ion chromatography
ICAP	inductively coupled argon plasma
ISO	International Organization for Standardization
K <sub>2</sub> CO <sub>3</sub>	potassium carbonate
K	Kelvin
K	potassium
kW	kilowatts
L/min	liters per minute
mg/dscm	milligrams per dry standard cubic meter
Mn	manganese

N	number concentration
N <sub>2</sub>	nitrogen gas
Na	sodium
NAAQS	National Ambient Air Quality Standards
NaOH	sodium hydroxide
NH <sub>3</sub>	ammonia
nm	nanometers
NYSERDA	New York State Energy Research and Development Authority
O <sub>2</sub>	molecular oxygen
O <sub>3</sub>	ozone
OC	organic carbon
pH	potential of hydrogen
PM <sub>0.32</sub>	particulate with aerodynamic diameter less than 0.32 micrometers
PM	particulate matter
PM <sub>10</sub>	particulate with aerodynamic diameter less than 10 micrometers
PM <sub>2.5</sub>	particulate with aerodynamic diameter less than 2.5 micrometers
ppm	parts per million
PTFE	polytetrafluoroethylene
S	sulfur
SMPS	scanning mobility particle sizer
SO <sub>2</sub>	sulfur dioxide
SO <sub>3</sub>	sulfur trioxide
SO <sub>3</sub> <sup>=</sup>	sulfite ion
SO <sub>4</sub> <sup>=</sup>	sulfate ion
TSI	Thermo Scientific Incorporated
XRF	x-ray fluorescence
Zn	zinc
ZnO	zinc oxide



APPENDIX B SI CONVERSION FACTORS

	<u>English (US) units</u>	X	<u>Factor</u>	=	<u>SI units</u>
Area:	1 ft <sup>2</sup>	x	9.29 x 10 <sup>-2</sup>	=	m <sup>2</sup>
	1 in <sup>2</sup>	x	6.45	=	cm <sup>2</sup>
Flow Rate:	1 gal/min	x	6.31 x 10 <sup>-5</sup>	=	m <sup>3</sup> /s
	1 gal/min	x	6.31 x 10 <sup>-2</sup>	=	L/s
Length:	1 ft	x	0.3048	=	m
	1 in	x	2.54	=	cm
	1 yd	x	0.9144	=	m
Mass:	1 lb	x	4.54 x 10 <sup>2</sup>	=	g
	1 lb	x	0.454	=	kg
	1 gr	x	0.0648	=	g
Volume:	1 ft <sup>3</sup>	x	28.3	=	L
	1 ft <sup>3</sup>	x	0.0283	=	m <sup>3</sup>
	1 gal	x	3.785	=	L
	1 gal	x	3.785 x 10 <sup>-3</sup>	=	m <sup>3</sup>
Temperature	°F-32	x	0.556	=	°C
	°R	x	0.556	=	K
Energy	Btu	x	1055.1	=	Joules
Power	Btu/hr	x	0.29307	=	Watts